AD NUMBER

AD884446

NEW LIMITATION CHANGE

TO

Approved for public release, distribution unlimited

FROM

Distribution authorized to U.S. Gov't. agencies only; Test and Evaluation; Mar 1971. Other requests shall be referred to Army Tank-Automotive Command, Warren MI.

AUTHORITY

USATAC ltr, 29 Oct 1971.

1935

313

AD884461

TECHNICAL REPORT NO. 11321

AN INVESTIGATION OF GAS TURBINE COMBUSTORS WITH HIGH INLET AIR TEMPERATURES
PART I: COMBUSTOR MODELLING

MARCH 1971

U. S. ARMY TANK-
AUTOMOTIVE COMMAND
CONTRACT NO.
DAAE07-68-C-0756

TACOM
PROPULSION SYSTEMS LABORATORY
U.S. ARMY TANK-AUTOMOTIVE COMMAND Warren, Michigan

The findings in this report are not to be construed as an official Department of the Army position.

The citation of commercial products in this report does not constitute an official indorsement or approval of such products.

CITATION OF EQUIPMENT IN THIS REPORT DOES NOT CONSTITUTE AN OFFICIAL INDORSEMENT OR APPROVAL OF THE USE OF SUCH COMMERCIAL HARDWARE.

DESTROY THIS REPORT WHEN IT IS NO LONGER NEEDED. DO NOT RETURN IT TO THE ORIGINATOR.

UNCLASSIFIED
Security Classification

DOCUMENT CONTROL DATA - R & D

(Security classification of title, body of abstract and indexing annotation must be entered when the overall report is classified)

1. ORIGINATING ACTIVITY (Corporate author)
JET PROPULSION CENTER
PURDUE UNIVERSITY

2a. REPORT SECURITY CLASSIFICATION
UNCLASSIFIED

2b. GROUP

3. REPORT TITLE
AN INVESTIGATION OF GAS TURBINE COMBUSTORS WITH HIGH INLET AIR TEMPERATURES, PART I: COMBUSTOR MODELLING

4. DESCRIPTIVE NOTES (Type of report and inclusive dates)
ANNUAL REPORT MARCH 1970 to MARCH 1971

5. AUTHOR(S) (First name, middle initial, last name)
Dean C. Hammond, Jr.
Arthur M. Mellor

6. REPORT DATE	7a. TOTAL NO. OF PAGES	7b. NO. OF REFS
March 1971	113	58

8a. CONTRACT OR GRANT NO.
DAAE07-69-C-0756

b. PROJECT NO.

c.

d.

9a. ORIGINATOR'S REPORT NUMBER(S)
TM-71-1

9b. OTHER REPORT NO(S) (Any other numbers that may be assigned this report)
11321

10. DISTRIBUTION STATEMENT
This document is subject to special export controls and each transmittal to foreign governments or foreign nationals may be made only with prior approval of U.S. Army Tank-Automotive Command ATTN: AMSTA-BSL

11. SUPPLEMENTARY NOTES

12. SPONSORING MILITARY ACTIVITY
U.S. Army Tank-Automotive Command
Propulsion Systems Laboratory
Warren, Michigan

13. ABSTRACT

DD FORM 1 NOV 68 1473 REPLACES DD FORM 1473, 1 JAN 64, WHICH IS OBSOLETE FOR ARMY USE

UNCLASSIFIED
Security Classification

14. KEY WORDS	LINK A		LINK B		LINK C	
	ROLE	WT	ROLE	WT	ROLE	WT
Gas Turbine Combustor Design						
Combustor						
Perfectly Stirred Reactor						
Analytical modelling						
Hydrocarbon Kinetics						
Gas Turbine emissions						

REPORT NO. 11321

PURDUE UNIVERSITY

AND

PURDUE RESEARCH FOUNDATION

AN INVESTIGATION OF GAS TURBINE COMBUSTORS WITH HIGH INLET AIR TEMPERATURES

SECOND ANNUAL REPORT

PART I: COMBUSTOR MODELLING

by

D. C. Hammond, Jr.
A. M. Mellor

Contract Number DAAE07-69-C-0756
U. S. Army Tank-Automotive Command
Warren, Michigan

Jet Propulsion Center
Purdue University
Lafayette, Indiana

March 1971

ACKNOWLEDGMENTS

The authors are indebted to Mr. B. W. Gerhold for a large part of the work on the equilibrium reactor program. Mr. W. C. Mayse assisted in preparing some of the experimental comparisons.

This work was sponsored by the U. S. Army Tank-Automotive Command under contract DAAE07-69-C-0756, Mod. P002. Mr. Hammond acknowledges partial financial support through a traineeship from the National Science Foundation.

ABSTRACT

An analytical model has been developed which will predict the performance and pollutant emissions of gas turbine combustors. The entire gas turbine combustor is approximated as a collection of perfectly stirred zones. Within each zone a general hydrocarbon combustion mechanism is used to predict the gas composition and temperature. The zone volumes and sizes are assigned from consideration of the theoretically predicted gas flows thereby approximating the mixing behavior of the system. The resulting combustor model is seen to possess several intrinsic merits, namely:

1. it is simple enough to facilitate solutions;
2. both mixing and kinetics are considered;
3. there is an exact correspondence between the flow zones in the model and in a combustor.

Selected predictions of the overall model for a "typical" aircraft combustor are presented. These results are seen to be qualitatively accurate and fall in the range of values typically observed in practical systems.

TABLE OF CONTENTS

LIST OF TABLES

LIST OF TABLES

LIST OF FIGURES

CHAPTER I

INTRODUCTION AND OBJECTIVES

It is now apparent that the gas turbine engine will take an important part in the field of vehicular propulsion in the near future. These engines are being considered as alternative powerplants both for heavy vehicles (trucks and military vehicles) and for automobiles. For vehicular applications a regenerator is usually included in the engine cycle, and this regenerator causes an increase in the combustor inlet air temperature. A similar but less severe inlet temperature increase is encountered in aircraft engines as the engine pressure ratios and flight Mach numbers increase. Lifting engines for STOL/VTOL applications also experience periods of hot gas ingestion which raises the inlet temperature significantly. For all of these situations large quantities of empirical design data are not available at elevated combustor inlet temperatures. Rather than attempting to scale up low inlet temperature data, it is felt that an analytical model of the combustor, valid for all inlet temperatures, will be eminently more useful.

The current emphasis on reducing the emission of atmospheric pollutants from all types of engines has also focused attention on the utility of the analytical modelling of combustion systems. Increased application of gas turbine engines can only increase interest in the control of their emissions. The primary gas-phase pollutants emitted from gas turbines are carbon monoxide and nitric oxide. The emissions of unburned hydrocarbons are usually negligible, but smoke emissions can be significant. The levels of carbon monoxide and nitric oxide are clearly dependent on the kinetic and mixing processes occuring inside the combustor. Smoke emissions are controlled primarily by the concentrations, temperatures, and flow pattern in the primary combustion zone. All of the processes mentioned can be

incorporated into an analytical model to permit prediction of emission levels.

The development of the overall gas turbine combustor model followed the same logical sequence as will be followed here. Firstly, the kinetics of hydrocarbon combustion are investigated resulting in a general hydrocarbon combustion theory for a single perfectly stirred reactor. The kinetics of nitric oxide formation are incorporated into the combustion mechanism. Secondly, several models of the turbulent mixing phenomena are considered. Thirdly, the flow processes inside the combustor are examined. Combining these three studies, a complete analytical model is postulated and used to make quantitative predictions.

CHAPTER II
A GENERALIZED HYDROCARBON COMBUSTION ANALYSIS FOR A PERFECTLY STIRRED REACTOR

The overall gas turbine combustor model to be used in this work was presented by Hammond and Mellor (1970a) and Hammond and Mellor (1970b). Certain modifications have been made to the original model, but it still remains basically a combination of perfectly stirred reactors. A kinetic analysis for the combustion of propane in a perfectly stirred reactor was previously developed (Hammond and Mellor, 1970a,b) for use in this model. This original analysis, upon detailed investigation, was shown to possess several undesirable limitations which subsequently resulted in its discard. Firstly, the analysis was valid only for propane which is an unrealistic fuel from a practical viewpoint. Secondly, an ill defined empirical parameter was involved in the analysis (cf. Schneider, 1960). Thirdly, predictions could only be obtained for a very limited range of equivalence ratios ($0.8 \leq \phi \leq 1.2$). Finally, the limitation on equivalence ratio precluded any realistic evaluation of accuracy by comparison with experimental data.

The analysis which follows was developed to allow a priori predictions of the combustion performance for a general hydrocarbon/air system in a single stage perfectly stirred reactor. All of the cited limitations inherent in the previous analysis have been successfully removed.

A. The generalized hydrocarbon combustion mechanism

The exact kinetic mechanisms for hydrocarbon/air combustion are poorly understood except for the simplest hydrocarbon species. In those cases where "complete" mechanisms have been postulated, the mechanisms contain a number of elementary reactions for which accurate

rate data are essentially unavailable. There have been many attempts to model the combustion process in a global manner; a number of these are summarized in Hammond and Mellor (1970a) and in Edelman and Fortune (1969). Our intent here is to formulate an approximate mechanism which will apply to a general hydrocarbon, and in order to do this we will first examine some of the "complete" mechanisms.

Chinitz (1965) used the methane combustion mechanism shown in Table 1 to study the constant-pressure combustion of methane/air systems. His predicted temperature-time histories compared very well with experimental values, but his predicted species concentration-time histories deviated significantly from experimental values. The predictions of ignition delay times were about a factor of 100 lower than experiment; however, Chinitz felt that mixing limitations in the physical experiment can be charged with some of the discrepancies. Note that Reactions [1-1] through [1-5] constitute a process of methane partial oxidation to carbon monoxide and water; that Reaction [1-6] is the only carbon monoxide destruction reaction; and that the remainder of the mechanism is concerned only with free radical production.

Morgan (1965) proposed the mechanism shown in Table 2 for methane/air combustion in a perfectly stirred reactor. Using this mechanism he was able to derive certain global rate expressions which agreed reasonably well with his own data. This mechanism differs only slightly from that of Chinitz, and can be similarily interpreted as consisting of partial oxidation to CO, carbon monoxide destruction, and free radical production processes. Morgan views Reactions [2-1] and [2-10] as being rate-limiting.

The mechanism shown in Table 3 was developed by Bowman and Seery (1968) and also by Bowman (1968) from shock tube studies of methane oxidation. Both works showed reasonable agreement between predicted and experimental values of the concentration-time histories and ignition delay time (defined as the time to the rapid increase in pressure) for mixtures around stoichiometric and temperatures above 2000°K. Bowman and Seery attributed the failure to predict behavior over the full range of temperature and stoichiometry to poorly understood reactions involving HCO which were omitted from their mechanism.

Table 1.

Methane combustion mechanism of Chinitz (1965)

Reaction	No.
$CH_4 + OH \rightleftarrows CH_3 + H_2O$	[1-1]
$CH_4 + O \rightleftarrows CH_3 + OH$	[1-2]
$CH_3 + O_2 \rightleftarrows HCHO + OH$	[1-3]
$HCHO + OH \rightleftarrows HCO + H_2O$	[1-4]
$HCO + OH \rightleftarrows CO + H_2O$	[1-5]
$CO + OH \rightleftarrows CO_2 + H$	[1-6]
$H + H_2O \rightleftarrows OH + H_2$	[1-7]
$O + H_2 \rightleftarrows OH + H$	[1-8]
$OH + OH \rightleftarrows H_2O + O$	[1-9]
$H + O_2 \rightleftarrows OH + O$	[1-10]
$O + O + M \rightleftarrows O_2 + M$	[1-11]
$H + H + M \rightleftarrows H_2 + M$	[1-12]

Table 2.

Methane combustion mechanism of Morgan (1967)

Reaction	No.
$CH_4 + OH \rightleftarrows CH_3 + H_2O$	[2-1]
$CH_4 + H \rightleftarrows CH_3 + H_2$	[2-2]
$CH_3 + O_2 \rightleftarrows HCHO + OH$	[2-3]
$CH_3 + O \rightleftarrows CH_2O + H$	[2-4]
$HCHO + OH \rightleftarrows HCO + H_2O$	[2-5]
$HCHO + H \rightleftarrows HCO + H_2$	[2-6]
$HCO + OH \rightleftarrows CO + H_2O$	[2-7]
$HCO + CH_3 \rightleftarrows CO + CH_4$	[2-8]
$HCO + H \rightleftarrows CO + H_2$	[2-9]
$CO + OH \rightleftarrows CO_2 + H$	[2-10]
$H + O_2 \rightleftarrows OH + O$	[2-11]
$H_2O + O \rightleftarrows OH + OH$	[2-12]
$H + H_2O \rightleftarrows OH + H_2$	[2-13]

Table 3.

Methane combustion mechanism of Bowman and Seery (1968)

Reaction	No.
$CH_4 + M \rightleftarrows CH_3 + H + M$	[3-1]
$CH_4 + O_2 \rightleftarrows CH_3 + HO_2$	[3-2]
$O_2 + M \rightleftarrows O + O + M$	[3-3]
$CH_4 + O \rightleftarrows CH_3 + OH$	[3-4]
$CH_4 + H \rightleftarrows CH_3 + H_2$	[3-5]
$CH_4 + OH \rightleftarrows CH_3 + H_2O$	[3-6]
$CH_3 + O \rightleftarrows HCHO + H$	[3-7]
$CH_3 + O_2 \rightleftarrows HCHO + OH$	[3-8]
$HCHO + OH \rightleftarrows HCO + H_2O$	[3-9]
$HCO + OH \rightleftarrows CO + H_2O$	[3-10]
$CO + OH \rightleftarrows CO_2 + H$	[3-11]
$H + O_2 \rightleftarrows O + OH$	[3-12]
$O + H_2 \rightleftarrows H + OH$	[3-13]
$O + H_2O \rightleftarrows OH + OH$	[3-14]
$H + H_2O \rightleftarrows H_2 + OH$	[3-15]
$H + OH + M \rightleftarrows H_2O + M$	[3-16]
$CH_3 + O_2 \rightleftarrows HCO + H_2O$	[3-17]
$HCO + O_2 \rightleftarrows CO + HO_2$	[3-18]
$H + HO_2 \rightleftarrows OH + OH$	[3-19]
$HCO + M \rightleftarrows H + CO + M$	[3-20]

Although the methane combustion mechanism of Bowman and Seery is rather more complex than the previous two mechanisms, it still possesses the three rather well defined processes. These processes are partial oxidation (Reactions [3-1], [3-2], [3-4]-[3-10], [3-17]-[3-20]), carbon monoxide destruction, and free radical production. The parametric studies of Bowman and Seery (1968) indicated the dominant reactions to be [3-11], [3-4]-[3-6], and [3-10]-[3-17].

Bowman and Seery (1968) also developed two mechanisms for acetylene combustion (cf. Table 4); the two mechanisms differ only in the choice of the oxygen atom attack reaction on acetylene from Reaction [4-2a] or [4-2b]. The ignition delays predicted using each mechanism were in good agreement with experimental values and with each other. The predicted temperature-time and concentration-time histories were different for the two mechanisms, and the predicted discrepancies were dependent on the rates of the reactions involving acetylene and acetylene fragments.

Surprisingly, this acetylene combustion mechanism can also be divided into the processes of partial oxidation (Reactions [4-11]-[4-8]), carbon monoxide destruction (Reactions [4-9]), and free radical production. Since acelylene has a triple bond structure and methane only single bonds, one might expect a significantly different combustion mechanism.

A detailed discussion of possible propane combustion mechanisms was presented by Hammond and Mellor (1970a). All of the mechanisms considered in that work could also be divided into the aforementioned three processes. Further, the partial oxidation process was assumed to be infinitely fast compared to the rate limiting process of carbon monoxide destruction through:

$$CO + OH \rightarrow CO_2 + H \qquad [24]$$

which was the only destruction reaction (in agreement with all of the above mechanisms). The two body branching reactions:

$$OH + H_2 \rightleftarrows H_2O + H \qquad [2]$$

$$H + O_2 \rightleftarrows OH + O \qquad [3]$$

Table 4.

The acetylene combustion mechanisms of Bowman and Seery (1968)

Reaction	No.	Mechanism 1 or 2
$C_2H_2 + C_2H_2 \rightleftarrows C_4H_2 + H + H$	[4-1]	1,2
$C_2H_2 + O \rightleftarrows CH_2 + CO$	[4-2]	2
$C_2H_2 + O \rightleftarrows C_2H + OH$	[4-2b]	1
$C_2H_2 + OH \rightleftarrows C_2H + H_2O$	[4-3]	1,2
$C_2H_2 + H \rightleftarrows C_2H + H_2$	[4-4]	1,2
$C_2H + O_2 \rightleftarrows CO + CO + H$	[4-5]	1,2
$C_2H + O \rightleftarrows CO + CH$	[4-6]	1
$CH_2 + O_2 \rightleftarrows HCO + OH$	[4-7]	2
$HCO + OH \rightleftarrows CO + H_2O$	[4-8]	2
$CO + OH \rightleftarrows CO_2 + H$	[4-9]	1,2
$H + O_2 \rightleftarrows OH + O$	[4-10]	1,2
$O + H_2 \rightleftarrows OH + H$	[4-11]	1,2
$O + H_2O \rightleftarrows OH + OH$	[4-12]	1,2
$H + H_2O \rightleftarrows H_2 + OH$	[4-13]	1,2
$H + OH + M \rightleftarrows H_2O + M$	[4-14]	1,2
$H + H + M \rightleftarrows H_2 + M$	[4-15]	1,2

$$O + H_2 \rightleftarrows OH + H \qquad [4]$$

were assumed to attain equilibrium (after Schneider, 1960; Hottel et al., 1965). Also the three-body radical recombination reactions:

$$H + H + M \rightleftarrows H_2 + M \qquad [6]$$
$$O + O + M \rightleftarrows O_2 + M \qquad [7]$$
$$O + H + M \rightleftarrows OH + M \qquad [8]$$
$$OH + H + M \rightleftarrows H_2O + M \qquad [9]$$

were allowed to proceed in the forward direction only. As noted previously, the results for C_3H_8 obtained using this mechanism were not good.

Chinitz and Baurer (1966) investigated the combustion of propane/air and ethane/air. They postulated a combined mechanism containing 69 basic reaction pairs and 31 chemical species; the ethane/air mechanism appeared as a subset of the propane/air mechanism. The complete mechanism is given in Table 5. In the table Reactions [5-1]-[5-12] pertain only to the propane/air combustion. Using an analytical definition for ignition delay time as 5% of the final temperature rise, the computed ethane ignition delay times were fair agreement with data determined in subsonic diffusion flames using vitiated air. However, the propane ignition delay times compared somewhat less well with some data obtained in a shock tube. The experimental ignition delay times were defined as the time to onset of luminosity, and thus the difference in definitions could account for some of the disagreement.

For this combined mechanism our division of the combustion into three processes fails. In particular, Reactions [5-18], [5-19], [5-21], [5-34]-[5-36], and [5-49] all produce carbon dioxide rather than carbon monoxide thus invalidating our separation of partial oxidation from carbon monoxide destruction. However, Reaction [5-61] is cited by Chinitz and Baurer as the predominant carbon monoxide destruction reaction, and the free radical reactions are essentially the same as in the previous mechanisms. To elucidate the coupling between the partial oxidation and carbon dioxide production processes, let us examine the temperature-time and carbon dioxide-time histories (cf. Figs. 1 and 2) from the work of Chinitz and Baurer. These histories show a brief

Table 5.

The combined propane/air; ethane/air
combustion mechanism of Chinitz and Baurer (1966)

Reaction	
$C_3H_8 + OH \rightleftarrows C_3H_7 + H_2O$	[5-1]
$C_3H_8 + O \rightleftarrows C_2H_6 + HCHO$	[5-2]
$C_3H_8 + H \rightleftarrows C_3H_7 + H_2$	[5-3]
$C_3H_7 + O \rightleftarrows C_2H_5CHO + H$	[5-4]
$C_3H_7 + O \rightleftarrows C_3H_6 + OH$	[5-5]
$C_3H_7 + OH \rightleftarrows C_3H_6 + H_2O$	[5-6]
$C_3H_7 + O_2 \rightleftarrows C_2H_5CHO + OH$	[5-7]
$C_3H_6 + O_2 \rightleftarrows CH_3CHO + HCHO$	[5-8]
$C_3H_6 + OH \rightleftarrows CH_3CHO + CH_3$	[5-9]
$C_3H_6 + O \rightleftarrows C_3H_4 + H_2O$	[5-10]
$C_3H_6 + O \rightleftarrows HCHO + C_2H_4$	[5-11]
$C_3H_4 + O_2 \rightleftarrows CH_3CO + CHO$	[5-12]
$C_2H_6 + O \rightleftarrows C_2H_5 + OH$	[5-13]
$C_2H_6 + OH \rightleftarrows C_2H_5 + H_2O$	[5-14]
$C_2H_6 + H \rightleftarrows C_2H_5 + H_2$	[5-15]
$C_2H_5CHO + OH \rightleftarrows C_2H_5CO + H_2O$	[5-16]
$C_2H_5CHO + H \rightleftarrows C_2H_5CO + H_2$	[5-17]
$C_2H_5CHO + O_2 \rightleftarrows C_2H_5 + CO_2 + OH$	[5-18]
$C_2H_5CO + O \rightleftarrows C_2H_5 + CO_2$	[5-19]

Table 5. Cont.

Reaction	No.
$C_2H_5CO + OH \rightleftarrows C_2H_5OH + CO$	[5-20]
$C_2H_5CO + O_2 \rightleftarrows C_2H_5O + CO_2$	[5-21]
$C_2H_5CO + H \rightleftarrows C_2H_5 + CHO$	[5-22]
$C_2H_5OH + O_2 \rightleftarrows CH_3OH + CO + H_2O$	[5-23]
$C_2H_5OH + H \rightleftarrows C_2H_5 + H_2O$	[5-24]
$C_2H_5O + O_2 \rightleftarrows CH_3O + CO + H_2O$	[5-25]
$C_2H_5O + O_2 \rightleftarrows CH_3OH + CO + OH$	[5-26]
$C_2H_5O + H \rightleftarrows C_2H_5 + OH$	[5-27]
$C_2H_5 + O_2 \rightleftarrows CH_3CHO + OH$	[5-28]
$C_2H_5 + O \rightleftarrows C_2H_4 + OH$	[5-29]
$C_2H_5 + O \rightleftarrows CH_3CHO + H$	[5-30]
$C_2H_5 + OH \rightleftarrows C_2H_4 + H_2O$	[5-31]
$CH_3CHO + OH \rightleftarrows CH_3CO + H_2O$	[5-32]
$CH_3CHO + H \rightleftarrows CH_3CO + H_2$	[5-33]
$CH_3CHO + O_2 \rightleftarrows CH_3 + CO_2 + OH$	[5-34]
$CH_3CO + O \rightleftarrows CH_3 + CO_2$	[5-35]
$CH_3CO + O_2 \rightleftarrows CH_3O + CO_2$	[5-36]
$CH_3CO + OH \rightleftarrows CH_3OH + CO$	[5-37]
$CH_3CO + H \rightleftarrows CH_3 + CHO$	[5-38]
$CH_3OH + O_2 \rightleftarrows CO + H_2O + H_2O$	[5-39]
$CH_3OH + H \rightleftarrows CH_3 + H_2O$	[5-40]
$CH_3O + O_2 \rightleftarrows CO + OH + H_2O$	[5-41]
$CH_3O + H \rightleftarrows CH_3 + OH$	[5-42]
$C_2H_4 + O \rightleftarrows CH_3 + CHO$	[5-43]

Table 5. Cont.

Reaction	No.
$C_2H_4 + O \rightleftarrows C_2H_2 + H_2O$	[5-44]
$C_2H_4 + OH \rightleftarrows CH_3 + HCHO$	[5-45]
$C_2H_2 + O \rightleftarrows C_2H + OH$	[5-46]
$C_2H_2 + OH \rightleftarrows C_2H + H_2O$	[5-47]
$C_2H + O_2 \rightleftarrows CO + CO + H$	[5-48]
$C_2H + O_2 \rightleftarrows CH + CO_2$	[5-49]
$CH + O_2 \rightleftarrows CO + OH$	[5-50]
$CH_4 + OH \rightleftarrows CH_3 + H_2O$	[5-51]
$CH_4 + O \rightleftarrows CH_3 + OH$	[5-52]
$CH_4 + H \rightleftarrows CH_3 + H_2$	[5-53]
$CH_3 + O \rightleftarrows HCHO + H$	[5-54]
$CH_3 + O_2 \rightleftarrows HCHO + OH$	[5-55]
$HCHO + OH \rightleftarrows CHO + H_2O$	[5-56]
$HCHO + H \rightleftarrows CHO + H_2$	[5-57]
$HCHO + O \rightleftarrows CHO + OH$	[5-58]
$CHO + O \rightleftarrows CO + OH$	[5-59]
$CHO + OH \rightleftarrows CO + H_2O$	[5-60]
$CO + OH \rightleftarrows CO_2 + H$	[5-61]
$OH + H_2 \rightleftarrows H + H_2O$	[5-62]
$OH + OH \rightleftarrows H_2O + O$	[5-63]
$O + H_2 \rightleftarrows OH + H$	[5-64]
$H + O_2 \rightleftarrows OH + O$	[5-65]
$O + H + M \rightleftarrows OH + M$	[5-66]
$O + O + M \rightleftarrows O_2 + M$	[5-67]
$H + H + M \rightleftarrows H_2 + M$	[5-68]
$H + OH + M \rightleftarrows H_2O + M$	[5-69]

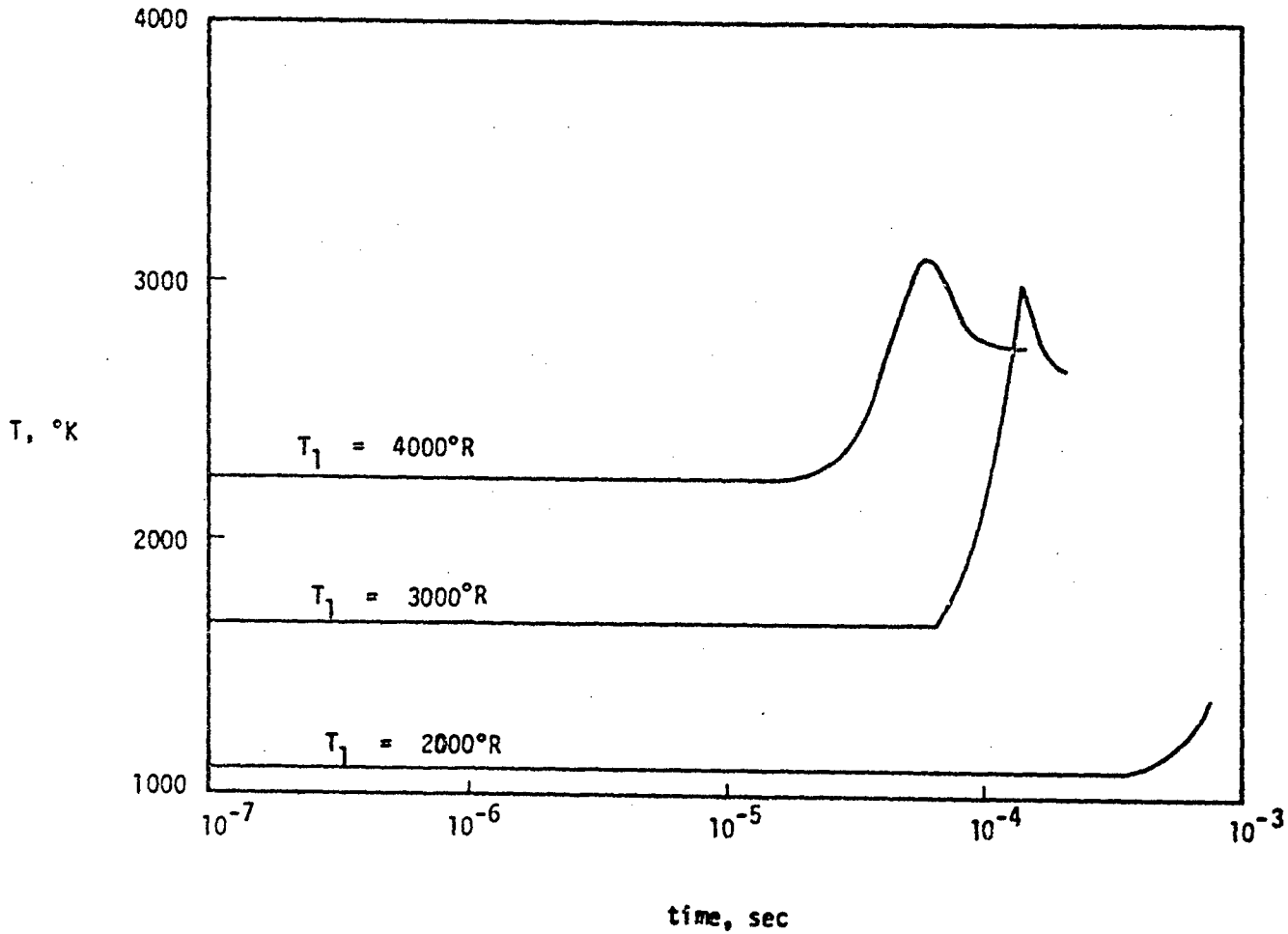

Fig. 1 The effect of initial temperature on C_3H_8/air combustion (1 atm) (Chinitz and Baurer, 1966)

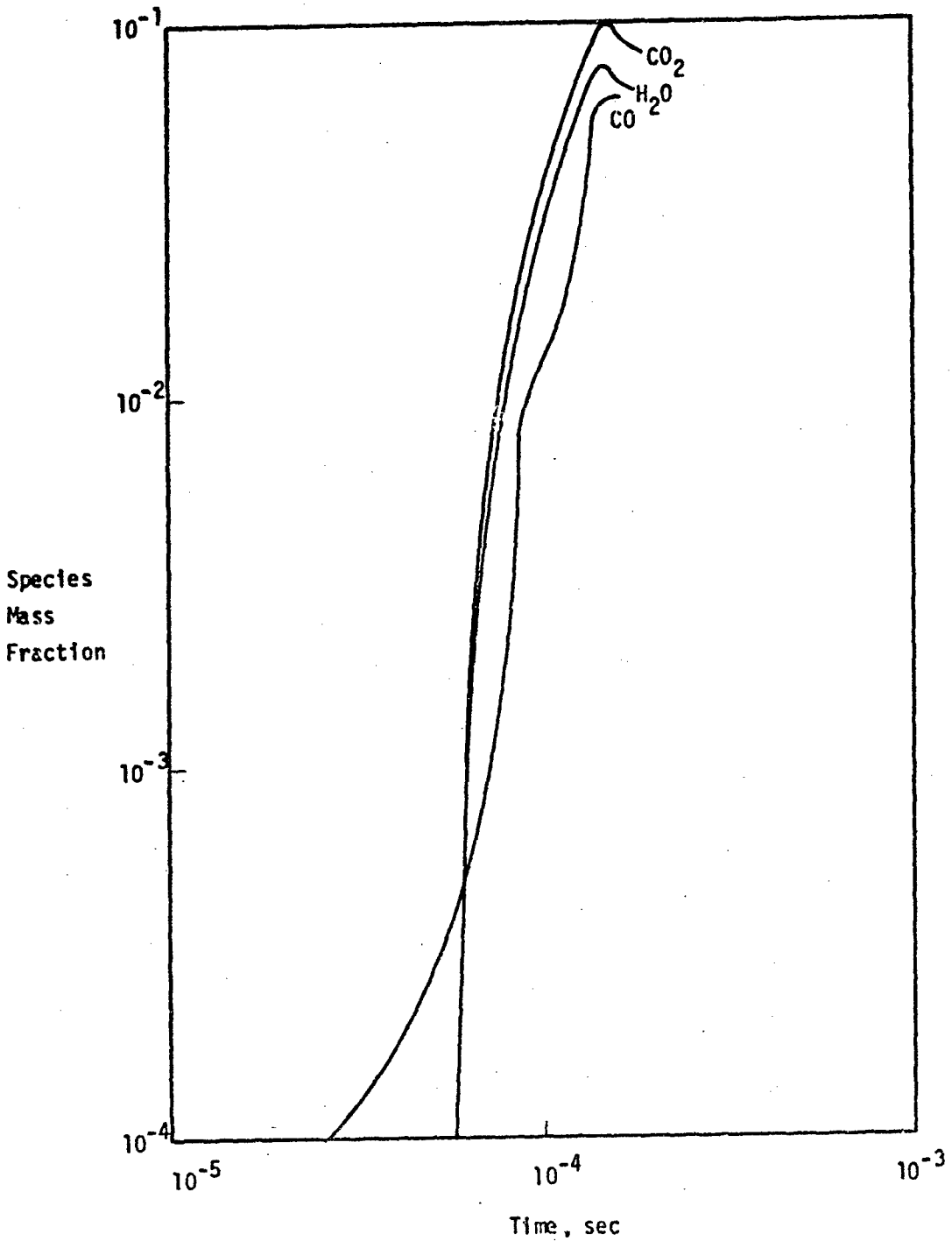

Fig. 2 Species concentration histories in C_3H_8/air combustion (1 atm, 3000°R) (Chinitz and Baurer, 1966)

carbon dioxide and temperature overshoot with a duration of approximately 10^{-4} seconds. Chinitz and Baurer attribute these overshoots to the inability of the CO-CO_2 equilibrium (Reaction [5-61]) to match the initial rapid production of carbon dioxide by the reactions mentioned above. They note that the magnitude and existence of the overshoots depend on the values of some of the less accurately known rate constants. If indeed the overshoot is a real effect (experimental verification is lacking) its duration is short and its effect is quickly damped. In fact, the overshoot can be thought of as indicating the high rate of the partial oxidation.

The common feature of all the hydrocarbon combustion mechanisms presented is that (with the exceptions noted) they can be divided into three basic processes:

1. rapid partial oxidation of the parent hydrocarbon to carbon monoxide and water,
2. A rate limiting step of carbon monoxide destruction through Reaction [24],
3. a sequence of free radical production reactions not involving carbon.

A similar division was made by Hammond and Mellor (1970a,b) and by Edelman (1970).

In the present work, in order to make the mechanism applicable to the combustion of any hydrocarbon the partial oxidation is modelled using the following general reaction:

$$C_aH_b + \left(\frac{a}{2} + \frac{b}{4}\right) O_2 \rightarrow aCO + \frac{b}{2} H_2O \qquad [37]$$

which is assumed to have an infinitely fast forward rate compared to the rate of Reaction [24]. The necessity of making such a gross characterization of the process becomes apparent when one considers the extremely complex mechanism which was developed for as relatively simple a hydrocarbon as propane (Chinitz and Baurer, 1966) and then envisions the complexity of the mechanism which will surely be required to model the combustion of a more realistic hydrocarbon fuel such as kerosene. Clearly, our present knowledge of complex hydrocarbon combustion is insufficient to allow development of accurate mechanisms.

Edelman (1970) has modelled the partial oxidation process by a reaction similar to Reaction [37] but producing carbon monoxide and diatomic hydrogen and having a finite but empirically determined rate. A similar division was also made by Marteney (1970) for methane combustion. In agreement with our postulate, he found that the "complete" mechanism results agreed with those using an infinitely fast partial oxidation.

The remainder of the general hydrocarbon combustion mechanism consists of the single carbon monoxide destruction reaction ([24]) and various generally accepted free radical production reactions not involving carbon. This portion of the mechanism is common to all of the cited mechanisms with minor deviations in the free radical production reactions. We have chosen to include those free radical reactions which are most well understood and have accurate accepted rate constants. Thus, the final general hydrocarbon combustion mechanism is shown in Table 6.

B. The nitric oxide formation mechanism

Since the nitric oxide emissions from gas turbine engines are of current interest from a pollution viewpoint, it would be advantageous to incorporate a nitrogen oxidation mechanism into the hydrocarbon combustion mechanism. Although the nitrogen oxidation chemistry is considerably simpler than the hydrocarbon oxidation chemistry, only recently has a well defined mechanism been developed.

The Zeldovich mechanism (Zeldovich et al., 1947) consisting of the reactions:

$$O + N_2 \rightleftarrows NO + N \qquad [20]$$

$$N + O_2 \rightleftarrows NO + O \qquad [21]$$

is generally accepted as the major source of nitric oxide (Bowman, 1970; Newhall, 1969; Camac and Feinberg, 1967; Marteney, 1970; Lavoie et al., 1970; Fletcher and Heywood, 1971). The only point of disagreement among these various authors is what other reactions also contribute significantly to the formation of nitric oxide. This point must be examined somewhat

Table 6.

The general hydrocarbon combustion mechanism (this ref.)

Reaction	No.
$C_aH_b + (\frac{a}{2} + \frac{b}{4})\ O_2 \rightleftarrows aCO + \frac{b}{2}\ H_2O$	[37]
$CO + OH \rightleftarrows CO_2 + H$	[24]
$O_2 + H_2 \rightleftarrows OH + OH$	[1]
$OH + H_2 \rightleftarrows H_2O + H$	[2]
$O_2 + H \rightleftarrows OH + O$	[3]
$O + H_2 \rightleftarrows OH + H$	[4]
$O + H_2O \rightleftarrows OH + OH$	[5]
$H + H + M \rightleftarrows H_2 + M$	[6]
$O + O + M \rightleftarrows O_2 + M$	[7]
$O + H + M \rightleftarrows OH + M$	[8]
$H + OH + M \rightleftarrows H_2O + M$	[9]

more closely.

Bowman (1970) feels that only Reactions [20] and [21] are significant. Camac and Feinberg (1967) favor including the reaction:

$$N + O + M \rightleftarrows NO + M \qquad [22]$$

for high temperatures in air and the reaction:

$$N_2 + O_2 \rightleftarrows NO + NO \qquad [23]$$

at low temperatures. Marteney (1970) includes only Reactions [20], [21], and [22] in his analytical work. Newhall (1969) initially includes all of the Reactions [20]-[23] and two additional formation paths involving the species NO_2 and N_2O but he then concludes from his result that the Zeldovich mechanism dominates. Lavoie et al. (1970) add the reaction:

$$N + OH \rightleftarrows NO + H \qquad [38]$$

giving the mechanism shown in Table 7. Fletcher and Heywood (1971) also use the mechanism of Table 7; however, both investigators found that only the first three reactions are significant.

The basic Zeldovich mechanism must clearly be incorporated into any reasonable mechanism of nitric oxide formation. Bowman (1970) established from his shock tube studies that Reaction [38] could become significant at temperatures below 2000°K, but we have not included it at present. In deference to the results of Camac and Feinberg (1967) Reaction [22] is included, but Reaction [23] is excluded since we are concerned only with high temperature processes. Our final mechanism thus appears in Table 8.

Bowman's (1970) work clearly shows an advantage which our total kinetic model gives over previous models which assume the hydrocarbon chemistry to be in equilibrium (Lavoie et al., 1970; Fletcher and Heywood, 1971). Note the discrepancy resulting from the equilibrium assumptions (Fig. 3). Bowman accurately attributes this deviation to a kinetic oxygen atom overshoot above its equilibrium value.

Table 7

Nitric oxide mechanism of Lavoie et al. (1970) and Fletcher and Heywood (1971)

Reaction	
$N_2 + O \rightleftarrows NO + N$	[20]
$N + O_2 \rightleftarrows NO + C$	[21]
$N + OH \rightleftarrows NO + H$	[38]
$H + N_2O \rightleftarrows N_2 + OH$	[39]
$O + N_2O \rightleftarrows N_2 + O_2$	[40]
$O + N_2O \rightleftarrows NO + NO$	[41]

Table 8.

Nitric oxide mechanism (this ref.)

Reaction	No.
$N_2 + O \rightleftarrows NO + N$	[20]
$N + O_2 \rightleftarrows NO + O$	[21]
$N + O + M \rightleftarrows NO + M$	[22]

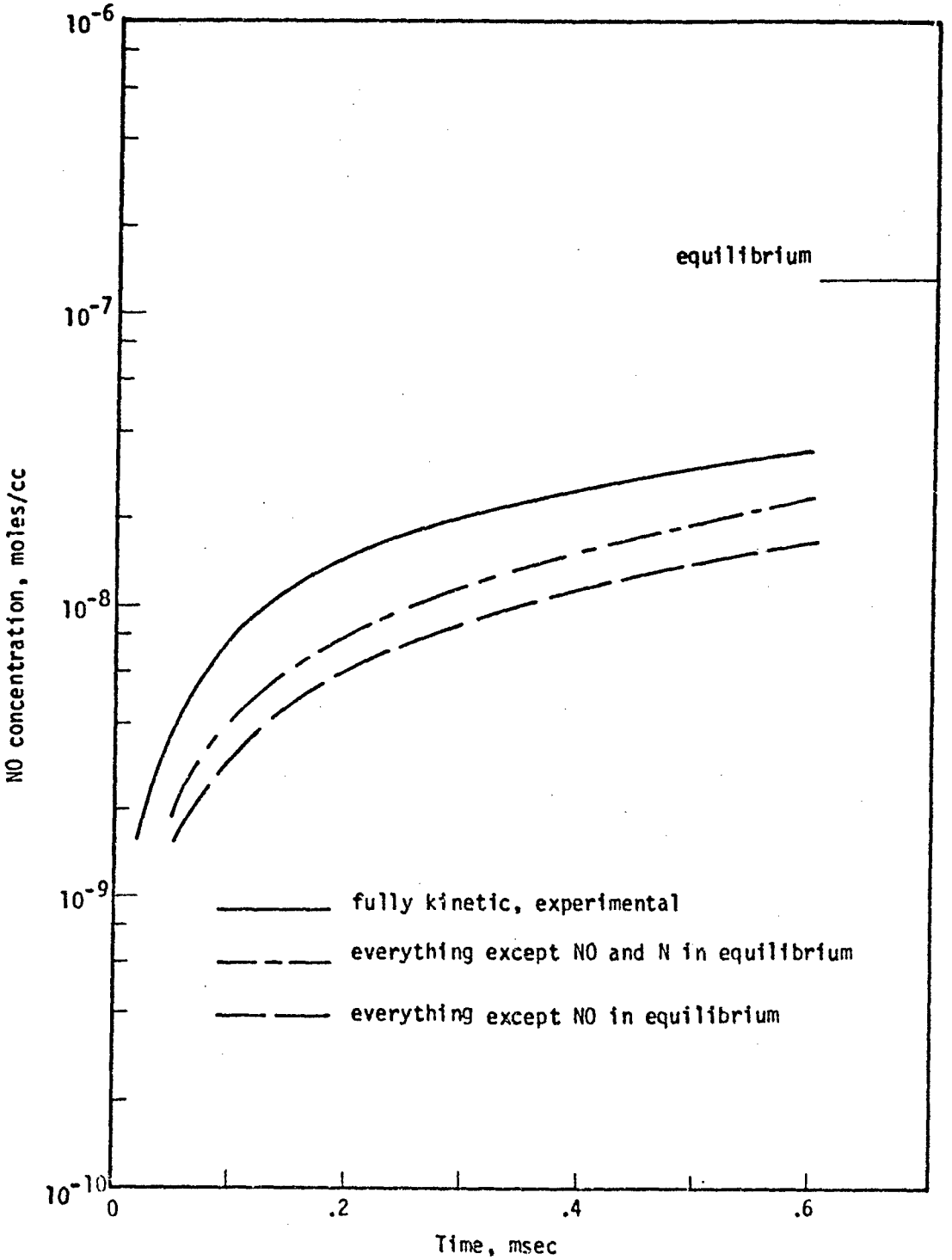

Fig. 3 NO concentration profiles (2% H_2-6% O_2-92% N_2, 2560 °K, 2.07 atm) (Bowman, 1970)

C. Hydrocarbon combustion rate data

The determination of accurate rate constants for use in kinetic calculations has long been a significant problem. For the reactions we are considering the comprehensive surveys of Baulch et al. (1968a, b, 1969a,b) have greatly simplified the problem. For each reaction pair in the final mechanism we have taken the more accurate of the forward and reverse rate constants from this reference where possible and expressed it in the modified Arrhenius form:

$$k_i = A_i T^{\delta i} \exp(-E_i/RT) \qquad (2\text{-}1)$$

where A_i, δ_i, E_i are the parameters for the i^{th} elementary reaction. The less accurate of the rate constant pair is then computed from the equilibrium constant (Stull, 1965) and the other rate constant and fitted to equation (2-1). The values of the forward and reverse rate parameters are given in Table 9 for all reactions in the combined hydrocarbon combustion-nitrogen oxidation mechanism.

D. Formulation of the governing equations for a perfectly stirred reactor

The classical concept of a stirred reactor is a zone of uniform and homogeneous composition and temperature through which a steady flow of mass passes (Fig. 4). Any mass entering this zone is assumed to be instantaneously mixed throughout the volume of the zone. Thus inside the zone mixing is infinitely fast, and kinetics completely control the reaction rates. Also, since the zone is perfectly mixed the composition and temperature of the exit flow are identical to the composition and temperature inside the zone. With this basic groundwork we can proceed to formulate the governing equations.

Using the generalized notation of Penner (1957) the chosen reaction mechanism may be represented by:

$$\sum_{i=1}^{I} \nu'_{ij} X_i \underset{k_{rj}}{\overset{k_{fj}}{\rightleftharpoons}} \sum_{i=1}^{I} \nu''_{ij} X_i \quad (j=1,2,\ldots J) \qquad (2\text{-}2)$$

Table 9.

Rate parameters*

Reaction No.	Forward Reaction A_{fi}	δ_{fi}	E_{fi}	Reverse Reaction A_{ri}	δ_{ri}	E_{ri}
[1]‡	8.000×10^{14}	0.	+45000	1.071×10^{12}	.39	25751
[2]+	2.190×10^{13}	0.	+5150	4.858×10^{14}	-.20	20727
[3]+	2.240×10^{14}	0.	+16800	6.647×10^{11}	.39	-469
[4]+	1.740×10^{13}	0.	+19450	7.737×10^{12}	0.	7467
[5]+	5.750×10^{13}	0.	18000	1.169×10^{12}	.20	444
[6]‡	5.000×10^{18}	-1.15	0	1.662×10^{19}	-1.14	103988
[7]‡	4.700×10^{15}	-.28	0	2.375×10^{18}	.66	119279
[8]‡	5.300×10^{15}	0.	-2780	8.477×10^{15}	0.	99246
[9]+	1.170×10^{17}	0.	0	8.629×10^{18}	-.19	119565
[20]+	6.192×10^{13}	.10	75241	3.100×10^{13}	0.	334
[21]+	6.430×10^{9}	1.00	6250	3.661×10^{8}	1.16	37847
[22]+	6.450×10^{14}**	-.50	0	1.856×10^{16}	-.72	150876
[24]+	5.600×10^{11}	0.	1080	1.455×10^{18}	-1.19	27047

* units, g-mole, cc, °K, cal

‡ forward parameters from Jenkins et al. (1967)

\+ forward parameters from Baulch et al. (1968a,b, 1969a,b)

** Due to a coding error this valve is lower by a factor of 100 than that of Baulch, et al.; however, calculations reveal that this error has a negligible effect on the predictions to be presented in Chapter V.

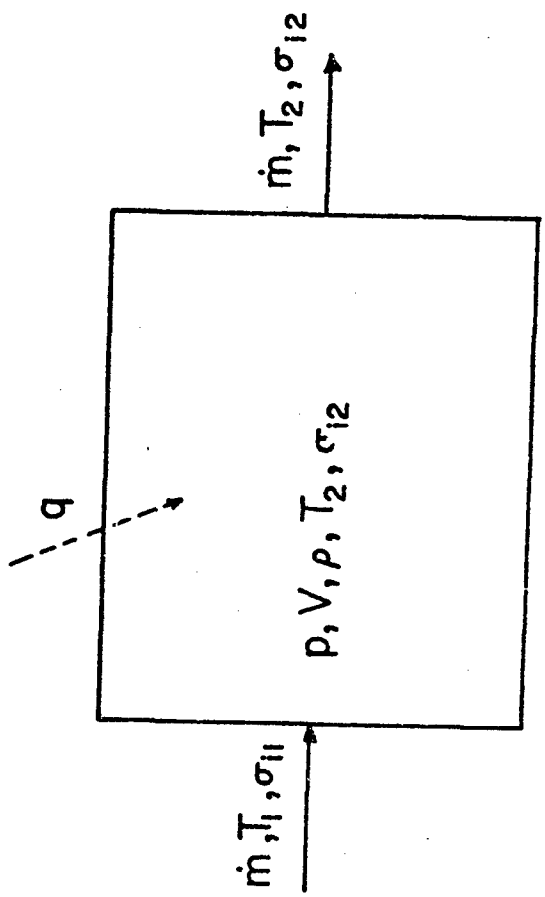

Fig. 4 Notation to be used in describing the performance of a single perfectly stirred reactor.

where X_i denotes the i^{th} species, ν'_{ij} its stoichiometric coefficient as a reactant, and ν''_{ij} its stoichiometric coefficient as a product, where there are I species and J reactions (here I = 12, J = 14). The symbols k_{fj} and k_{rj} denote the forward and reverse rate constants for the j^{th} reaction, respectively.

The species conservation equations are given in general by:

$$\dot{m}_{i1} - \dot{m}_{i2} = - \dot{m}'''_i V \qquad (i=1,2,\ldots I) \qquad (2\text{-}3)$$

where $\dot{m}_i$ is the total mass flow of the i^{th} species, $\dot{m}'''_i$ is the volumetric mass production rate of the i^{th} species inside the reactor due to chemical reaction, and V is the reactor volume. The subscripts 1 and 2 denote inlet and exit (also internal) conditions, respectively. After Jones and Prothero (1968) equation (2-3) can be recast as:

$$\frac{\dot{m}}{V} (\sigma_{i1} - \sigma_{i2}) = - \frac{\dot{m}'''_i}{W_i} \qquad (i=1,2,\ldots I) \qquad (2\text{-}4)$$

where σ_i is the concentration of the i^{th} species (mole i/gm), $\dot{m}$ is the total mass flow rate, and W_i is the molecular weight of the i^{th} species.

Assuming local thermal equilibrium, a mixture of thermally perfect gases, and constant reactor pressure, the source term in equation (2-4) can be written explicitly giving:

$$\frac{\dot{m}}{V} [\sigma_{i1} - \sigma_{i2}] = \sum_{j=1}^{J} (\nu'_{ij} - \nu''_{ij}) \left[k_{fj} \prod_{i=1}^{I} (\rho \sigma_{i2})^{\nu'_{ij}} - k_{rj} \prod_{i=1}^{I} (\rho \sigma_{i2})^{\nu''_{ij}}\right] \qquad (i=1,2,\ldots I) \qquad (2\text{-}5)$$

and the gas law:

$$\rho = \frac{P}{RT_2 \sum_{i=1}^{I} \sigma_{i2}} \qquad (2\text{-}6)$$

Assuming negligible changes in kinetic and potential energy and no shaft work, the energy equation can be written as:

$$\sum_{i=1}^{I} (\sigma_{i2} h_{i2} - \sigma_{i1} h_{i1}) = q \qquad (2\text{-}7)$$

where h_i is the total (chemical + sensible) enthalpy of the i^{th} species (cal/mole i) and q is the heat added (cal/g of flow).

The set of equations (2-5), (2-6), and (2-7) number I + 2, and there are I + 2 dependent variables (σ_{i2}, T_2, ρ); therefore the problem is well posed. A computer program was written to solve the set of equations simultaneously (cf. Appendix A). We will now present a discussion of the predictions obtained from the program.

E. Comparison of the predicted results with experimental data

The true measure of the usefulness of this perfectly stirred reactor analysis in building an overall gas turbine combustor model will be its ability to predict the combustion performance of physical systems. Any error incurred in predicting the performance of a single perfectly stirred reactor will certainly manifest itself in an error in the overall predictions. For this reason we have checked the accuracy of our analysis in two ways: the first is an asymtotic comparison with equilibrium results, and the second is a comparison with experimental data for a single-stage reactor.

It is expected that the kinetic predictions approach equilibrium values as the mass flow rate is decreased or the inlet temperature increased. To check this correspondence Fig. 5 was prepared. In this and subsequent figures completeness of combustion ϵ is defined by:

$$\epsilon = \frac{x_{CO_2,2}}{x_{CO_2,2} + x_{CO,2}} \qquad (2\text{-}8)$$

where x_{i2} is the reactor and exit mole fraction of the indicated species. The curve denoted as equilibrium is the result of an independent computation for the same conditions based on accepted values of the equilibrium constants (Stull, 1965). The equilibrium computer program is described in Appendix B. In the figure the kinetic results are seen to tend towards equilibrium as the flow rate per unit volume is decreased

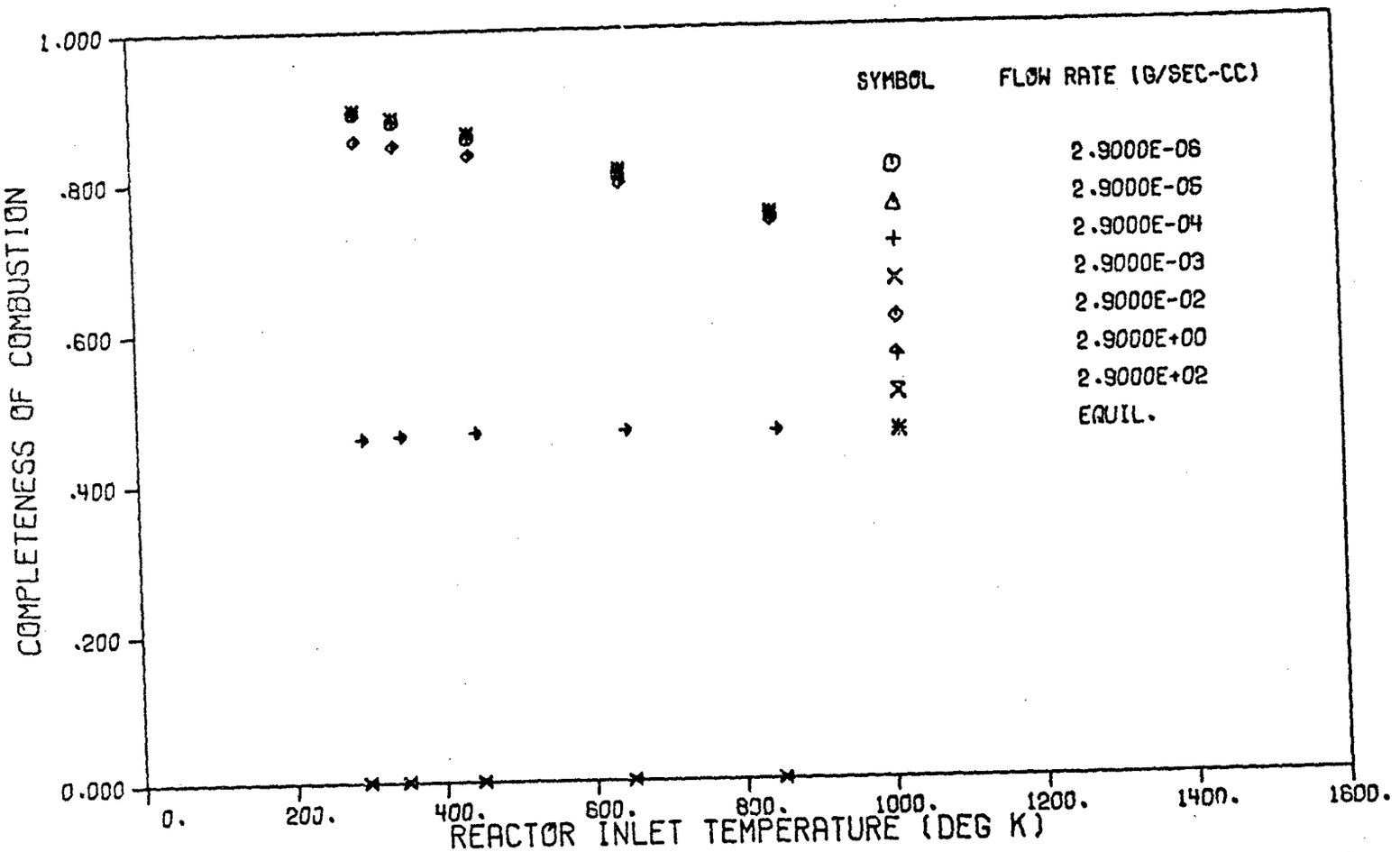

FIGURE 5 INLET TEMPERATURE DEPENDENCE OF THE COMPLETENESS OF COMBUSTION
PROPANE/AIR PRES. = 1.000 (ATM) EQUIV. RATIO = 1.00

(for a constant pressure of one atm). The results also exhibit the correct inlet temperature trend, i.e. for constant flow rate per unit volume and constant pressure the results tend toward equilibrium values with increasing inlet temperature. Finally, at a given loading the completeness of combustion ϵ (a measure of combustion efficiency) decreases with increasing inlet temperature. This trend, observed in our earlier results (Hammond and Mellor, 1970a), is consistent with the explanation of increased carbon dioxide dissociation at higher reactor temperatures.

In order to further define the accuracy of our single stage stirred reactor program for various fuels, comparisons were made with experimental data for the combustion of carbon monoxide/air in a spherical combustor (Nerheim, 1960), methane/air in conical and cylindrical combustors (Morgan, 1967), and propane/air in a spherical combustor (Schneider, 1960). These comparisons are shown in Figs. 6-11.

Considering first the carbon monoxide/air data (Figs. 6-9), one would expect the theory to be most accurate for this fuel since our hydrocarbon combustion scheme is based on a rate limiting carbon monoxide combustion mechanism. This comparison should thus provide a test of the validity of this generally accepted carbon monoxide combustion mechanism. Fig. 6 reveals a rather large discrepancy between the predicted and experimental values, i.e. theory predicts blow-out while the experimental values clearly indicate the presence of combustion. The discrepancy in Fig. 6 results from our use of Reaction [24] as the only carbon monoxide destruction reaction. In the presence of high water concentrations (and thus an ample supply of hydroxyl radicals) Reaction [24] is truly dominant, but as the amount of water is reduced other reactions have been shown to become significant (Newhall, 1969). Therefore, for "dry" carbon monoxide/air combustion the following reactions should be considered:

$$CO + O_2 \rightleftarrows CO_2 + O \qquad [25]$$

$$CO + O + M \rightleftarrows CO_2 + M \qquad [26]$$

Since these reactions are not included in our mechanism the rate of

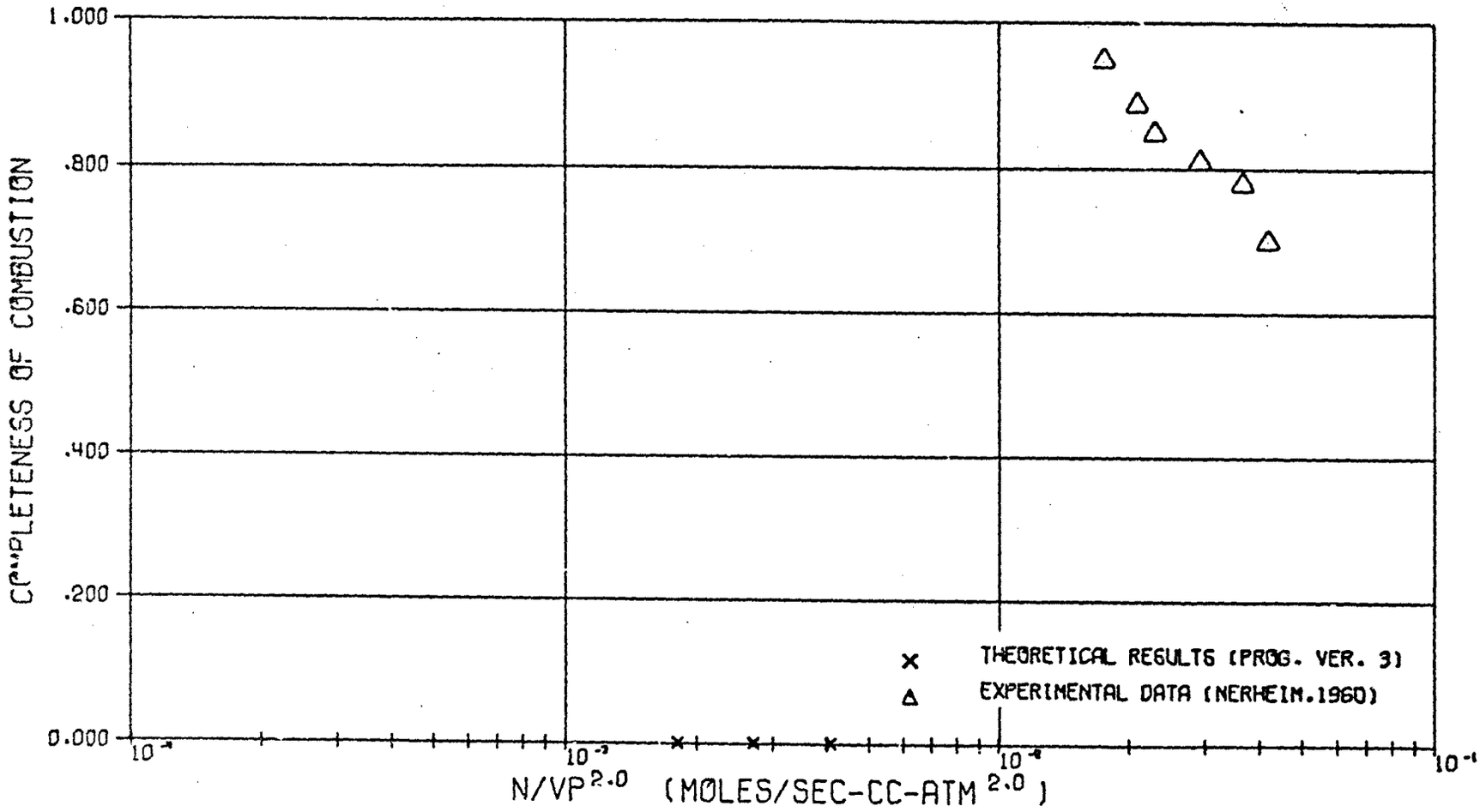

FIGURE 6 THEORETICAL STIRRED REACTOR PERFORMANCE

CARBON MONOXIDE/AIR T1= 338 (DEG K) EQUIV. RATIO = 0.43

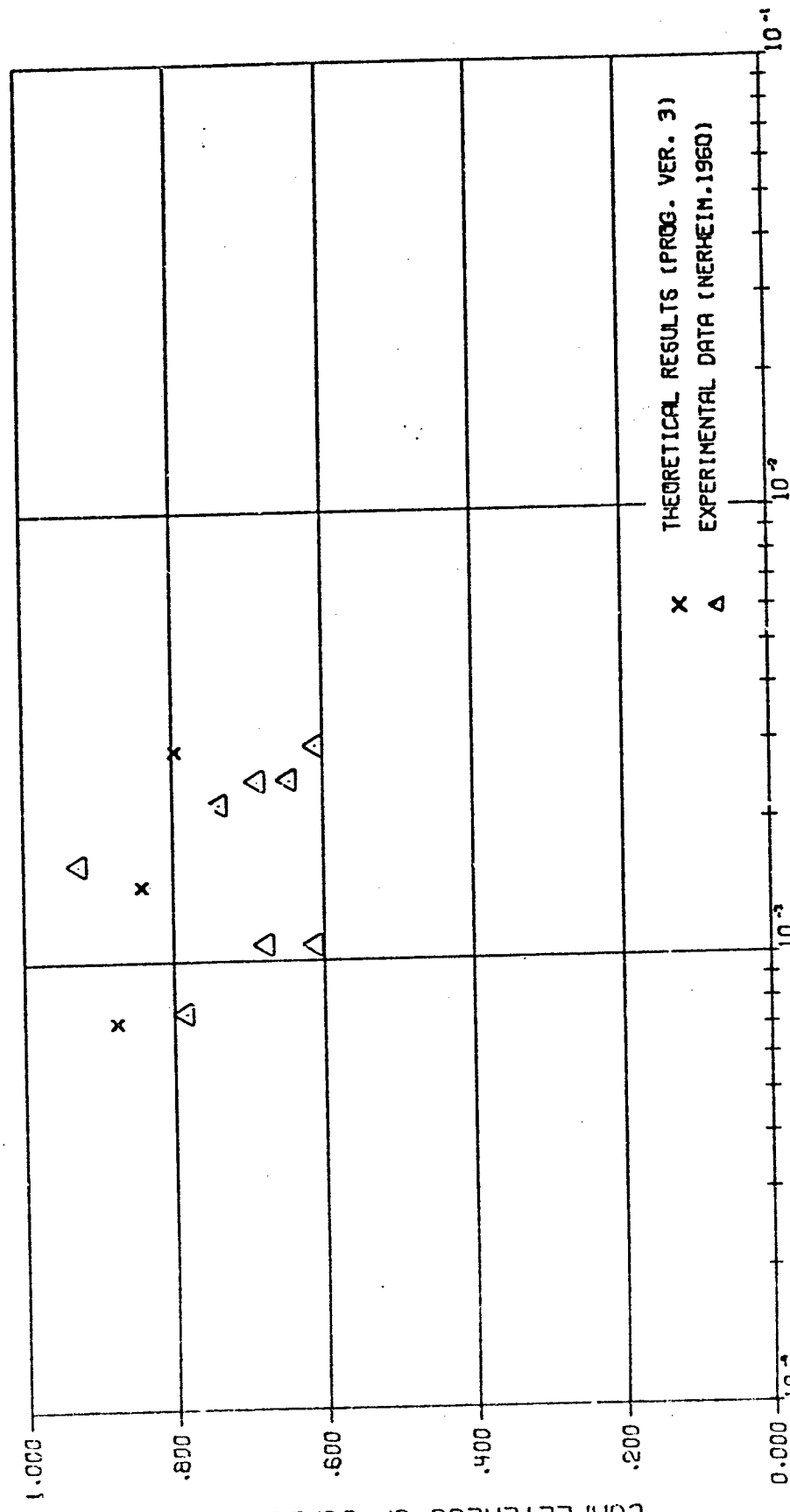

FIGURE 7 THEORETICAL STIRRED REACTOR PERFORMANCE
CARBON MONOXIDE/AIR T1= 340 (DEG K) EQUIV. RATIO = 0.59

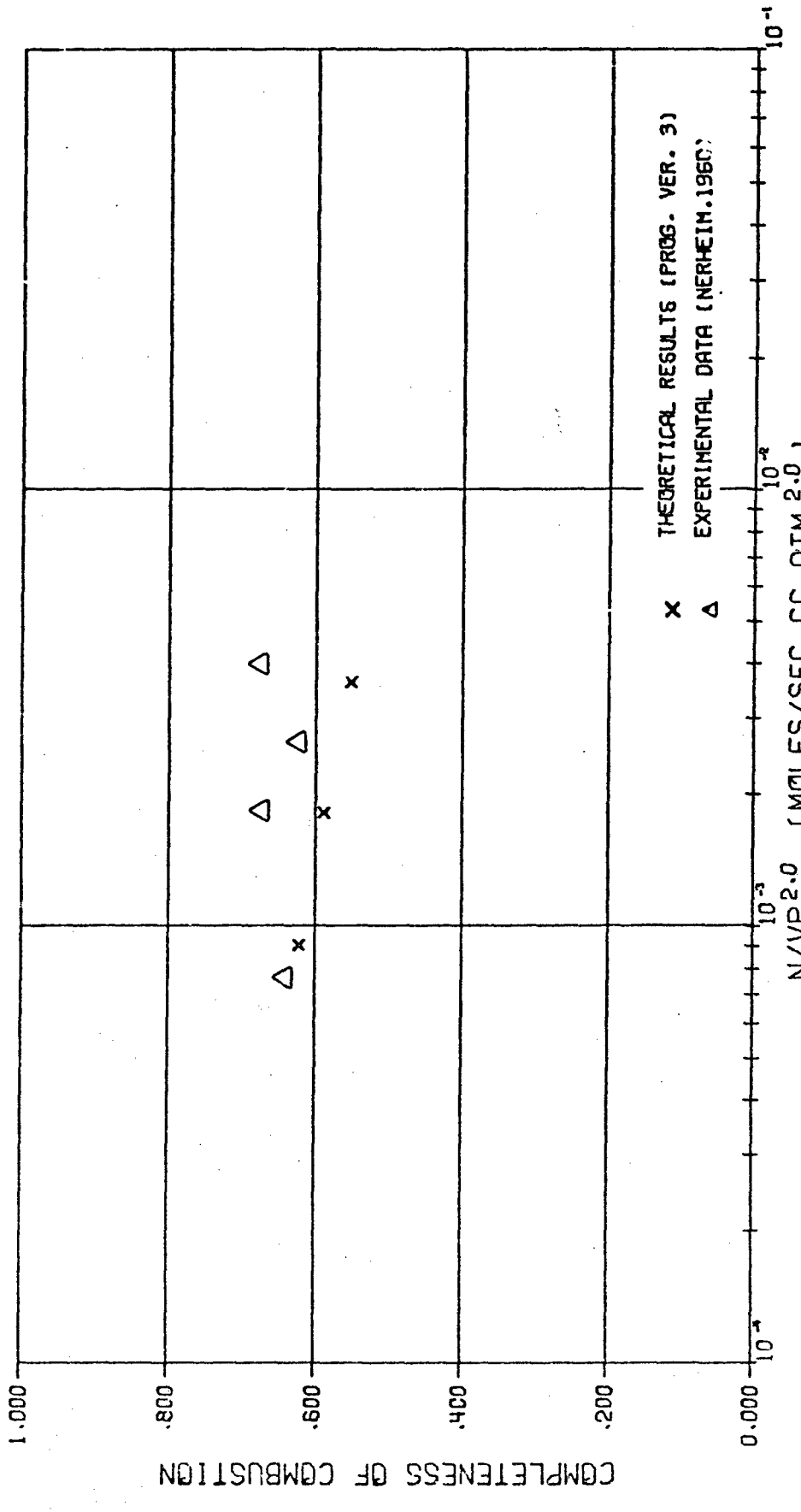

FIGURE 8 THEORETICAL STIRRED REACTOR PERFORMANCE
CARBON MONOXIDE/AIR TI= 335 (DEG K) EQUIV. RATIO = 1.30

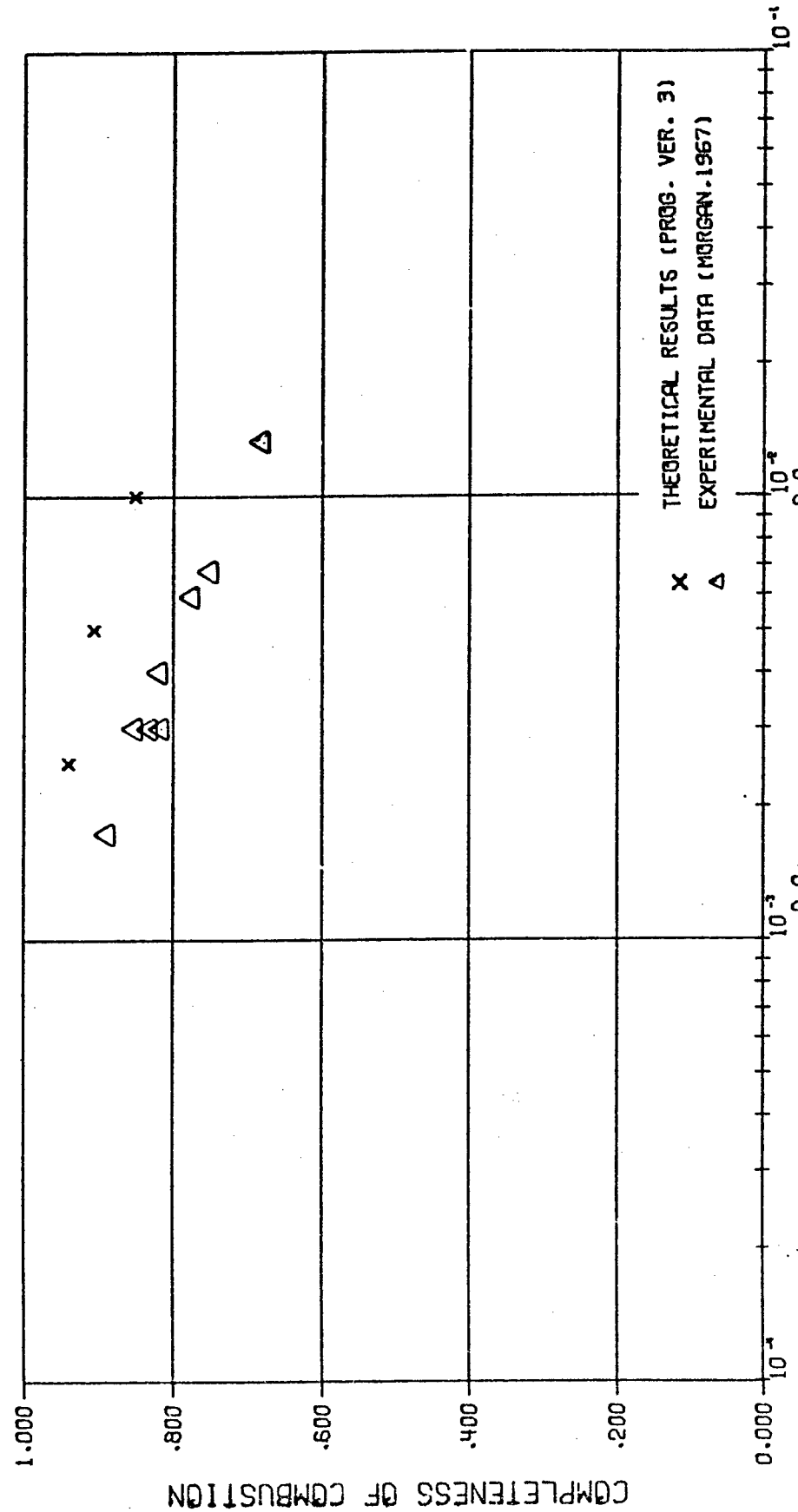

FIGURE 9 THEORETICAL STIRRED REACTOR PERFORMANCE
METHANE/AIR TI= 300 (DEG K) EQUIV. RATIO = 0.58

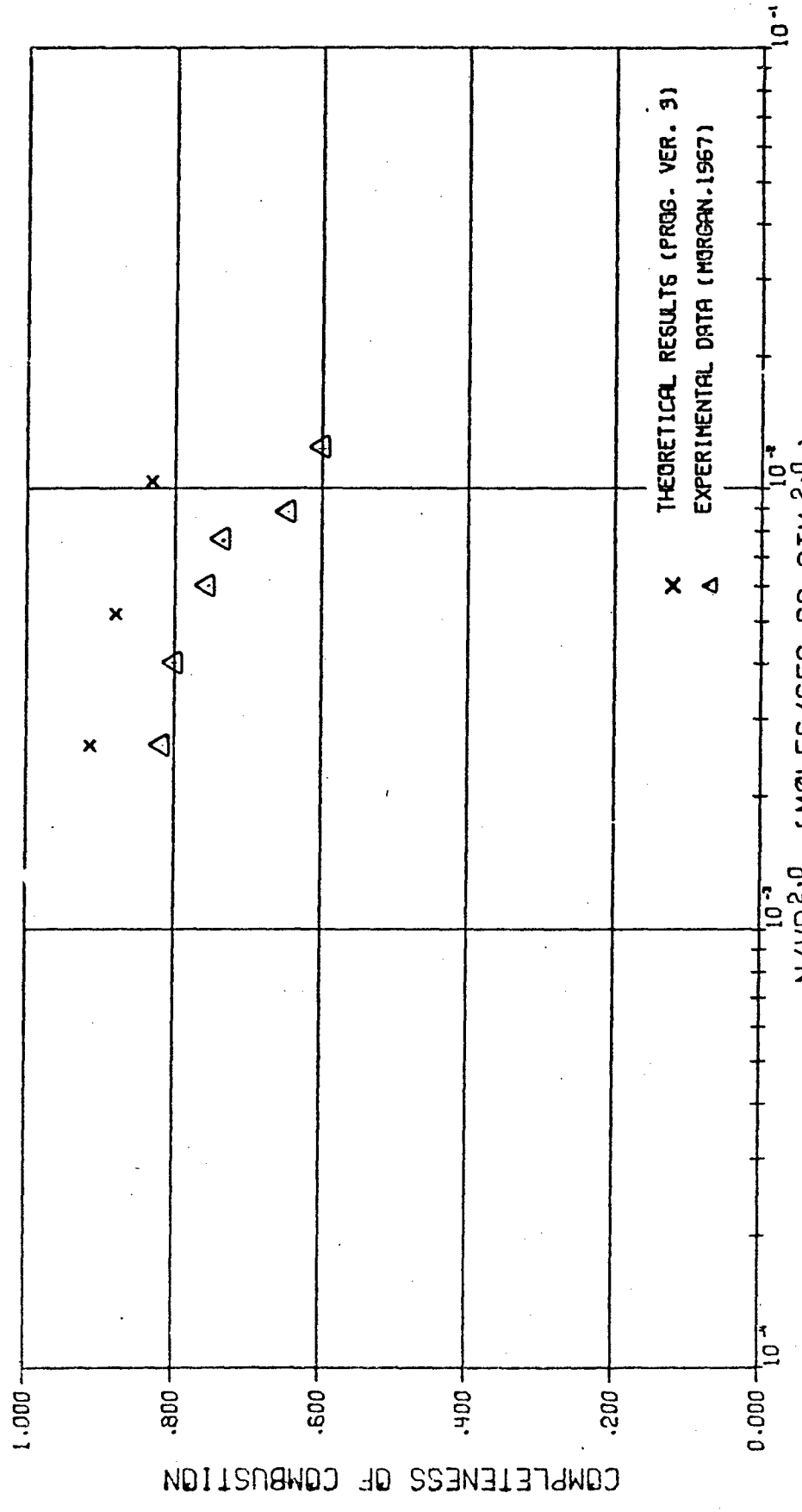

FIGURE 10 THEORETICAL STIRRED REACTOR PERFORMANCE
METHANE/AIR T1= 300 (DEG K) EQUIV. RATIO = 0.83

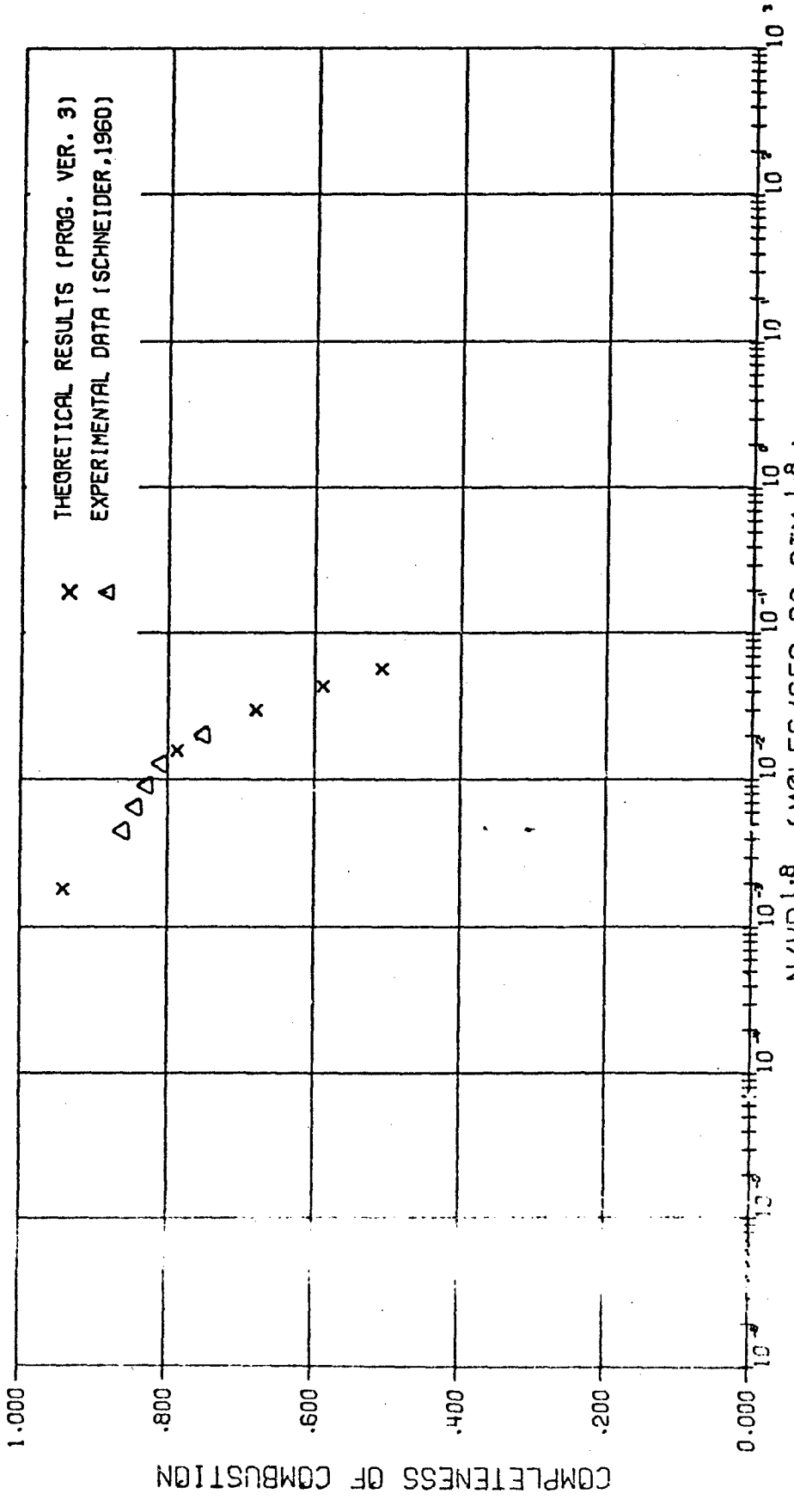

FIGURE 11 THEORETICAL STIRRED REACTOR PERFORMANCE
PROPANE/AIR T1= 460 (DEG K) EQUIV. RATIO = 0.53

carbon monoxide destruction will be underestimated as the hydroxyl radical concentration decreases. Fortunately, for the hydrocarbon/air systems we seek to model sufficient hydroxyl radical concentrations are insured by the hydrogen content of the fuel. Thus, the discrepancy evidenced is considered to result primarily from a decrease in the rate due to neglecting Reactions [25] and [26] and a reduction in the rate of Reaction [24] due to a lack of hydroxyl radicals and will therefore not be important for hydrocarbons.

Mixing in the physical system would play some role in the performance degradation of the experimental data of Figs. 8-9, but the large scatter in the experimental data makes definite conclusions difficult.

The methane/air combustion data are presented in Figs. 10-11. Although the discrepancy between theory and experiment still persists, its magnitude is somewhat smaller than for the previous data. In both cases the trends predicted are completely correct. The predicted performance for CH_4 exceeds the experimental performance as a result of assuming an infinitely fast partial oxidation step. It has been reasonably well established that Reaction [2-1] constitutes a second rate limiting step in the methane combustion process (Morgan, 1967). Therefore, the partial oxidation process cannot have an infinite rate, and as a result the predicted values are high. Mixing limitations as always could further reduce the experimental performance.

In general Reaction [2-1] has not been found to be rate-limiting in the combustion of hydrocarbons higher than methane. The assumption of an infinitely fast partial oxidation should thus improve for higher hydrocarbons. The data for propane/air combustion shown in Fig. 11 appear to substantiate this hypothesis. The agreement is extremely good over the range of the data, except for a slight deviation in the region of low loadings. This deviation is most likely a result of increased segregation in the physical system as the mixing rate decreases with decreasing flow rate.

To establish the ability of the kinetic analysis for a single stage perfectly stirred reactor to realistically predict nitric oxide formation, its predictions were compared with the aforementioned equilibrium calculations (Fig. 12). In all cases the predicted nitric oxide

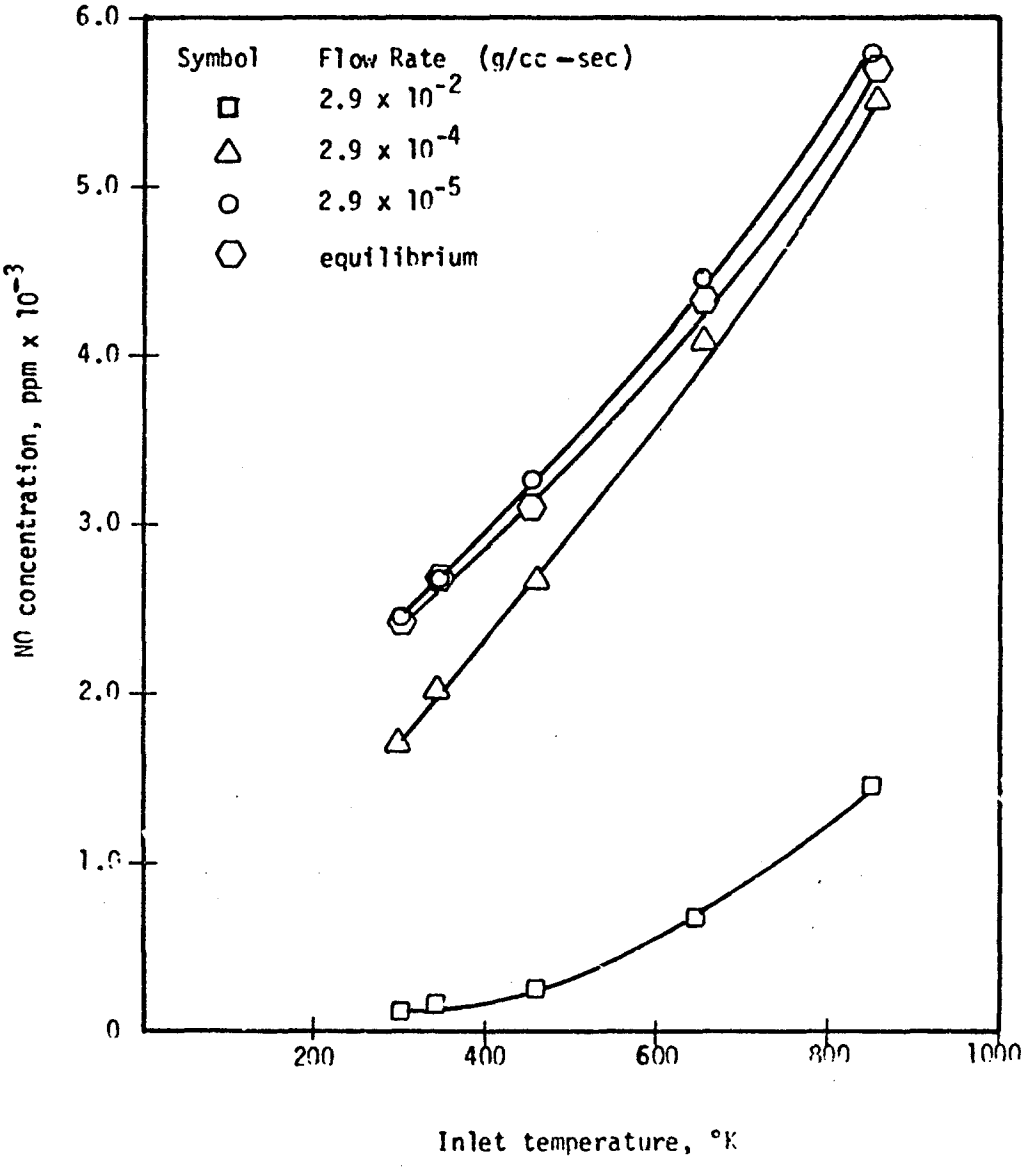

Fig. 12 Predicted exit NO concentrations for a single perfectly stirred reactor burning a propane/air mixture (ϕ = 1.0; P = 1.0 atm).

concentration increases with increasing inlet temperature, and as the flow rate is decreased the results tend toward equilibrium. At very low flows the equilibrium and kinetic curves essentially coincide; in fact, the discrepancy between them is a measure of the numerical accuracy, and is less than 1%.

In view of the good correspondence between theory and experiment for propane and the fair correspondence for methane, the analysis will be used "as is" for hydrocarbons above and including propane. Investigation of a more appropriate model for partial oxidation is continuing; however, a vast number of reactions which would seriously increase computational cost is clearly undersirable.

In all of the comparisons above mixing has been blamed for at least a portion of the discrepancy observed between theory and experiment. To further define the exact effects of mixing we now will investigate it in more detail.

CHAPTER III

THE INFLUENCE OF MIXING ON THE COMBUSTION PROCESS

The performance of any physical combustion system will be determined by the rates of two processes: chemical reaction and mixing. In the previous chapter systems having infinite mixing rates were considered. In this chapter we turn to an investigation of the effects of a finite mixing rate on such systems both through its effect on the residence time distribution and through segregation. Considering a zone of given volume, the residence time distribution gives the time which each fluid element (which may have finite or molecular size) has been in the system and the degree of segregation indicates the freedom with which these fluid elements may intermix. Each of these concepts will be considered in turn, but first it is advantageous to consider the turbulent mixing process in general.

In the theory of micro-volume combustion reviewed by Hammond and Mellor (1970a,b) it was stated that the turbulent mixing process could be characterized by the formation and subsequent decay of eddies in the flow, and this concept is useful here. These eddies are visualized as reasonably discrete aggregates of fluid which retain their identity for some lifetime determined by the turbulent parameters of the flow. If the properties inside each individual eddy are assumed to the uniform (in the limit of zero eddy volume the assumption is exact), then the segregation of the fluid is directly related to the scale of the eddies, and the decay of segregation is directly related to their lifetimes.

If in a certain flow the eddies posses infinite lifetimes, the flow is said to be completely segregated, and the fluid is said to behave as a macrofluid. On the other hand, if the eddy lifetime is zero, the flow is said to have no segregation, and the fluid is said to behave as a microfluid. The terms macromixing and micromixing have been used to describe the

accompanying mixing processes (Levenspiel, 1962). Fig. 13 shows a physical interpretation of a microfluid and a macrofluid. A quantitative definition of segregation was given by Danckwerts (1958b).

Therefore, several items must be known to completely define the mixing performance: the residence time distribution of the eddies, the rate of eddy intermixing, and the initial distribution of reactants within the various eddies. Firstly, we will consider the determination of the residence time distribution, secondly, the initial distribution of reactants, and finally, the rate of eddy intermixing.

A. The determination of residence time distributions

The residence time behavior of a system is generally described in terms of four distribution functions. These descriptions were first presented in part by Gilliland and Mason (1949, 1952) and expanded by Danckwerts (1953) and Levenspiel (1962). Any flow reactor is characterized by a certain mean residence time defined by:

$$\tau = \bar{\rho}V/\dot{m} \qquad (3\text{-}1)$$

where $\bar{\rho}$ is the mean fluid density inside the reactor, V the reactor volume, and $\dot{m}$ the mass flow rate. For further analysis it is convenient to nondimensionalize time on the mean residence time, thus:

$$\theta = t/\tau \qquad (3\text{-}2)$$

where t is dimensional time and θ is called the reduced time. Except in certain extreme cases τ is not known, since $\bar{\rho}$ is not known until the internal gas composition is known from the solution; therefore a distribution of residence times must be considered.

Intuitively one would not expect all of the fluid within the vessel to possess identically the same residence time; therefore the internal age distribution function I is defined such that $I d\theta$ is the fraction of material inside the reactor with residence time between θ and $\theta + d\theta$. Since each fluid element must possess a residence time between zero and infinity, integral of I over all time must be unity.

In an analogous manner, E, the exit residence time distribution

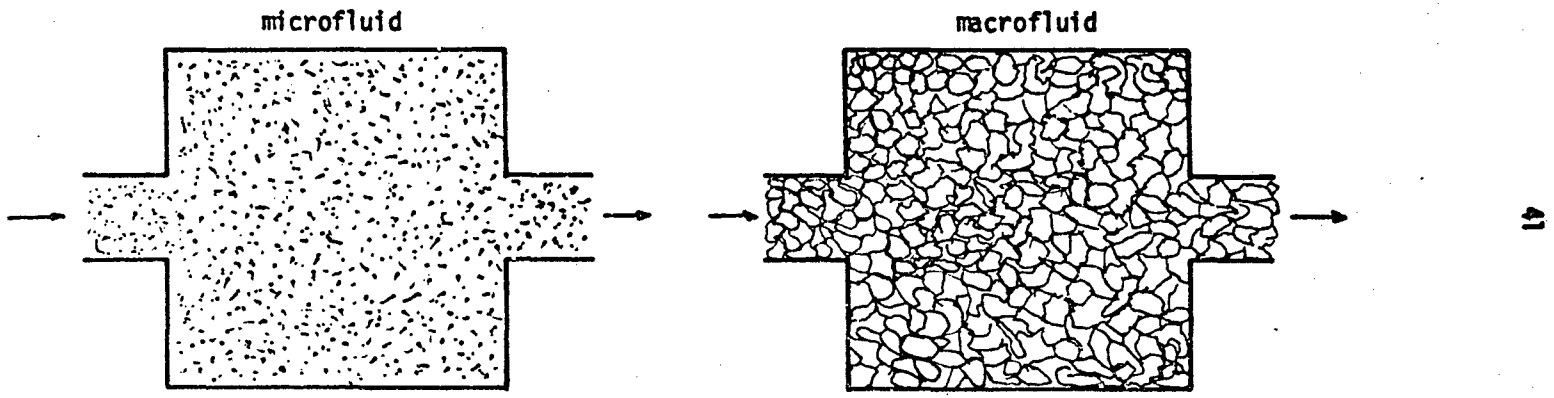

Fig. 13 Reactors containing a microfluid and a macrofluid (after Levenspiel, 1962).

function, is defined such that $Ed\Theta$ is the fraction of material leaving the reactor with residence time between Θ and $\Theta + d\Theta$. E must satisfy the same normalization condition as I. Note that in the case of complete or no segregation the E function can be used as a weighting function to integrate the set of equations defining the chemical reaction rate, thereby giving the overall performance (assuming the initial reactant distribution is known). The performance of partially segregated systems cannot be similarily obtained, since the reaction rate then also depends on the rate of eddy intermixing.

The E and I distribution functions are related to two other functions which can be evaluated experimentally. Consider now some tracer fluid whose presence can be easily detected. The F function is defined as the nondimensional tracer concentration response to a unit step function tracer input. Similarily, the C function is the nondimensional tracer concentration response to a unit delta function tracer input. The derivation of the following relations among these functions is straightforward and will not be repeated here (for details see Levenspiel, 1962 and Danckwerts, 1953):

$$F + I = 1 \tag{3-3}$$

$$C = E \tag{3-4}$$

$$E = \frac{dF}{d\Theta} \tag{3-5}$$

The I, F, and E functions for the two idealized cases of perfectly stirred flow and plug flow are shown in Figs. 14 and 15, respectively, both for a unit step input function. As pointed out by Levenspiel (1962), and E and F functions are not sufficient to ascertain the segregation of the system. Only in the extreme of complete segregation can the residence time distribution derived with the aid of the F and C functions be interpreted as the eddy residence time distribution, because only in this case does an eddy retain its identity as a discrete fluid element.

Two basic models have been developed to treat the effects of

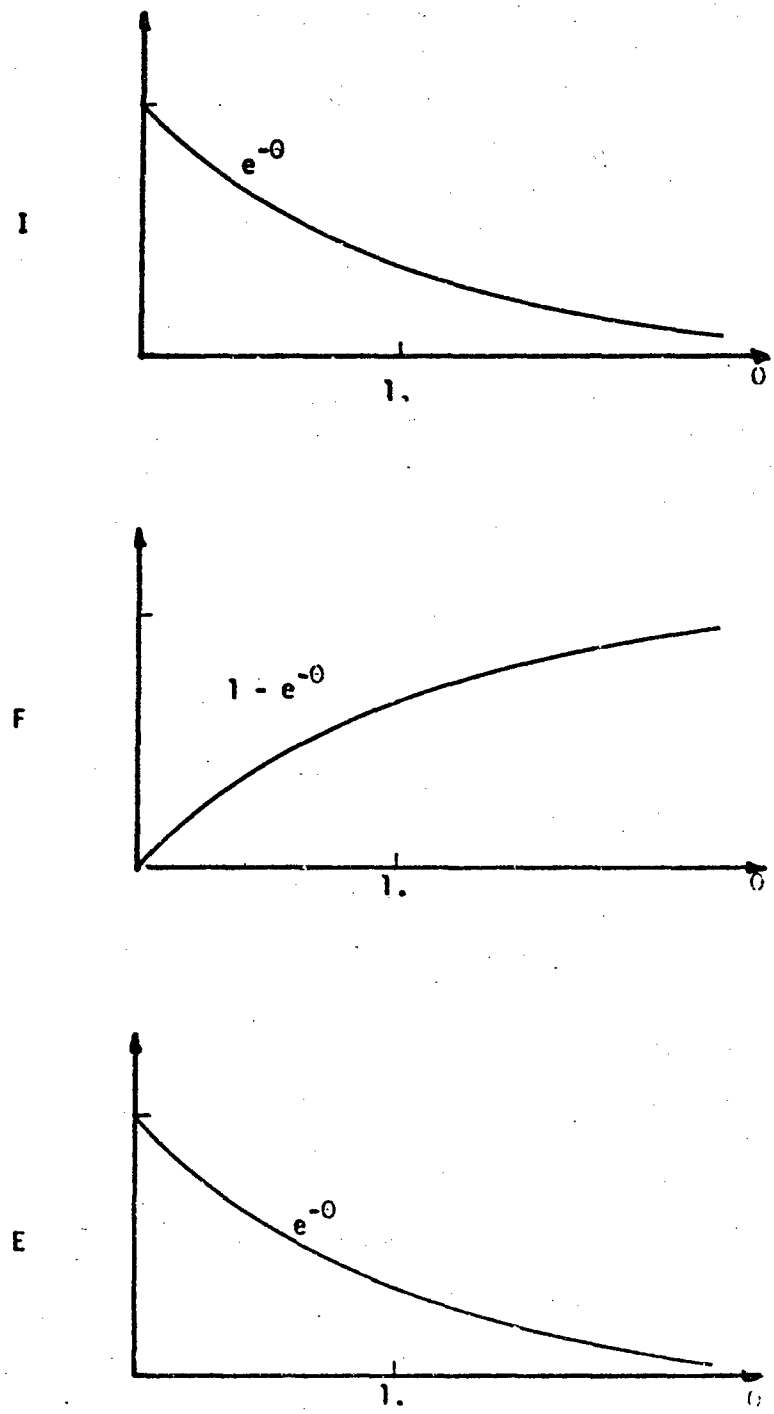

Fig. 14 I, F, and E functions for a perfectly stirred reactor (after Levenspiel, 1962)

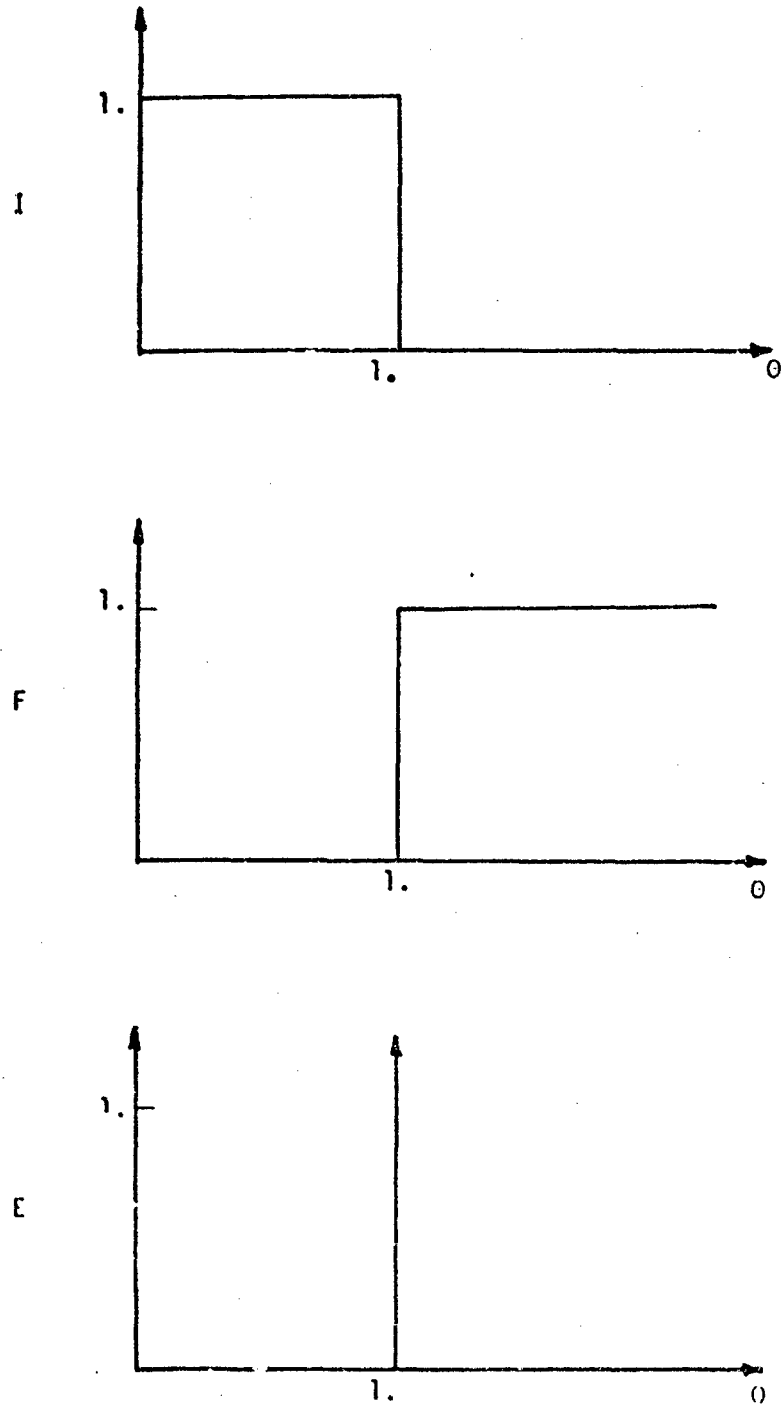

Fig. 15 I, F. and E functions for a plug flow reactor (after Levenspiel, 1962).

imperfect mixing on the residence time distribution functions. The first is called the dispersion model (Levenspiel, 1962) and treats mixing as a deviation from ideal plug flow. Considering a reactor of characteristic length L through which fluid passes with a bulk velocity U, the action of turbulent and molecular transport will certainly act to produce some mixing in the flow direction of fluid elements having different residence times. Danckwerts (1953) derived an analytical form for the F function from which the E function can be obtained as:

$$E(\theta) = \frac{1 + \theta}{4\theta\sqrt{\frac{\pi\theta D}{LU}}} \exp\left[-\left(\frac{1 - \theta}{2\sqrt{\frac{\theta D}{LU}}}\right)^2\right] \qquad (3\text{-}6)$$

where D is a turbulent mass diffusivity. Eqn. 3-6 applies for the case $4D/LU << 1$. The form of the E function is more clearly shown in Fig. 16, and the predicted deviation from plug flow can be seen. The figure shows that for $D/LU = 0$ the E function is that of plug flow, and for increasing D/LU the function deviates more strongly from that for plug flow. The complete range of mixing from plug to perfectly stirred flow cannot be predicted because the solution is restricted to $4D/LU << 1$ as noted.

The second model, called the tanks-in-series model, approximates mixing as a deviation from perfectly mixed flow. After Levenspiel (1962), the reactor to be modelled is divided into a series of equal volume zones which are perfectly stirred reactors. The predicted E function is:

$$E(\theta) = \frac{N^N \theta^{N-1}}{(N-1)!} \exp(-N\theta) \qquad (3\text{-}7)$$

where N is the number of zones. The E function for this model is shown in Fig. 17. Note that the full range of behavior from perfectly stirred ($N=1$) to plug flow ($N\to\infty$) can be predicted. Therefore, this model is better from a practical viewpoint than the dispersion model.

The previous two models are used in practice either by arbitrarily setting the value of D/LU and N or by using these values as parameters to curve fit experimental data. In general, these models alone are not

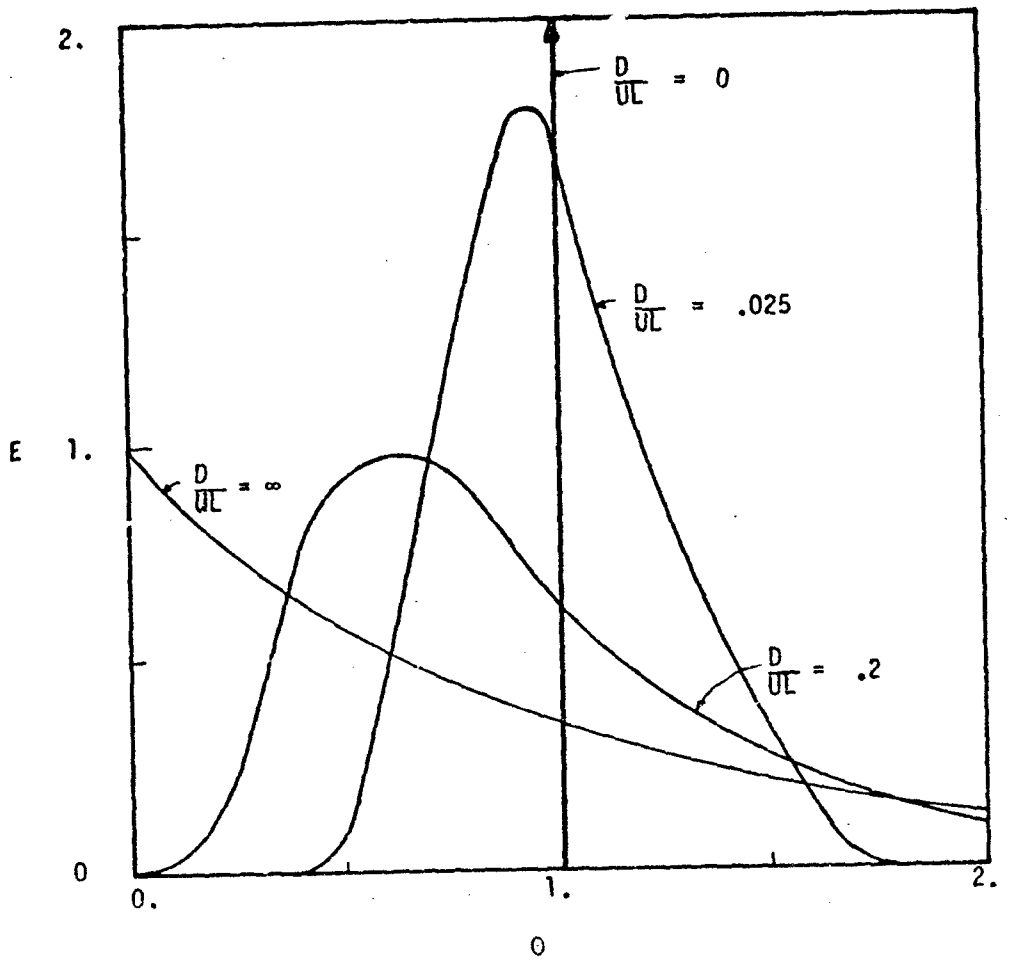

Fig. 16 The E functions predicted by the dispersion model (after Levenspiel, 1962).

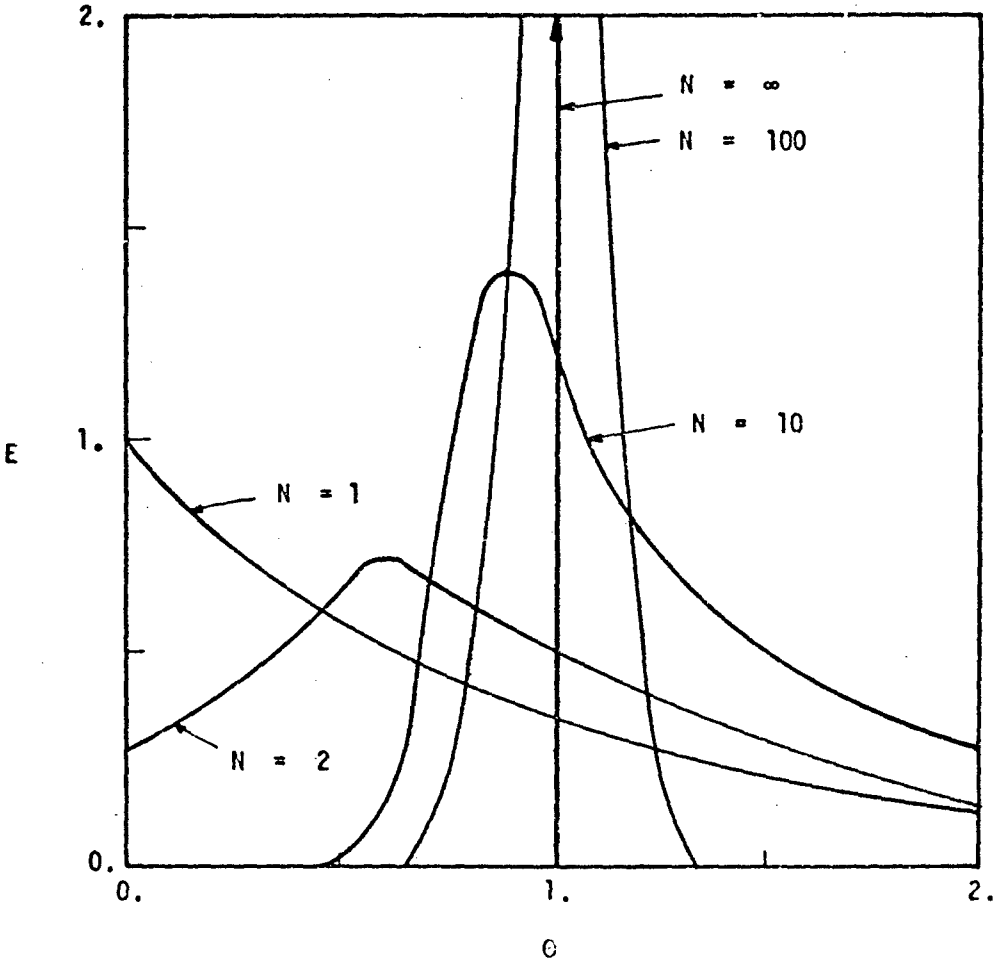

Fig. 17 The E functions predicted by the tanks-in-series model.

sufficient to model a combustor. By using various combinations of these models in conjunction with pure plug and perfectly stirred flow, bypass flow, and recirculation flow one can approximate a known residence time distribution. Two major difficulties remain, however: 1) these results are useful only if complete or no segregation is assumed; 2) unless the volumes and flows are arbitrarily assigned a model cannot be formulated without testing a physical system.

As a direct result of the two difficulties mentioned above, all current models attempting to predict the various residence time distribution functions for practical systems are either purely postulative or of a semi-empirical nature. We propose to discuss only the most promising models here.

Beér and Lee (1965) derived an empirical residence time distribution for the IJmuiden tunnel furnace using a 1/10 scale water model with salt tracer. The system was essentially a confined, cylindrical, swirling jet. They were able to approximate their experimental F functions by a perfectly stirred and a plug flow reactor in series. The fraction of total residence time (and hence total volume) devoted to perfectly stirred flow was determined as a function of the swirl number:

$$S = \frac{G_\phi}{G_x r_o} \qquad (3\text{-}8)$$

where G_ϕ is the total swirl angular momentum, G_x is the total axial linear momentum, and r_o is the inlet jet radius. This function is shown in Fig. 18. With no swirl the ratio has a value of 0.5 and shows a rapid decrease with increasing S up to a value of S = 1.0. For S > 1.0 the fraction devoted to perfectly stirred flow increases steadily. Beér and Lee explain their curve from the following sequence of physical events involving a wall and a central core recirculation zone. Initially a recirculation zone is formed along the chamber walls due to the entrainment effect of the jet. Viewing the jet as devoted primarily to plug flow and the recirculation regions to perfectly stirred flow, the initial increase in swirl serves only to increase the jet spread angle reducing the wall recirculation zone volume with-

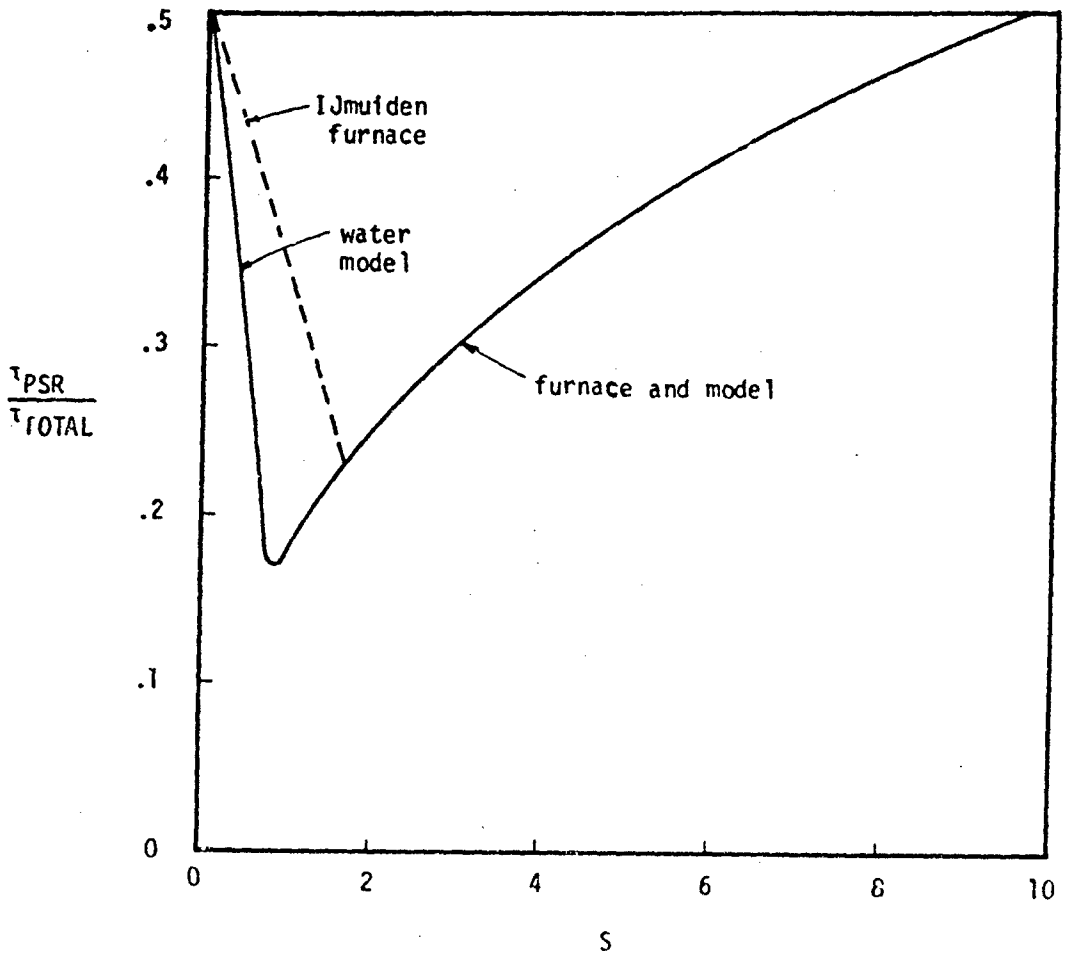

Fig. 18 Residence time fraction devoted to perfectly stirred flow (Beér and Lee, 1966).

out forming the central recirculation zone. Hence, a drop in perfectly stirred volume occurs. At S ≃ 1 the central recirculation zone starts to form (Chigier and Chervinsky, 1967) due to the radial pressure gradient and increases in size with increasing S; therefore the net perfectly stirred volume increases. Using this model Beér and Lee obtained reasonable agreement with experiment.

Pratt (1970) also considered a confined, swirling jet. He used the empirical recirculation model of Thring and Newby (1953) as modified by Field et al. (1965) and the mass entrainment function of Kerr and Frazer (1965). By considering differential equations for the conservation of a tracer substance he indicated how to evaluate the F function for the jet. He was able to predict a characteristic delay time θ_d which is the time of first change in the F function to some input and noted that it should correspond to the volume fraction devoted to plug flow as defined by Beér and Lee (1965). His work was restricted to low swirl (S < 1), but fair agreement with the data of Beér and Lee was obtained in that range.

Crowe and Pratt (1970) studied the conical reactor of Jain and Spalding shown in Fig. 19. Following Jain and Spalding, they defined a certain fraction R of the inlet flow which recirculates inside the reactor. Using the analysis of Pratt (1970) they predicted the F functions of the system (Fig. 20). The net result is a one parameter model for the residence time distribution since R cannot be predicted. The advantage of this model is that it predicts a characteristic delay time.

The two parameter recirculation model of Hottel et al. (1958) was discussed in previous work (Hammond and Mellor, 1970a, b). It was shown to predict a wide variation in mean residence time but always predicts a zero characteristic delay time.

In summary, we see that the residence time distribution functions can be approximated using a number of various models having one or more parameters, but that no priori analyses exist. We now consider determining the initial distribution of reactants.

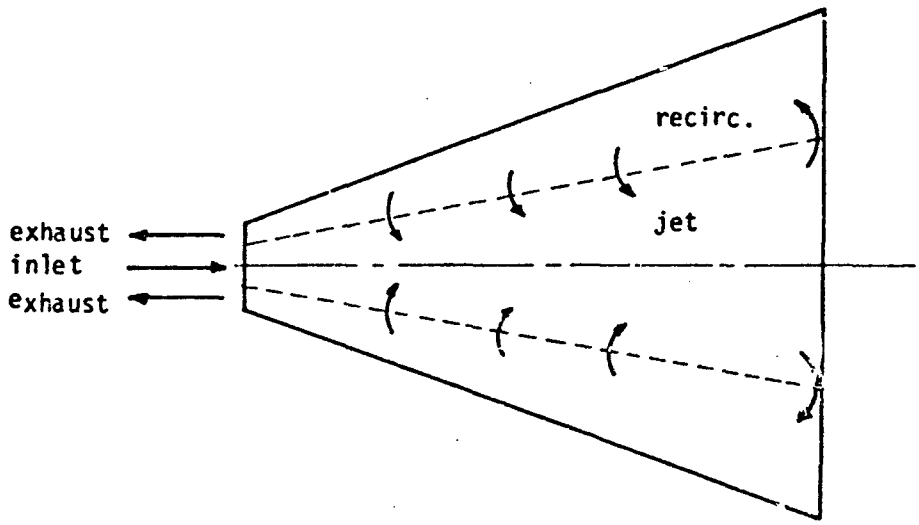

Fig. 19 The conical combustor of Jain and Spalding (1966).

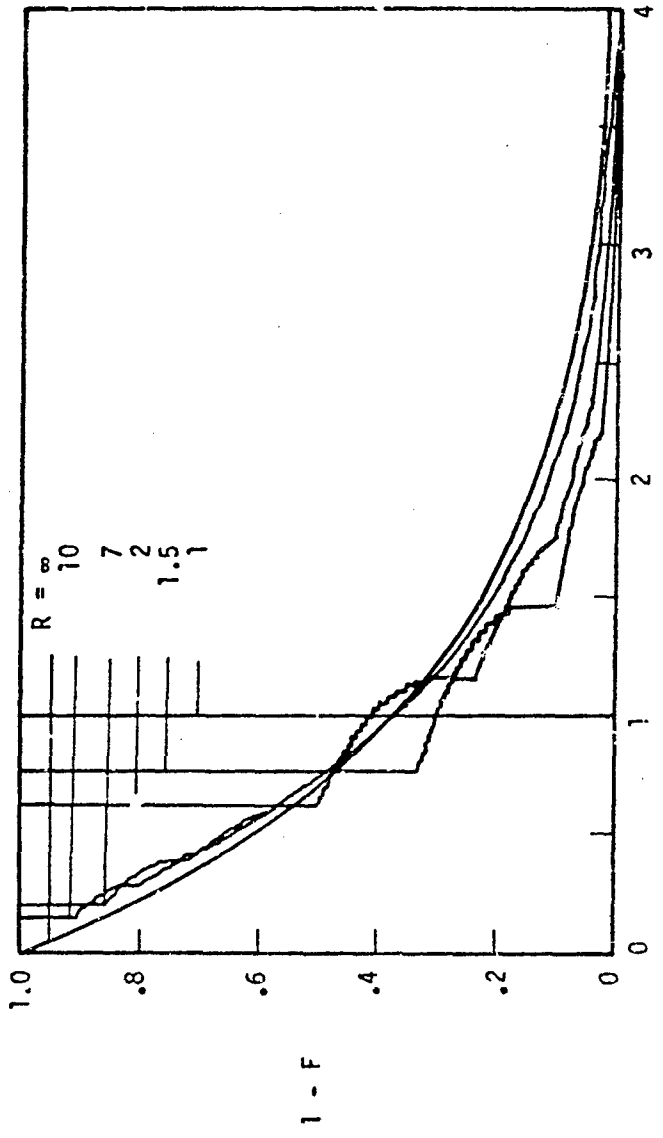

Fig. 20 Predicted F functions of Crowe and Pratt (1970).

B. The determination of the initial distribution of reactants

Currently only two attempts have been made to model the initial distribution of reactants. The first is a three parameter permutation of the recirculation model of Hottel el al. (1958) which has an additional fuel injection point (Fig. 21). Since each reactor is assumed to be micromixed, in essence two large "eddies" are considered.

Fletcher and Heywood (1971) modelled the primary zone of a gas turbine combustor as a single, completely segregated perfectly stirred reactor. At the reactor inlet a certain normal distribution of equivalence ratio was assumed, and both the mean and standard deviation could be varied arbitrarily. A normal distribution was chosen, apparently from consideration of fuel spray characteristics.

C. The determination of the rate of eddy intermixing

The rate of eddy intermixing is important in evaluating reactions in partially mixed flows since it is the single mechanism for bringing reactants together. The eddy mixing or lifetime problem has been discussed by Hammond and Mellor (1970a,b).

Fletcher and Heywood (1971) attacked the problem by assuming that the eddy decays over some arbitrary length, and at the end of that length the flow is micromixed. This was accomplished by forcing the standard deviation of their species concentration distributions to zero.

Summarizing the net contributions of all these mixing models we see that:

1) the exit residence time distribution function can be determined working from semi-empirical equations;

2) the initial distribution of reactants is usually assumed to be uniform, but in some cases an educated guess at a distribution can be made;

3) some sort of eddy intermixing function must be assumed.

We must now consider how this limited knowledge of mixing may be applied to aid performance predictions in a practical combustion system.

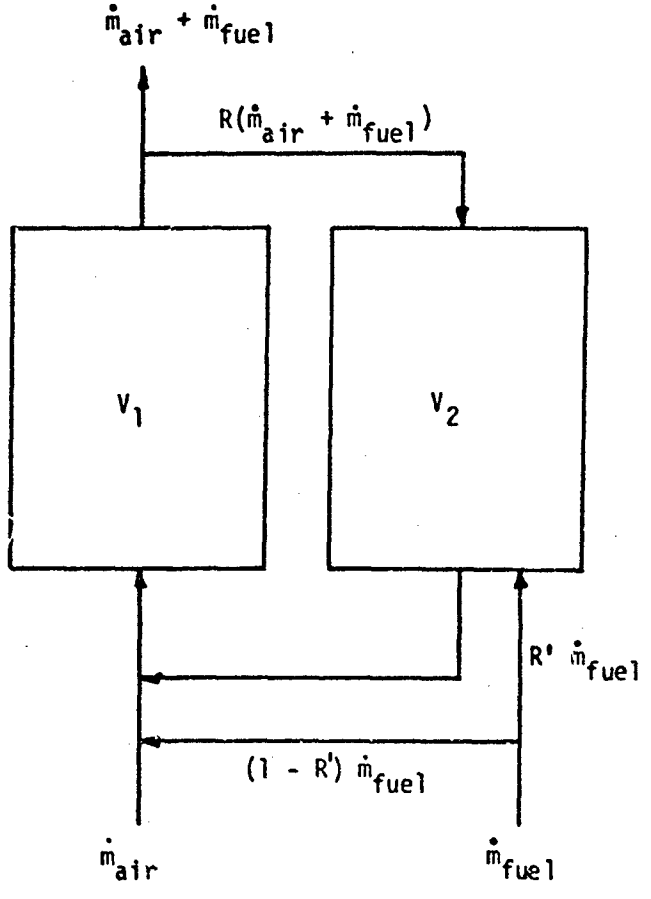

Fig. 21 Recirculation perfectly stirred reactor model with inlet fuel distribution (after Hottel et al., 1958).

CHAPTER IV
DEVELOPMENT OF AN ANALYTICAL GAS TURBINE COMBUSTOR MODEL

The previous two chapters have been devoted to detailed investigations of the two rate processes which interact to define the overall behavior of any physical combustion system. It now remains to assemble the results of these two studies into an integrated and workable form for application to the problem of analytically modelling gas turbine combustors. To elucidate the most realistic merging of mixing and kinetics, the physical characteristics of gas turbine combustors will be examined.

A. Pertinent physical and flow processes in gas turbine combustors

The configuration of a representative gas turbine combustor is shown in Fig. 22 and the flow pattern is schematically indicated. For tubular and tuboannular configurations the figure shows a centerline cross-section of the axisymmetric configuration; for an annular configuration the section is taken on a plane passing through the engine centerline and the combustor is considered to be two-dimensional. For either case the essential features of the flow pattern and the discussion which follows are identical.

Consider first the primary zone of the combustor which is taken as the volume contained in the flame tube from the start of the combustor up to the centerline of the first row of penetration holes. There may or may not be some addition of film cooling air in this zone. Examining the schematic flow pattern in this zone and the experimental flow pattern of Hiett and Powell (1962) shown in Fig. 23, it is apparent that the primary zone contains a complex recirculating flow pattern. Also all of the fuel is injected in this zone and must mix with the available air and hot gases.

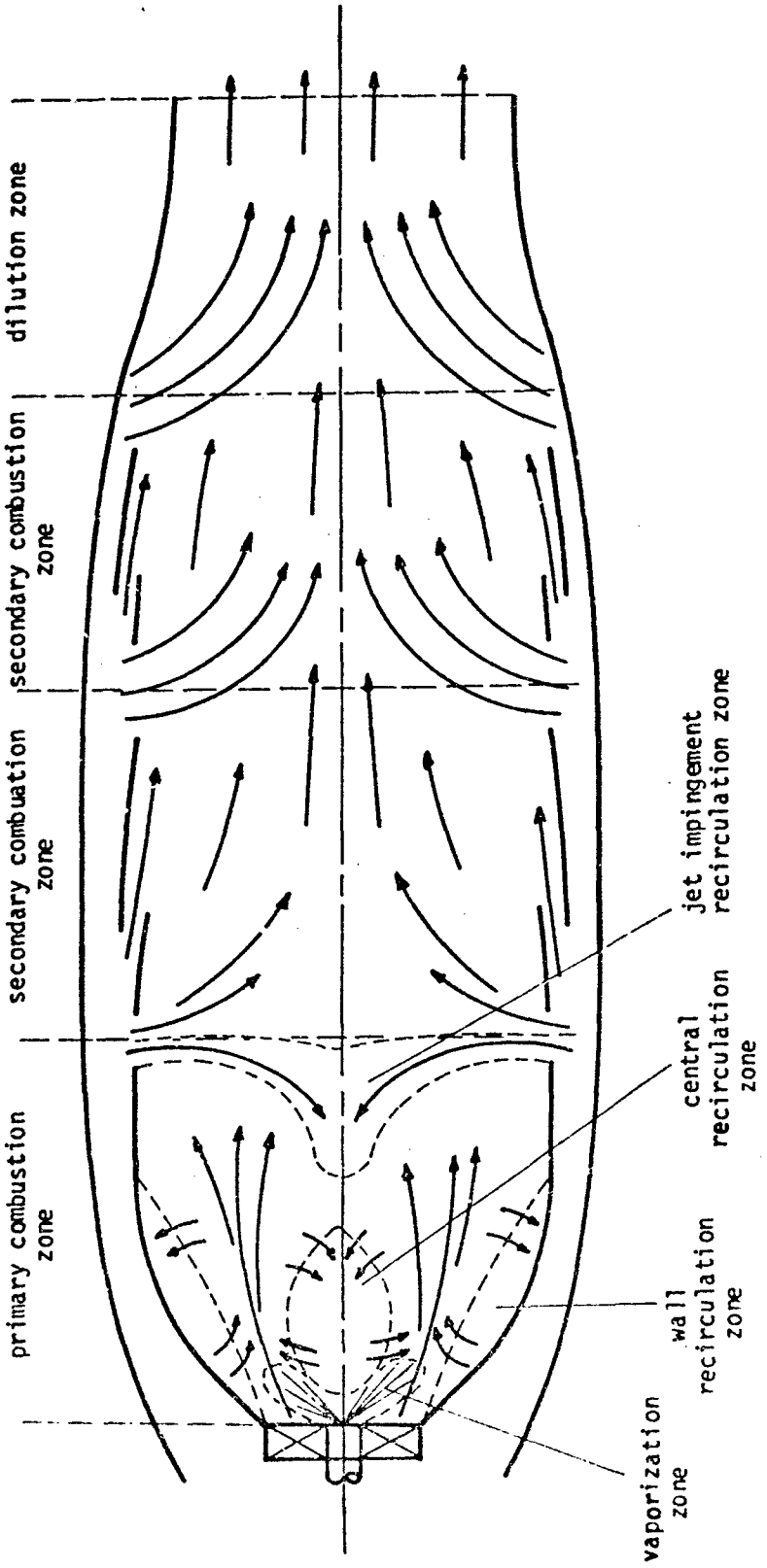

Fig. 22 Typical combustor cross-section showing various flow regions

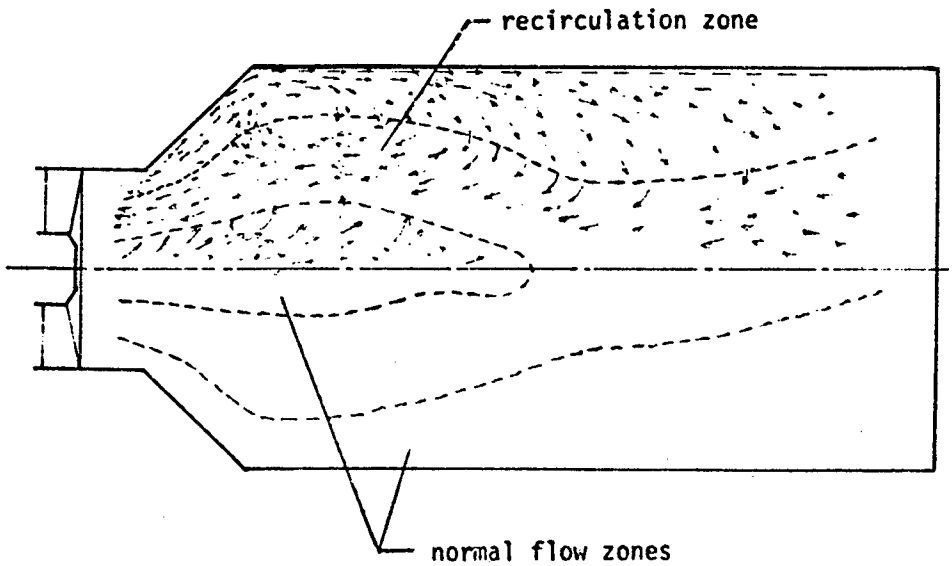

Fig. 23 Experimental primary zone flow pattern
(Hiett and Powell, 1962)

Heywood et al. (1970) view the fuel evaporation and mixing process as proceeding with negligible combustion until the fuel is in the vapor phase entirely. They postulate an extremely fuel rich region close to the injector where the atomized fuel spray droplets evaporate. No combustion is allowed in this region due to a lack of air as well as the postulate that the fuel drops have such a large velocity relative to the gas phase that a droplet type diffusion flame cannot be sustained. The size and shape of the vaporization zone will of course depend on the injector and swirler characteristics. Both the swirler air and recirculating hot gases entrain vaporized fuel from this region, and thus combustion takes place predominantly in the homogeneous mode. The initial distribution of vaporized fuel over the combustor cross section will determine the initial concentration distribution function. Heywood and Fletcher (1971) assumed this to be a normal distribution as mentioned previously; unfortunately this is the only available solution at present. In consensus, this treatment of vaporization and mixing implies that the actual rate of vaporization is not important and that the only significant parameter is the initial distribution. The effects of finite evaporation rates have been studied qualitatively by Lefebvre (1966, 1967).

Although the actual primary zone flow pattern is heavily dependent on the physical configuration of the flame tube in the area (the swirler-injector assembly and the first row of secondary air penetration holes), three distinct recirculation modes can usually be defined;

1. a reverse flow zone established along the flame tube wall as a result of the abrupt increase in diameter of the flame tube over that of the swirler;
2. a central core reverse flow zone established by the adverse centerline pressure gradient set up by swirl (in some cases this zone becomes annular as a result of injector interference);
3. a centerline reverse flow at the downstream end of the primary zone resulting from the central impingement of the first row of secondary air penetration jets (in some cases this merges with the reverse flow central core).

A similar division is made by Way (1955). To reasonably model the

primary zone each of these flow reversals must be investigated.

The first type of recirculation was considered by Pratt (1970) and results primarily from the inability of the inlet jet to follow the initial flame tube wall contour. This behavior leaves a "dead" zone or recirculation region adjacent to the flame tube wall from which fluid is entrained by the inlet jet, thus establishing a recirculating flow. His predictions for this situation were discussed previously. This mode of reverse flow would be expected to diminish with increasing swirl of the inlet jet since the jet will thus spread faster and reach the flame tube wall sooner reducing the available recirculation volume. Decreasing the abruptness of the initial flame tube wall contour and increasing the ratio of swirler diameter to initial flame tube diameter will also diminish the magnitude of this recirculation mode. Therefore, it is reasonable to neglect this mode except for combustors with low swirl ($S < 1$), abrupt initial flame tube contours, and small inlet jets.

The second mode of recirculation which occurs at high swirl can assume two forms: the first a reverse flow zone along the centerline of the combustor and the second an annular recirculation zone with flow occurring in the normal direction in the center. The first form of recirculation was observed experimentally by Gradon and Miller (1967), Cooper and Marek (1965), and Chigier and Chervinsky (1967). Chigier and Chervinsky covered the low swirl range up to $S = .64$ which marked the onset of centerline reverse flow; they were able to correlate their axial velocity profiles as error curves. Pratt (1970) outlined an analytical technique for determining the tracer response characteristics for this case, but no empirical or analytical solution has been found. The central core recirculation is usually evidenced in gas turbine combustors.

The annular type of recirculation was observed experimentally by Hiett and Powell (1962). This type of recirculation (Fig. 23) appears to result from the influence of the fuel injector flow which penetrates the center of the reverse flow region establishing normal flow along the centerline. When air-atomizing fuel injectors are used with high air flows this type of flow is likely.

The third mode of reverse flow is distinct from the other two which

recirculate hot, reacting gases. In this mode fresh secondary combustion air is forced upstream as a result of penetration jet interaction. The fraction of secondary air flow directed into the primary zone was given empirically by Rosenthal (Anon. 1968) as:

$$\frac{\dot{m}_{S,P}}{\dot{m}_S} = 0.5 \sin \phi \left(\frac{T_S}{T_P}\right)^{1/2} \qquad (4\text{-}1)$$

where ϕ is the penetration jet angle, T_S is the jet temperature, and T_P is the mean primary zone temperature.

Verduzio and Campanaro (1969) performed a theoretical analysis of the secondary jet recirculation in tubular combustors by solving the axial momentum equation for jet impingement. Their equations are too numerous to be presented here, but the analysis showed that the fraction of recirculated flow is dependent on the ratios of jet and primary mass flows and densities, the primary zone equivalence ratio, and the ratio of secondary hole diameter to flame tube diameter. They were also able to show good agreement with experimental data. The flow pattern of Fig. 23 shows this type of reverse flow, and in general one would expect it to be significant in gas turbine combustors.

The primary zone of gas turbine combustors will be dominated by the latter two recirculation modes. Of these two modes the secondary jet impingement reverse flow is fairly well understood both analytically and empirically, while the central recirculation for realistic values of swirl is poorly understood. The lack of good definition of these primary zone flows will necessarily hamper the primary zone modelling effort.

The secondary combustion zones do not exhibit any reverse flow regions (or other peculiarities) and the problem here reduces to modelling the turbulent mixing of the secondary and dilution air jets and cooling jets with the reacting main flow inside the flame tube. Turbulent jet mixing has been studied predominantly by empirical techniques. A good summary of the available empirical results is presented in the work of N.R.E.C. for NASA Lewis Research Center (Anon., 1968), and we will utilize their results for computing the rate of air addition in the secondary zones. A typical analytical jet mixing approach is

given by Hubble (1967).

We do have available a computer program from NASA Lewis Research Center (Anon. 1968) capable of accurately predicting the air flow and pressure distributions for a gas turbine combustor (Tacina and Grobman, 1969). This program has three major limitations which restrict its utility from a practical viewpoint:

1. The primary zone is treated as a single stirred reactor;
2. The flow inside the flame tube is considered as being one-dimensional;
3. The fraction of fuel consumed as a function of axial position in the combustor must be input.

If our combustion model can predict the fuel consumption function accurately, the error incurred in the airflow and pressure distributions from the first assumption will be reduced. It is possible that an inter-program iteration will be required if the predicted airflow distribution is heavily dependent on the fuel consumption function, but presently this is not thought to be necessary. Since this program can compute the air addition by various jet mixing models, a realistic estimate of the air available for combustion can be incorporated into the combustion model. A major difficulty in this program is that it considers only the third recirculation mode and completely neglects the primary zone flow structure.

We have now considered the major flow characteristics found in gas turbine combustors, at least qualitatively. The accurate airflow and pressure distributions predicted by the NASA combustor analysis program can be used as input to the combustion model. It remains to formulate an overall combustion model incorporating a realistic primary zone model and integrating the predicted airflow distribution with the reaction kinetics in the secondary combustion zones.

B. A refined analytical gas turbine combustor model

It has been previously postulated that as a direct result of the high turbulence level present in gas turbine combustors and the correspondingly high mixing rate that certain zones inside the flame tube could approach the stirred reactor in behavior. By considering the overall features of the flow pattern these zones were connected to

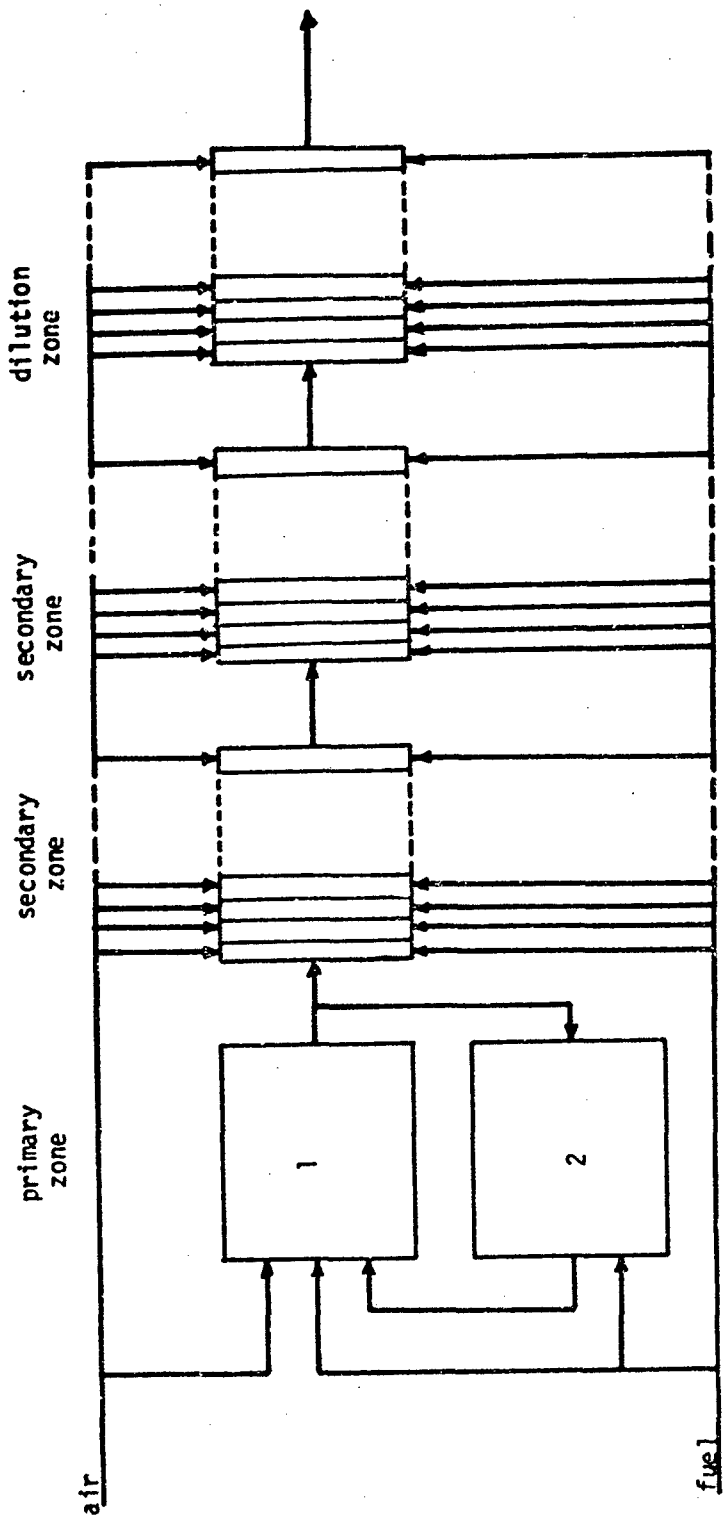

Fig. 24 Overall model of the combustion process in gas turbine combustors.

form an overall combustor model (cf. Hammond and Mellor, 1970a,b). The basic overall model has subsequently been refined to reflect the results obtained in the previous chapters, and this refined model will be presented here. The refined model is shown schematically in Fig. 24.

The primary zone model remains much the same; however an additional fuel inlet into the recirculation reactor is considered after Hottel et al. (1958). The additional fuel distribution point permits studying the effects of the initial reactant distribution. Addition of fuel into both zones more closely corresponds to the physical situation in which fuel vapor is entrained by both swirler air and hot recirculating gases. The two reactor structure is retained for simplicity with the main flow reactor accounting for reaction in flow of the normal direction, and the single recirculation reactor must account for the reaction in all three possible recirculation flow zones. Note that although this model can predict a wide variation in primary zone residence times and some variation in initial reactant distributions, it lacks the ability to predict a characteristic delay time as observed by Beér and Lee (1965). This deficiency can be easily rectified by the inclusion of a series plug flow reactor in the primary zone or by the recirculating plug flow pair of Morgan (1967) shown in Fig. 25. The ability of the recirculation pair model to predict flame stabilization phenomena has been discussed previously (Hammond and Mellor, 1970a,b; Hottel et al., 1958).

Our model of the secondary combustion zones has also been slightly altered. Each of the "plug flow reactors" is now modelled as a sequence of perfectly stirred reactors of finite and equal volume. Altering the reactor volumes gives a variation in the residence time distribution as discussed in the tanks-in-series model, since the standard deviation of the residence time distribution depends on the number of reactors incorporated in a given volume (cf. Eqn. 3-7). Each individual perfectly stirred reactor now has its own discrete amount of air and fuel addition; therefore the predicted mixing behavior can be altered by changing the fuel distribution function. The semi-continuous air additions permit closer approximations of the airflow distribution computed using turbulent jet mixing phenomena. This is particularly important when considering film-cooled combustors. By varying the volumes of the perfectly stirred reactors, the spread (or deviation) of the

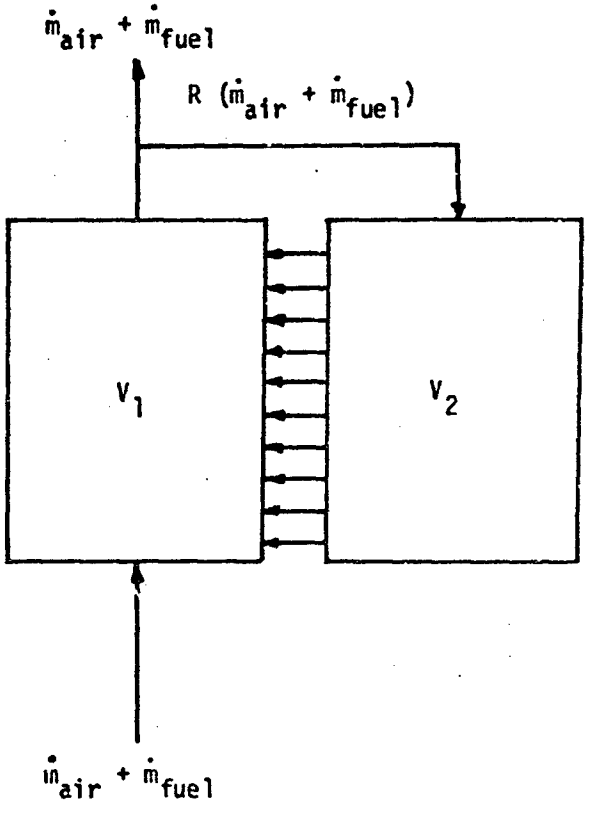

Fig. 25 Recirculation model using a plug flow reactor pair (after Morgan, 1967).

residence time distribution can be changed as a function of axial position.

The current overall model has several intrinsic merits. Firstly, it is simple enough to facilitate computer solution without consuming vast amounts of time. Secondly, both mixing and kinetics are considered. Thirdly, an exact correspondence exists between the flow regions in the model and those in the physical combustor; therefore, the internal composition and temperature patterns will be approximately predicted. This ability to approximate the internal structure of the reacting flow separates the model from those relying heavily on exit tracer response functions to predict overall performance and which neglect internal structure entirely. In fact, to obtain more exact and detailed results the coupled turbulent governing equations must be integrated.

Having presented what we feel to be a realistic overall combustor model let us examine the current models of other investigators before presenting the predictions of our own model.

C. Other recently proposed combustor models

There exist only two other complete analytical models for gas turbine combustors. The first was proposed by Heywood et al. (1970) for use in predicting air pollutant emissions. They modelled the primary combustion zone as a single plug flow reactor and the secondary combustion zones as a one-dimensional equilibrium flow with continuous air addition. Although this model gave fair agreement for nitric oxide emissions, because it assumes perfect mixing in the radial direction in the primary zone and thus neglects the recirculation flow, it cannot predict combustor blowout and flame stability. The use of C-H-O equilibrium neglects the kinetic nature of nitric oxide formation and can lead to serious error as shown by Bowman (1970).

The other complete gas turbine combustor model was developed by Fletcher and Heywood (1971) to predict the nitric oxide emission levels of aircraft gas turbine combustors. The primary zone is modelled as a single segregated perfectly stirred reactor with an assumed initial normal distribution of mixture ratio. The effects of such assumptions have been discussed in the section on segregation. An arbitrary fraction of the total fuel flow is assumed to burn in the primary zone,

the rest being carried downstream. The primary zone is followed by an intermediate zone which is modelled by forcing the standard deviation of the mixture ratio distribution to zero over an arbitrary zone length. This corresponds to the intermixing of eddies in a segregated plug flow, and at the exit of the zone the flow is micromixed plug. The final or dilution zone is then modelled as micromixed plug flow with air addition.

One major limitation of this model is that it holds the carbon-hydrogen-oxygen chemistry in equilibrium and treats only the nitric oxide formation kinetically, since it is assumed that the entire process is mixing limited. As mentioned previously, the work of Bowman (1970) discredits the equilibrium assumption. Also, this model contains a number of arbitrary parameters which must be assigned values intuitively (as does our model to a lesser degree).

The predicted nitric oxide emission levels exhibited the correct trends and reasonable values. The strong point of this model (and our refined model) is its ability to examine the effect of segregation of primary zone mixture ratio. The initial calculations used only the primary and dilution zones, but showed an interesting variation in nitric oxide emissions with initial reactant distribution (Fig. 26). This result indicates that the primary zone mixing should receive attention in our future work.

We now see that most investigators agree on the basic premise of using combinations of perfectly stirred and plug flow reactors to model gas turbine combustors. However, there exist differences in opinion as to the correct techniques for handling segregation, mixing, and kinetics. The true test in each case will be the experimental confirmation of the analytical predictions. For this reason we now turn to a discussion of our predicted results.

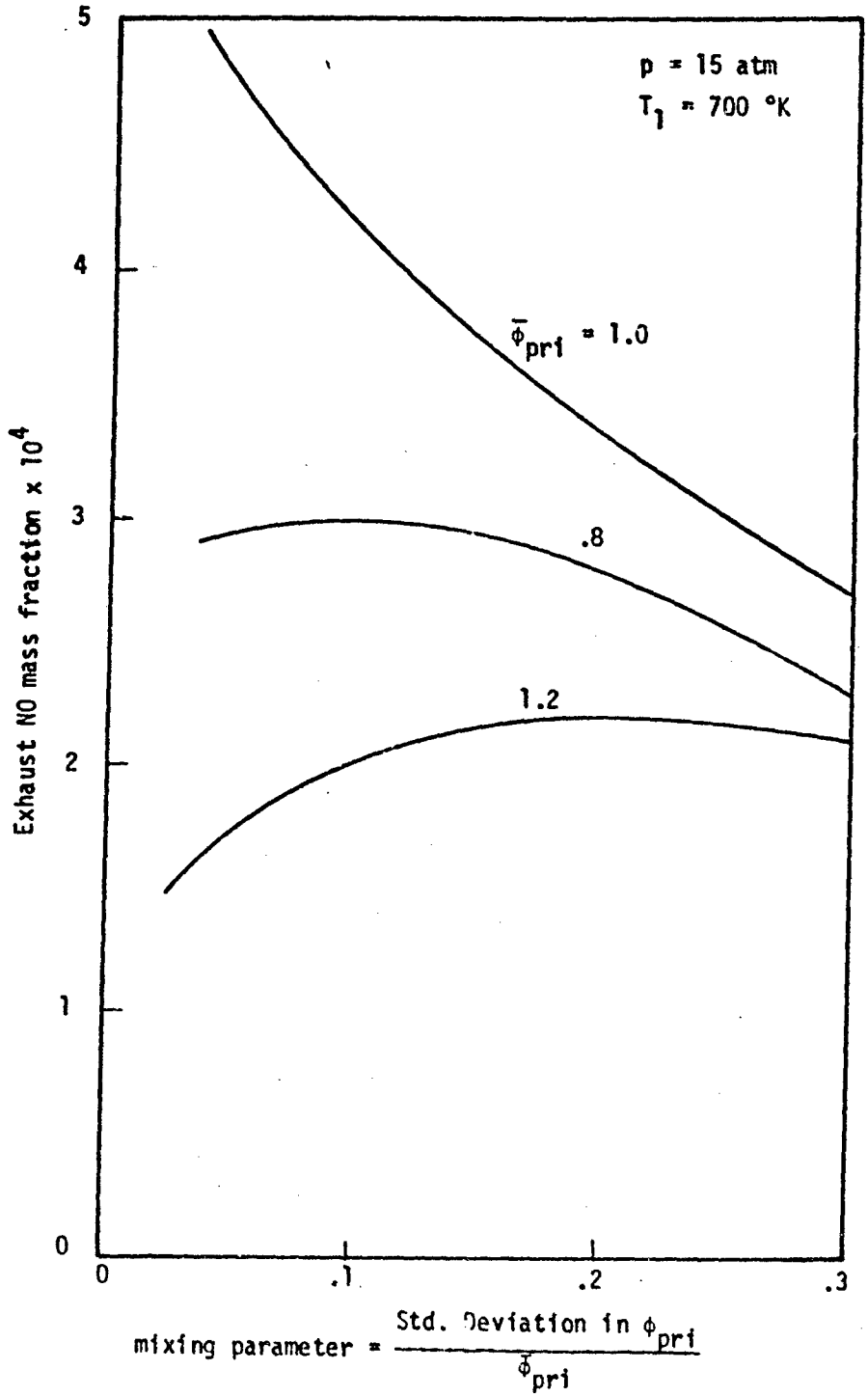

Fig. 26 Influence of assumed mixing model on nitric oxide predictions (after Fletcher and Heywood, 1971).

CHAPTER V
PREDICTIONS OF THE ANALYTICAL GAS TURBINE COMBUSTOR MODEL

As a result of difficulties with the NASA combustor program (Anon., 1968) only their test case air flow and pressure distributions have been available. We have, however, analyzed the combustion process in this test case combustor (denoted No. 3) using the overall combustor analysis program (unfortunately the NASA Test Case Combustor No. 3 is not known to correspond to any actual combustor). Although this is an annular configuration our analysis applies equally well. To reduce computation time, the combustor was modelled using single perfectly stirred reactors for all secondary combustion zones. The heavy hydrocarbon fuel originally used was replaced with an equivalent flow of propane, all of which was injected into V_1. Arbitrarily, a recirculation ratio R = 0.5 and a primary zone volume split $V_1/V_2 = 1.0$ were assumed. The configuration, airflow, and pressure distributions taken from the NASA output and used as input to the modelling program are shown in Figs. 27-29. The other operating conditions are:

air mass flow rate	= 4358	g/sec
inlet air temperature	= 895	°K
fuel mass flow rate	= 40	g/sec
inlet fuel temperature	= 298	°K
mean primary zone equivalence ratio	= 1.34	

The details of the gas turbine combustor analysis program are given in Appendix C. We will now discuss the predictions of the program both from a performance and from a pollution viewpoint.

A. Performance predictions

The temperature, completeness of combustion, and the mole fractions

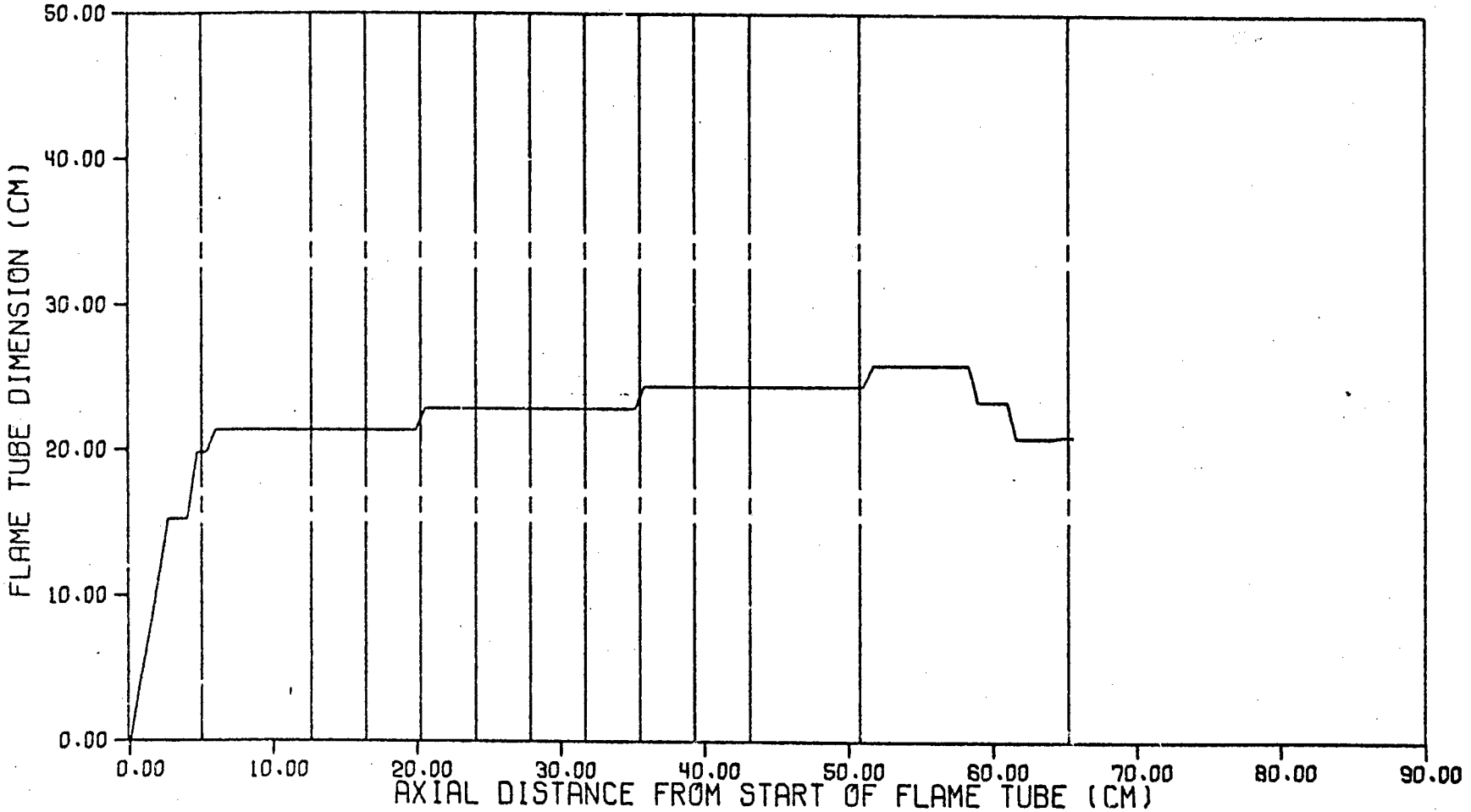

FIGURE 27. CONFIGURATION OF NASA TEST CASE COMBUSTOR NO. 3.

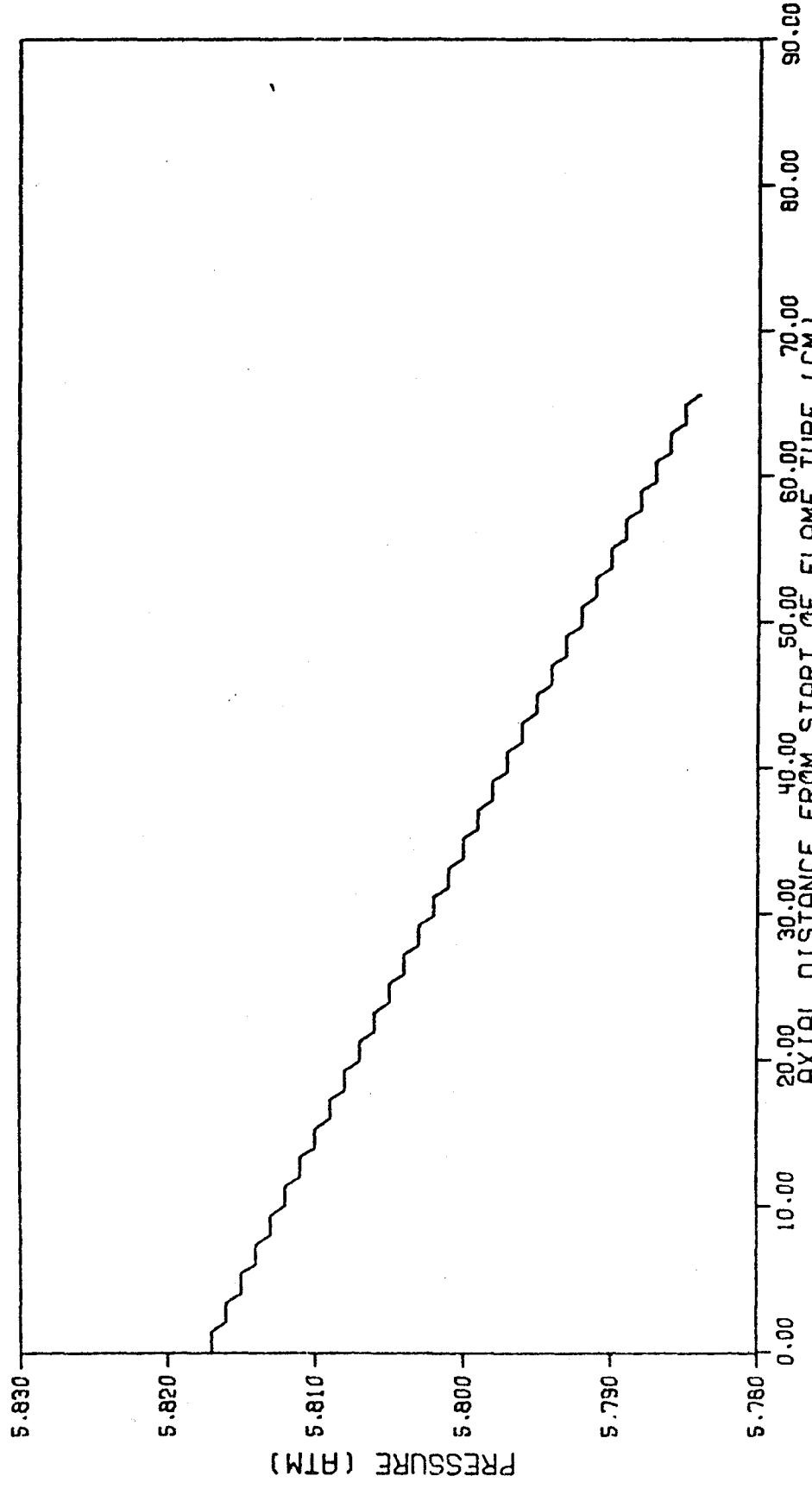

FIGURE 29. PRESSURE DISTRIBUTION OF NASA TEST CASE COMBUSTOR NO. 3.

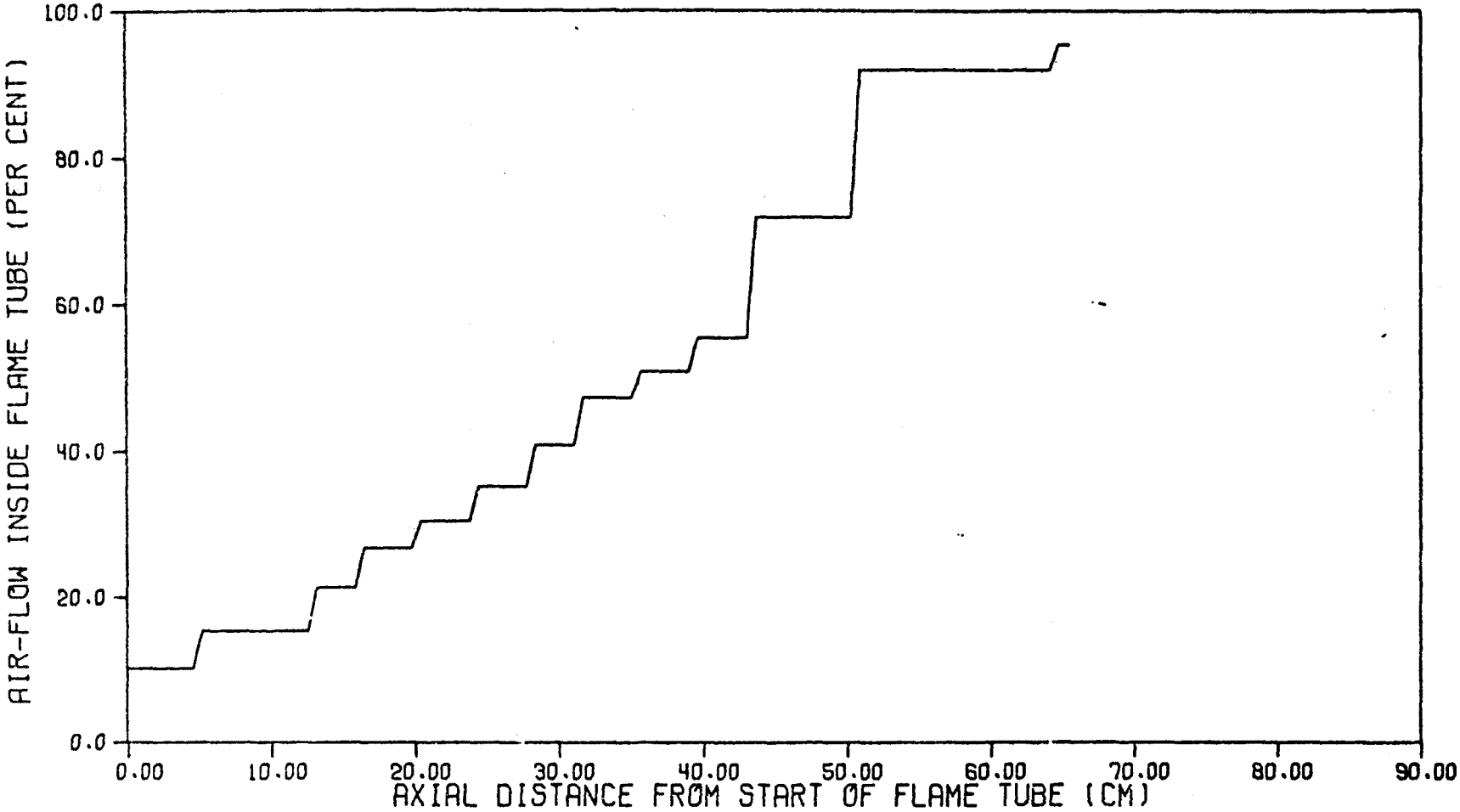

FIGURE 28. AIR-FLOW DISTRIBUTION OF NASA TEST CASE COMBUSTOR NO. 3.

of all species have been plotted versus axial position in the combustor; these results are shown in Figs. 30-42. Those most closely related to combustion performance are the temperature, completeness of combustion, and carbon monoxide mole fraction profiles (Figs. 30,31, and 41).

The temperature profile peaks in the primary zone and decreases downstream as expected. The slightly reduced temperature in the recirculation zone results from the increased dissociation in this region indicating that the C-H-O reactions in the recirculation zone have had time to more closely approach equilibrium than those in the primary zone. This dissociation (particularly of carbon dioxide) also reduces the completeness of combustion in the recirculation zone. Carbon monoxide is shown to peak in the recirculation zone since the high primary zone equivalence ratio favors the formation of that species over carbon dioxide. The primary zone also contains the maxima of all species having a highly reactive nature (free radicals), most notably the oxygen atom and the hydroxyl radical.

Considering results of an overall nature, we see that combustion is essentially complete in roughly half the length of the combustor. This indicates that a considerable length reduction could be realized for this combustor without significant performance degradation if a turbine inlet temperature of 1500°K could be tolerated. The final combustion efficiency is essentially 100% in correspondence with values observed in well-designed systems. Note that the predicted exit temperature of about 1200°K is physically reasonable.

B. Pollutant emissions

The primary pollutant species of interest are carbon monoxide and nitric oxide (hydrocarbon emissions are presently not predicted because of the assumed infinitely fast and complete partial oxidation to CO). The carbon monoxide profile indicates that a negligible amount of this species will be emitted. The exit carbon monoxide concentration of 19 ppm is in agreement with typical values for practical systems (Cornelius and Wade, 1970).

Examining the predicted nitric oxide concentration profile reveals two interesting points. Firstly, the nitric oxide level peaks in the recirculation zone in complete agreement with the concept that the

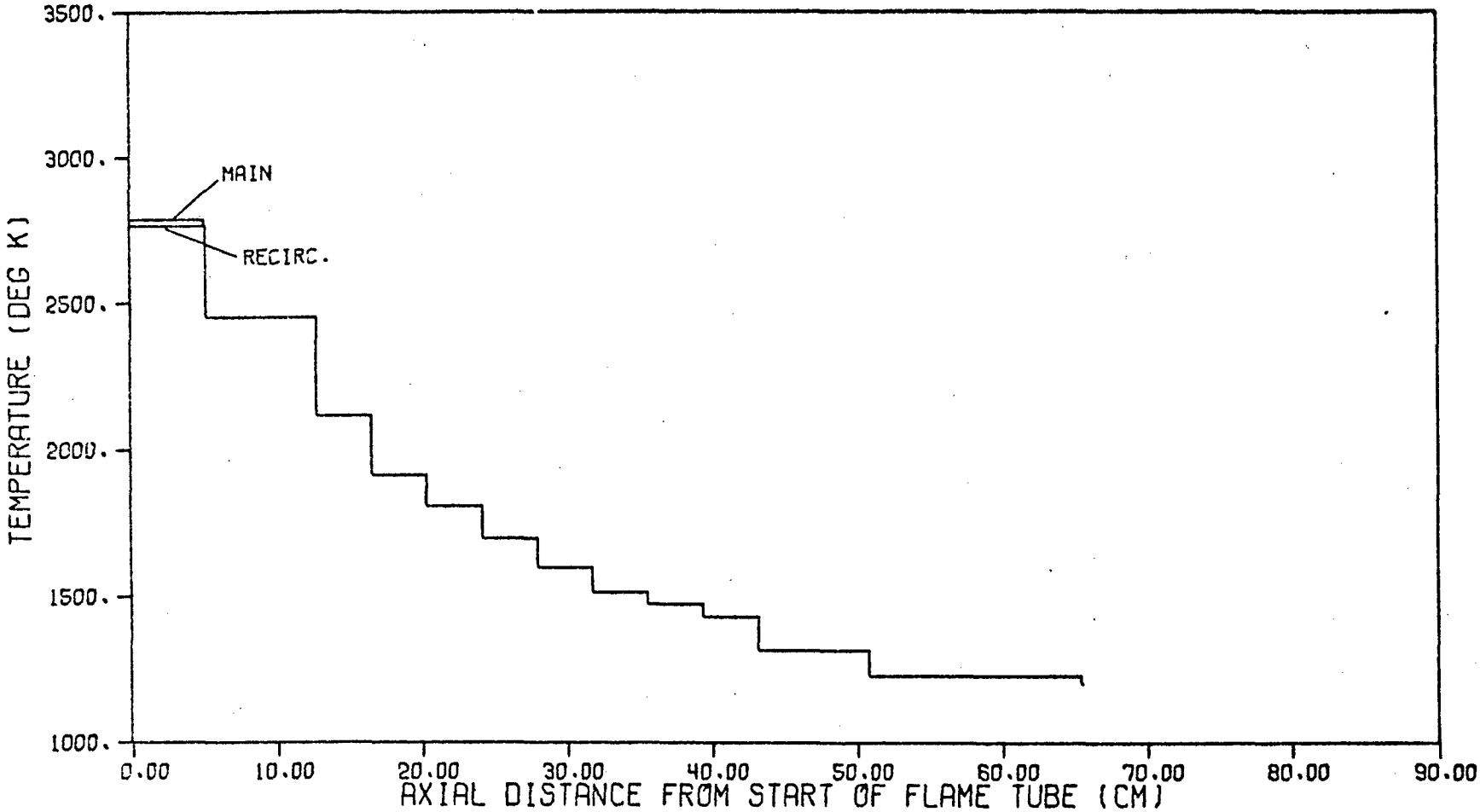

FIGURE 30. TEMPERATURE DISTRIBUTION PREDICTED FOR NASA TEST CASE COMBUSTOR NO. 3 (RECIRC. RATIO=0.5\VOLUME RATIO=1.0).

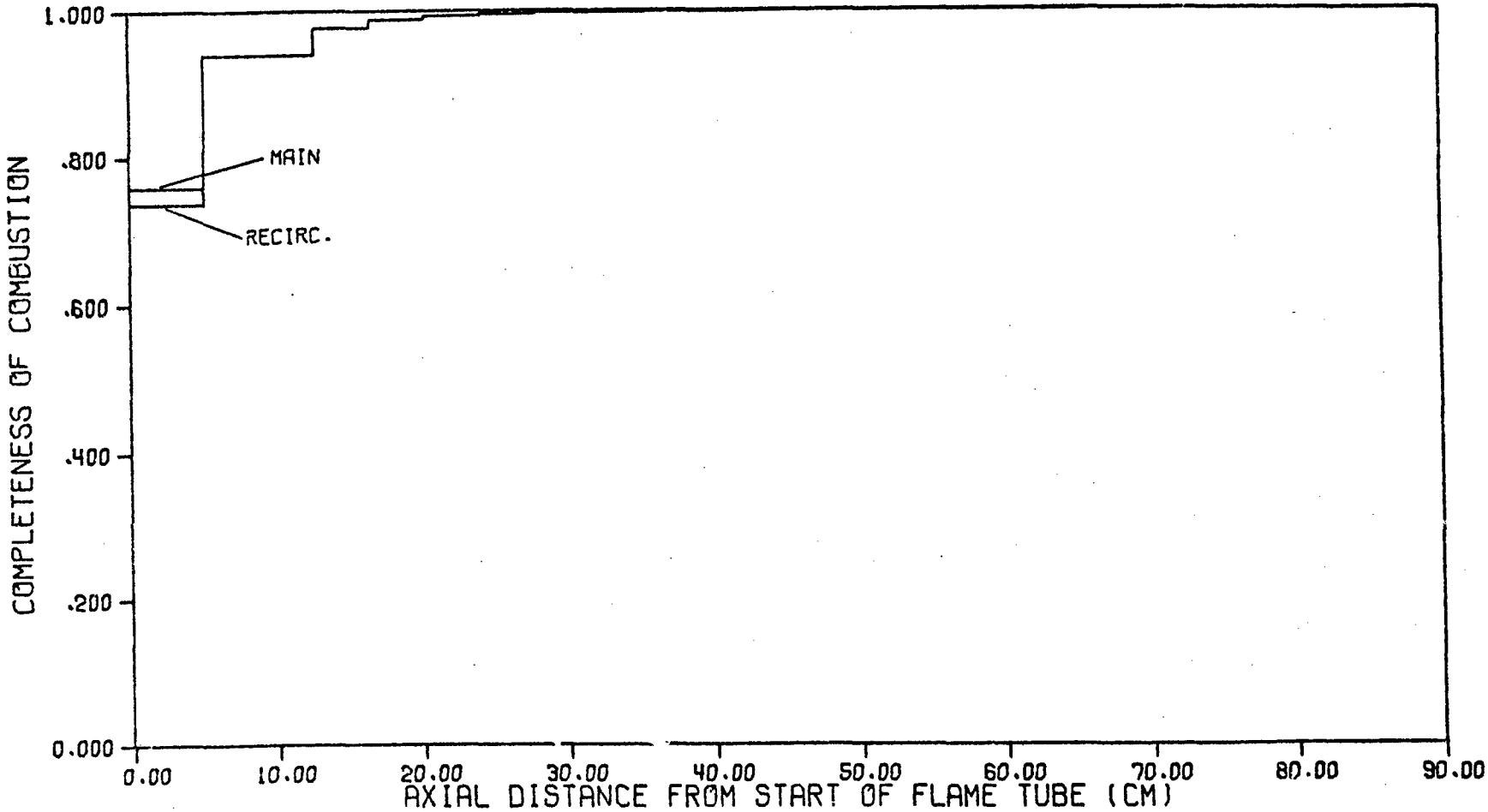

FIGURE 31. COMPLETENESS OF COMBUSTION PREDICTED FOR NASA TEST CASE COMBUSTOR NO. 3 (RECIRC. RATIO=0.5\VOLUME RATIO=1.0).

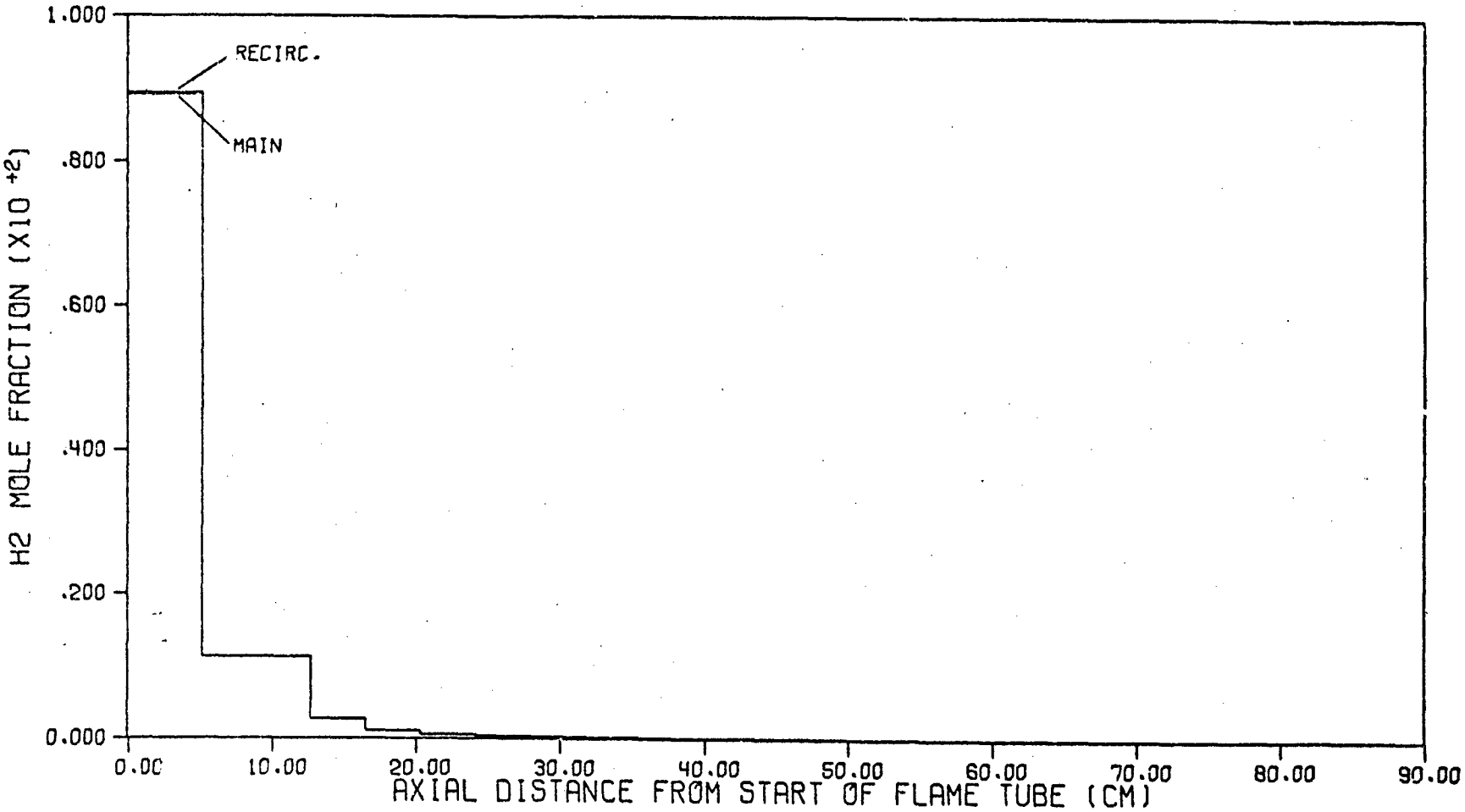

FIGURE 32. H2 MOLE FRACTION DISTRIBUTION PREDICTED FOR NASA TEST CASE COMBUSTOR NO. 3 (RECIRC. RATIO=0.5\VOLUME RATIO=1.0).

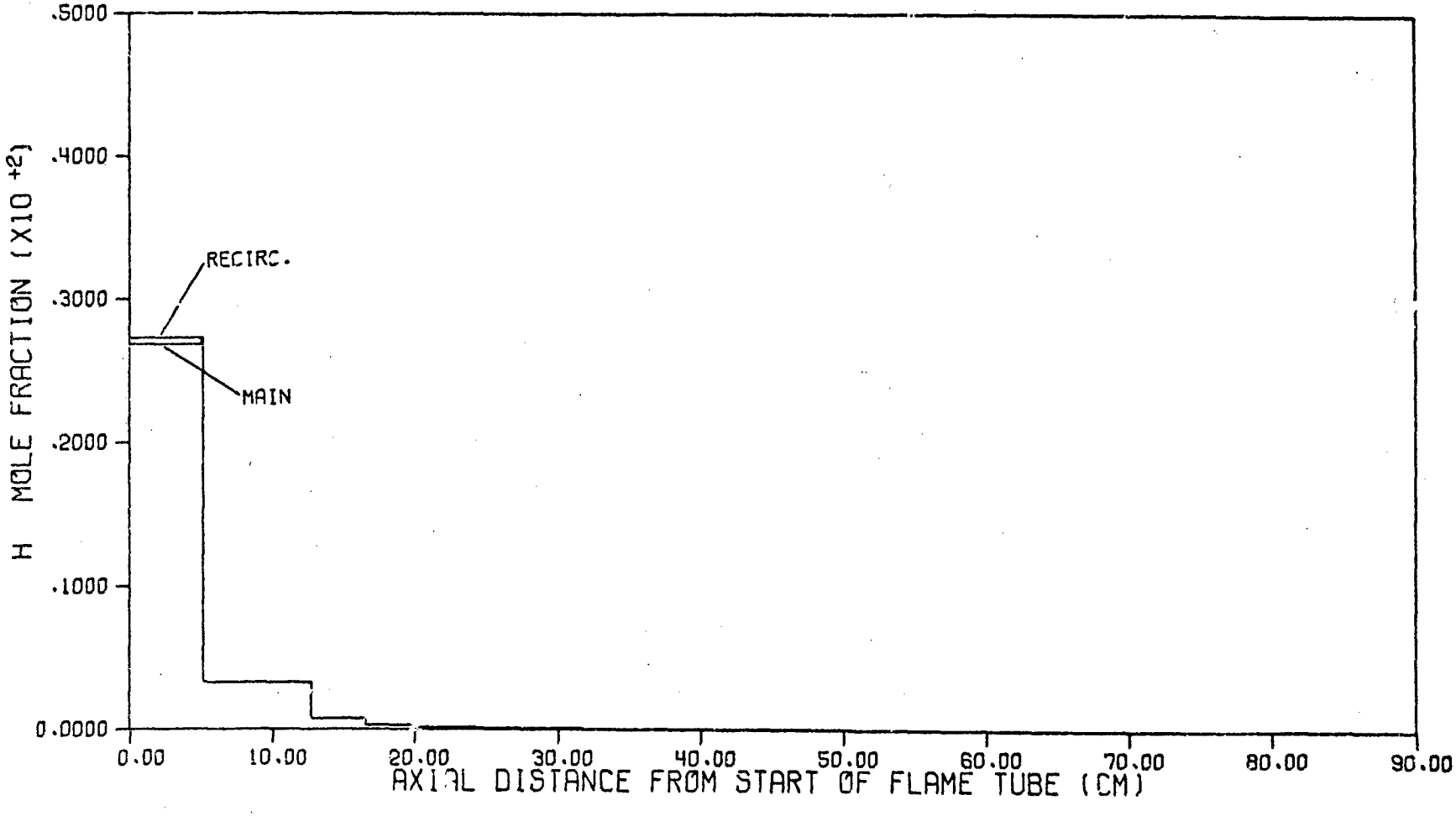

FIGURE 33. H MOLE FRACTION DISTRIBUTION PREDICTED FOR NASA TEST CASE COMBUSTOR NO. 3 (RECIRC. RATIO=0.5\VOLUME RATIO=1.0).

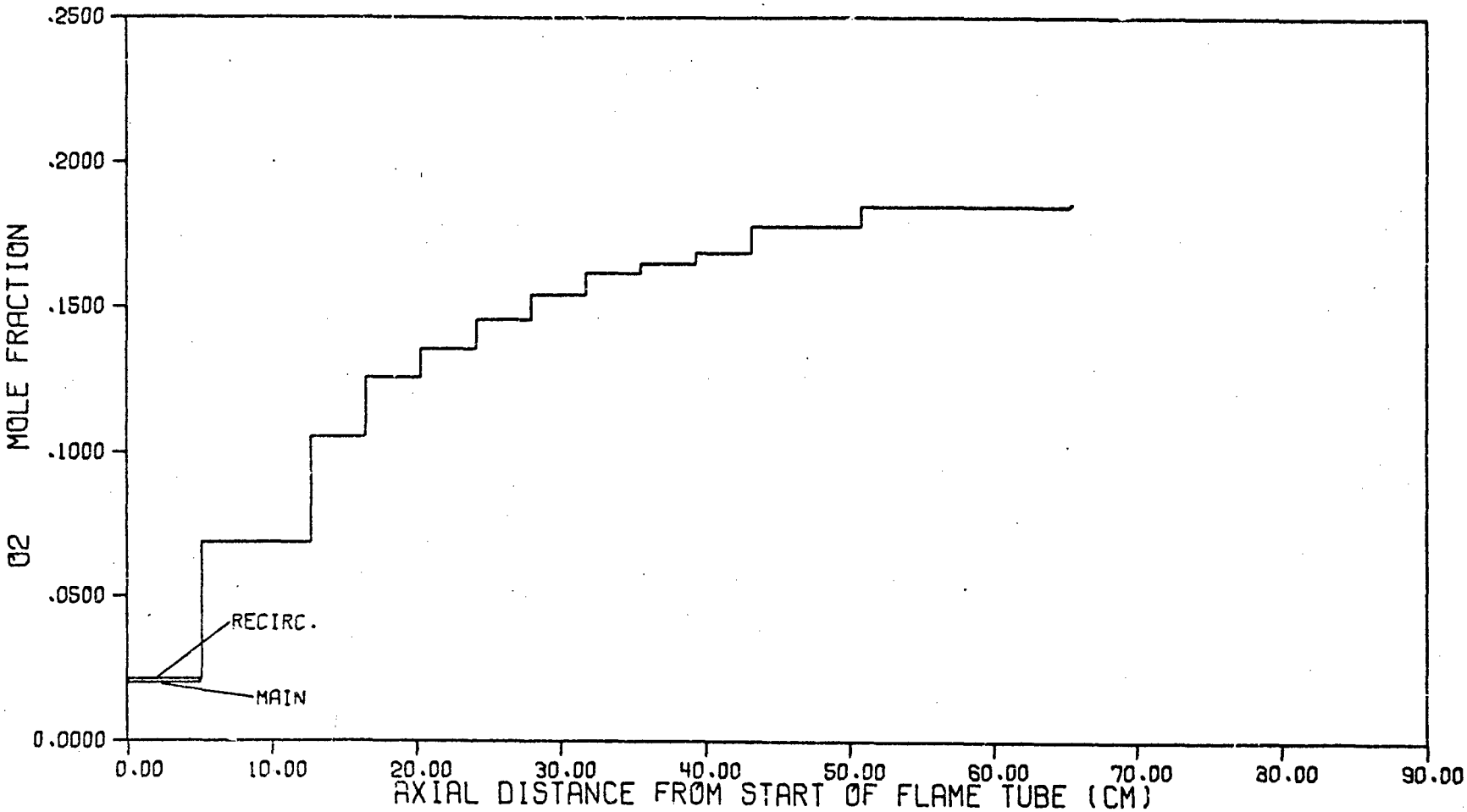

FIGURE 34. O2 MOLE FRACTION DISTRIBUTION PREDICTED FOR NASA TEST CASE COMBUSTOR NO. 3 (RECIRC. RATIO=0.5\VOLUME RATIO=1.0).

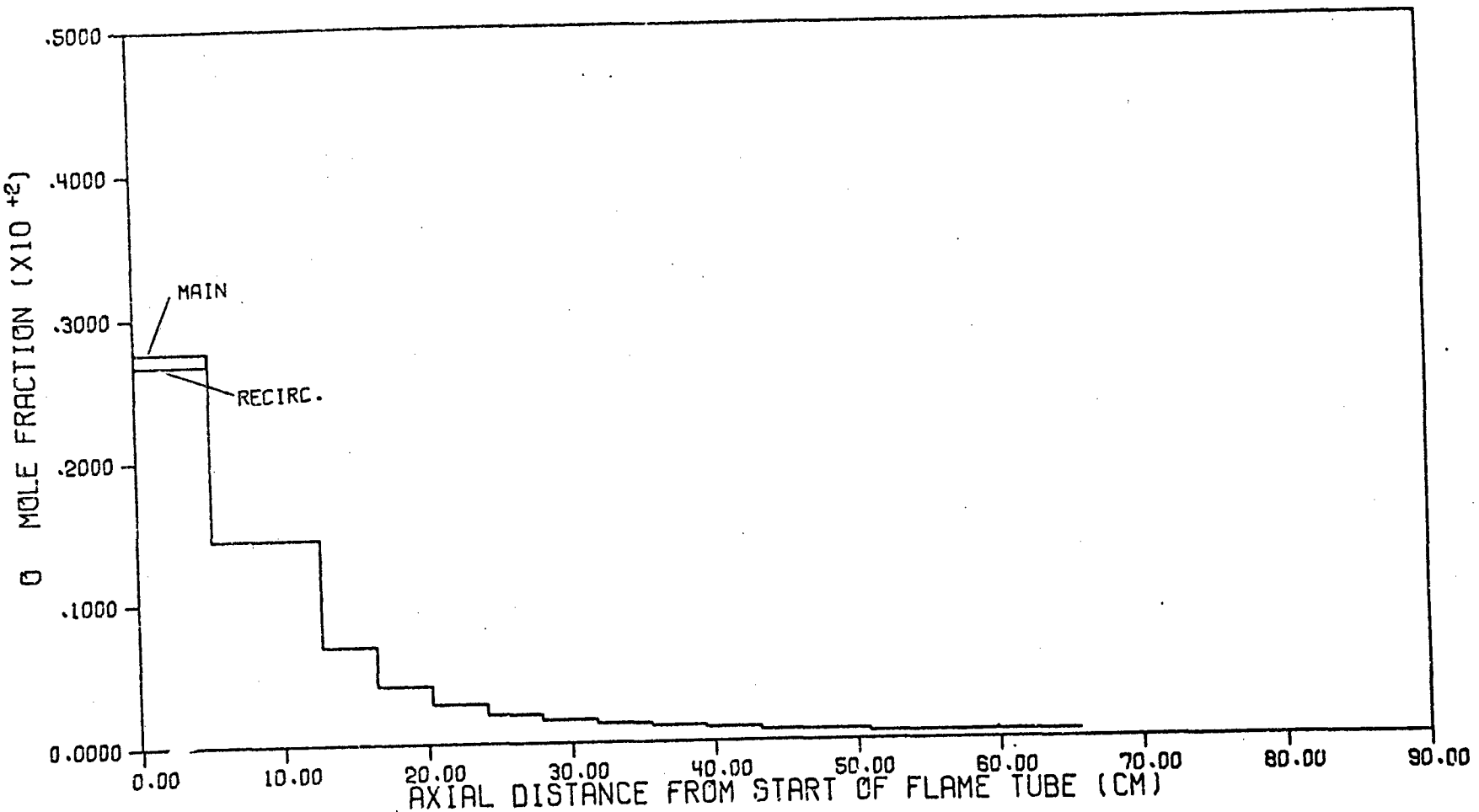

FIGURE 35. O MOLE FRACTION DISTRIBUTION PREDICTED FOR NASA TEST CASE COMBUSTOR NO. 3 (RECIRC. RATIO=0.5\VOLUME RATIO=1.0).

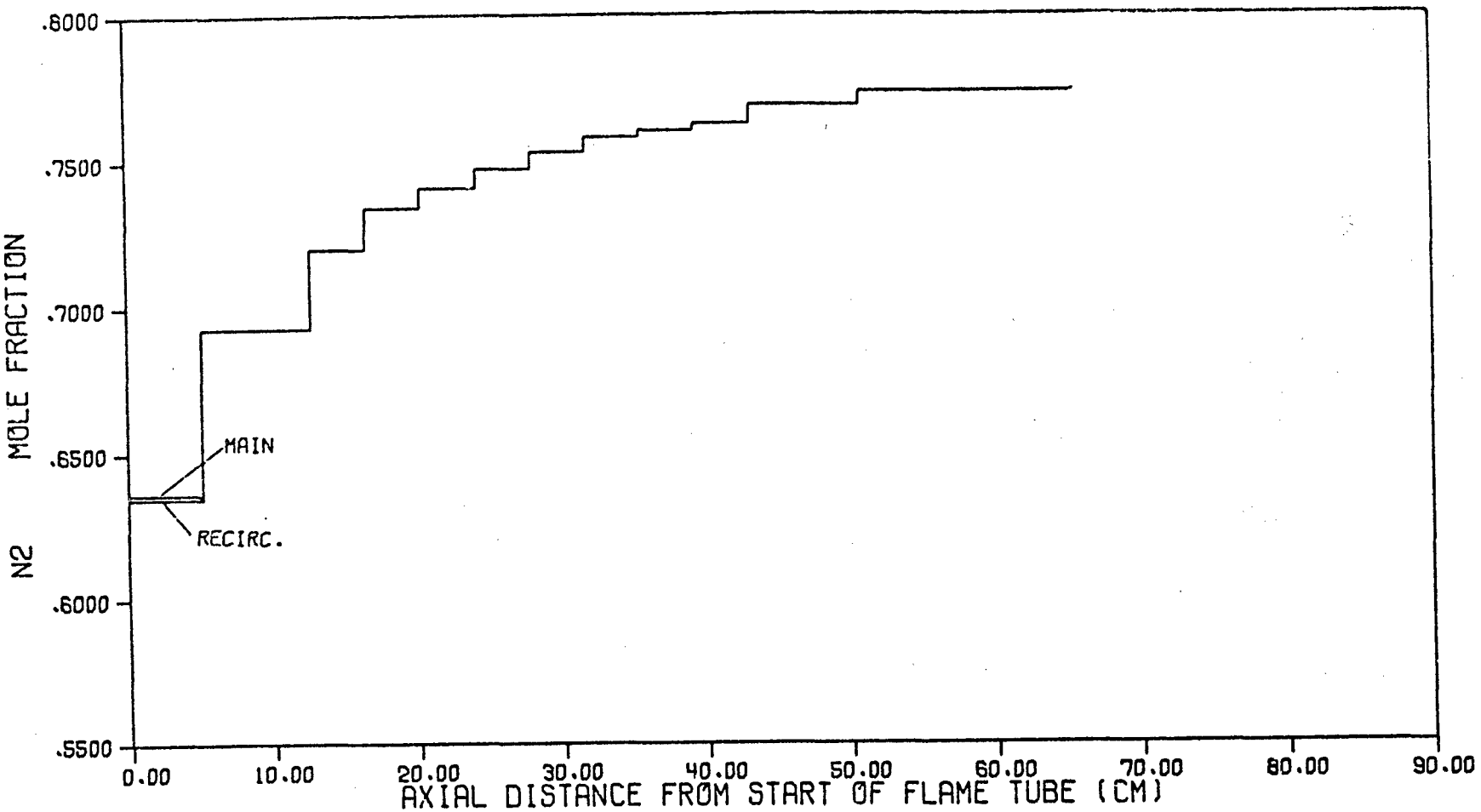

FIGURE 36. N2 MOLE FRACTION DISTRIBUTION PREDICTED FOR NASA TEST CASE COMBUSTOR NO. 3 (RECIRC. RATIO=0.5\VOLUME RATIO=1.0).

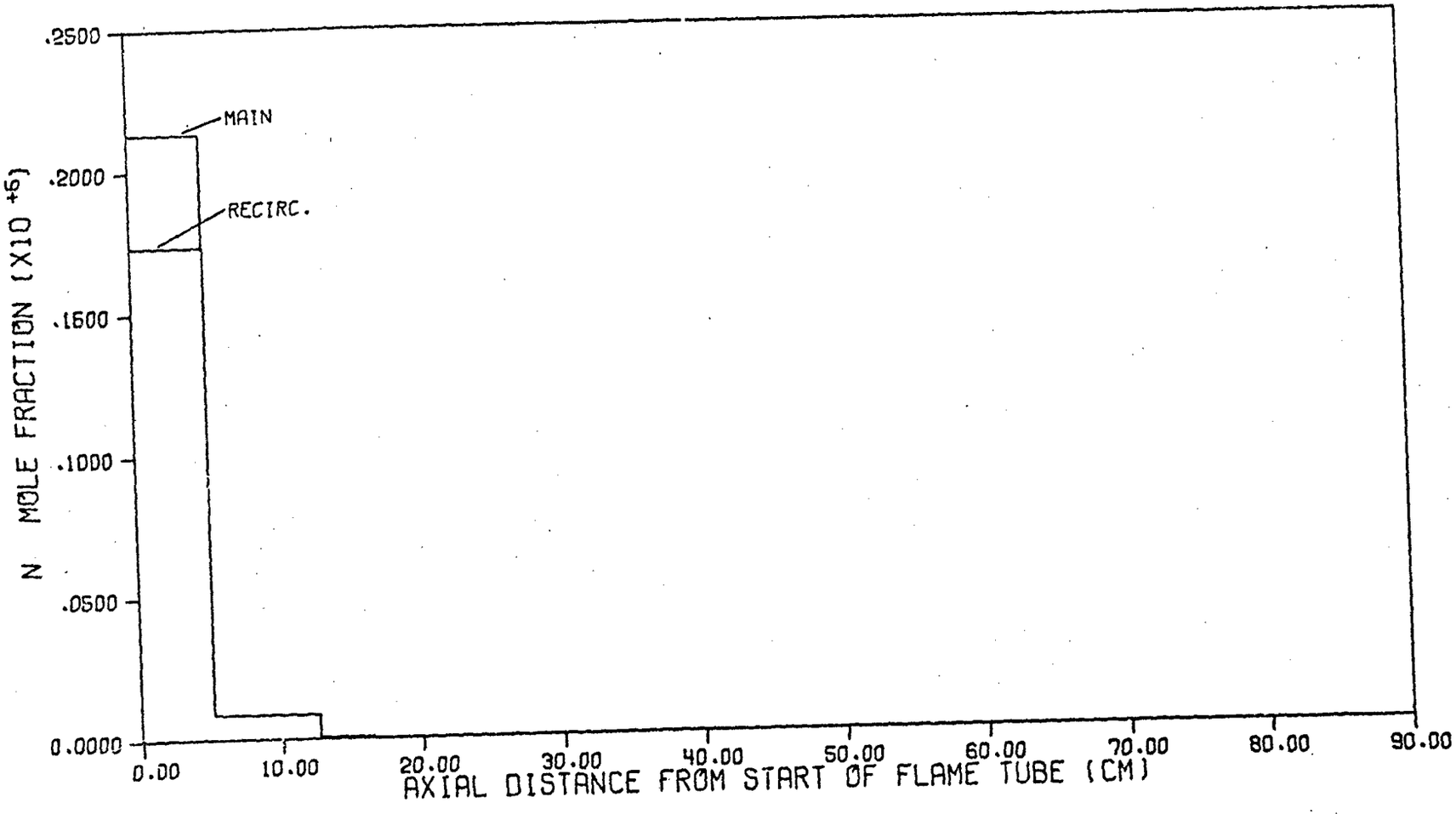

FIGURE 37. N MOLE FRACTION DISTRIBUTION PREDICTED FOR NASA TEST CASE COMBUSTOR NO. 3 (RECIRC. RATIO=0.5\VOLUME RATIO=1.0).

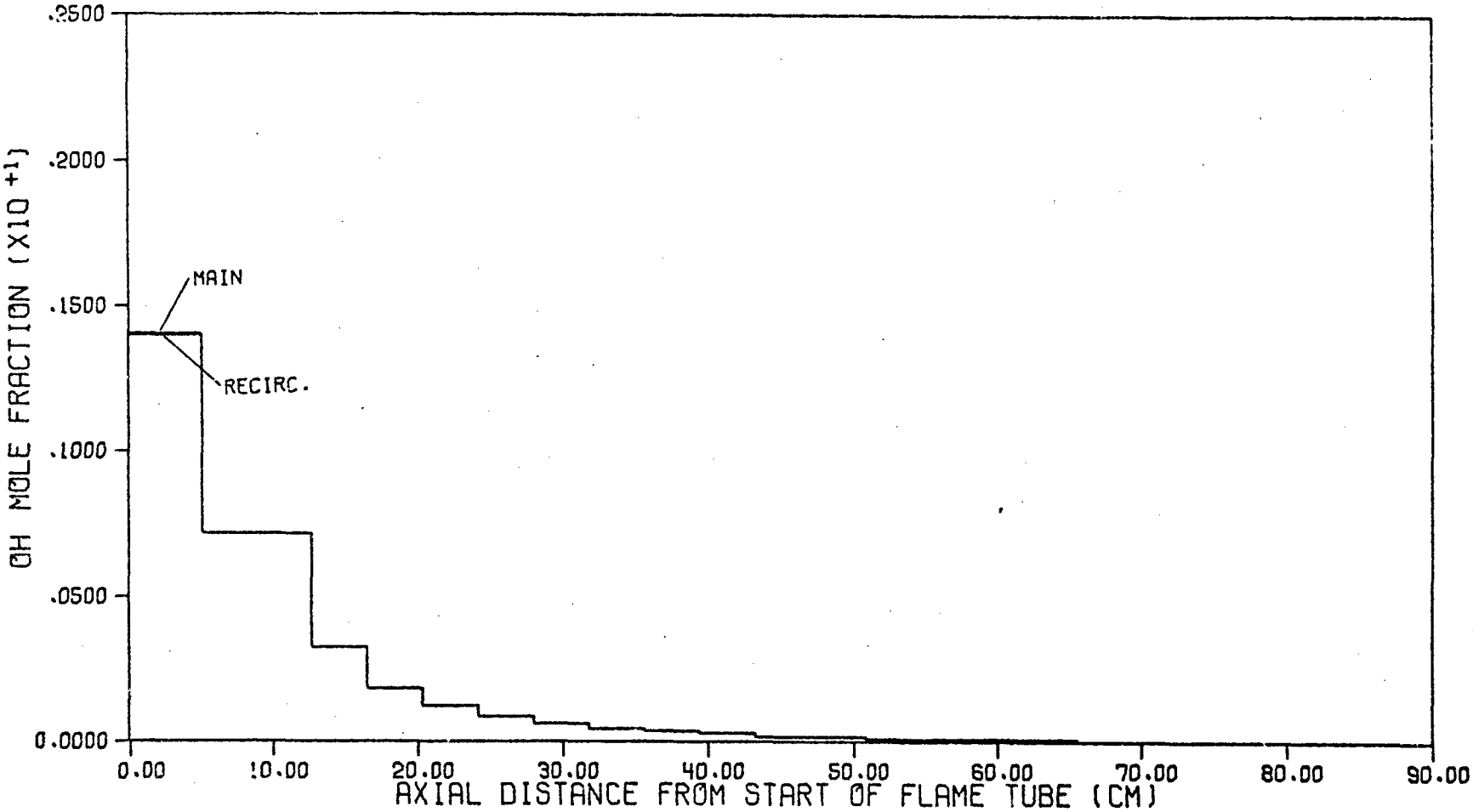

FIGURE 38. OH MOLE FRACTION DISTRIBUTION PREDICTED FOR NASA TEST CASE COMBUSTOR NO. 3 (RECIRC. RATIO=0.5\VOLUME RATIO=1.0).

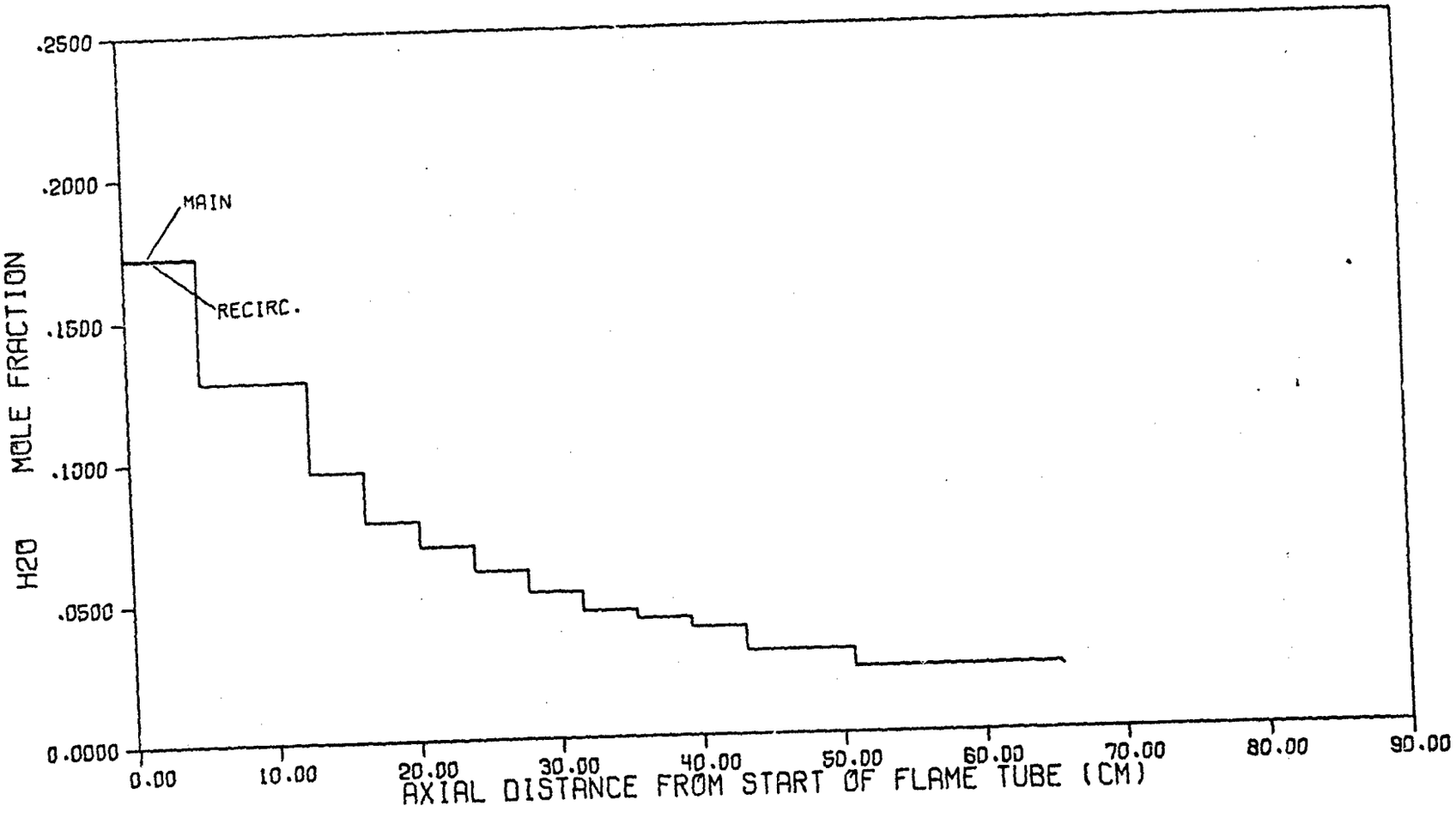

FIGURE 39. H20 MOLE FRACTION DISTRIBUTION PREDICTED FOR NASA TEST CASE COMBUSTOR NO. 3 (RECIRC. RATIO=0.5\VOLUME RATIO=1.0).

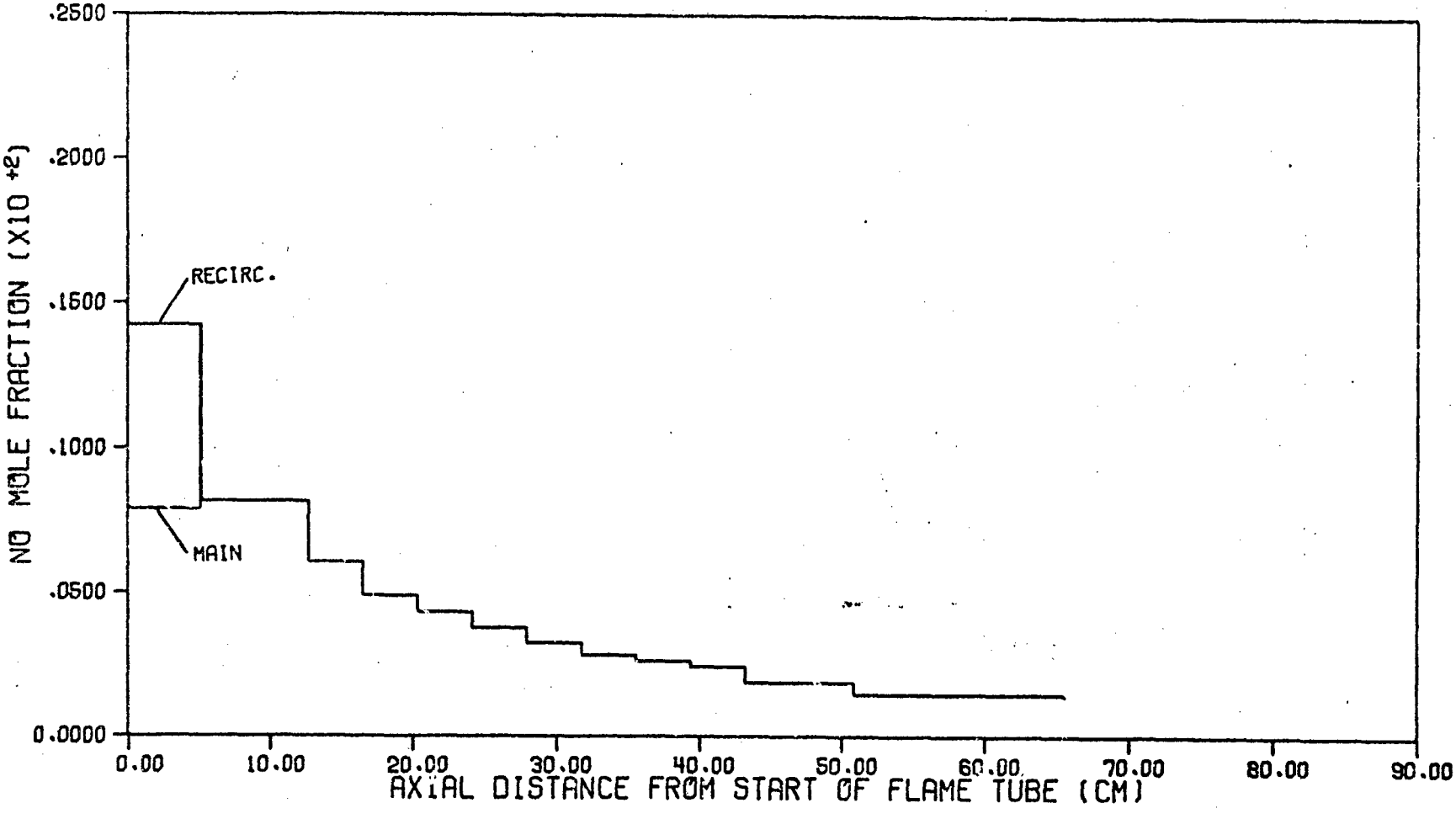

FIGURE 40. NO MOLE FRACTION DISTRIBUTION PREDICTED FOR NASA TEST CASE COMBUSTOR NO. 3 (RECIRC. RATIO=0.5\VOLUME RATIO=1.0).

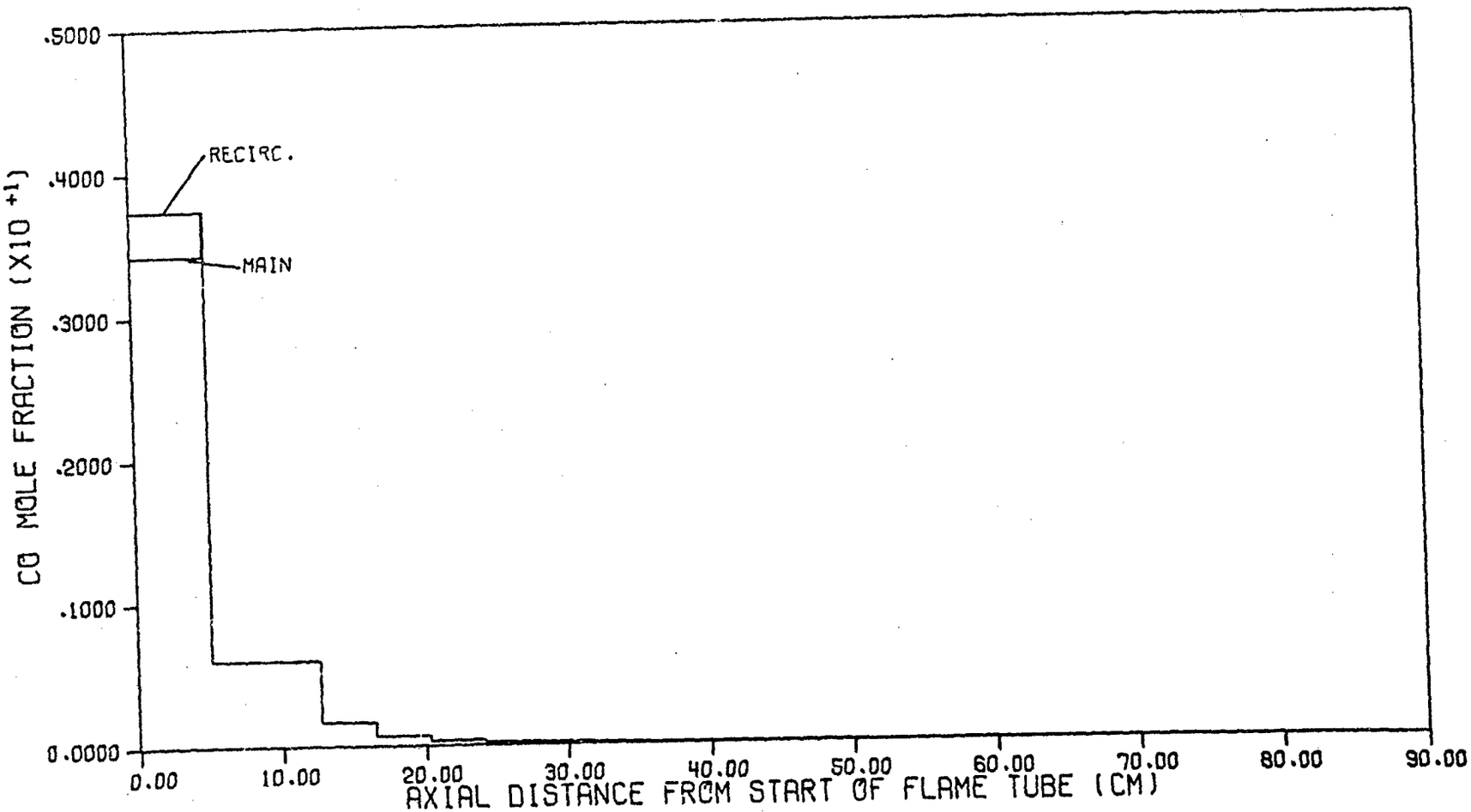

FIGURE 41. CO MOLE FRACTION DISTRIBUTION PREDICTED FOR NASA TEST CASE COMBUSTOR NO. 3 (RECIRC. RATIO=0.5\VOLUME RATIO=1.0).

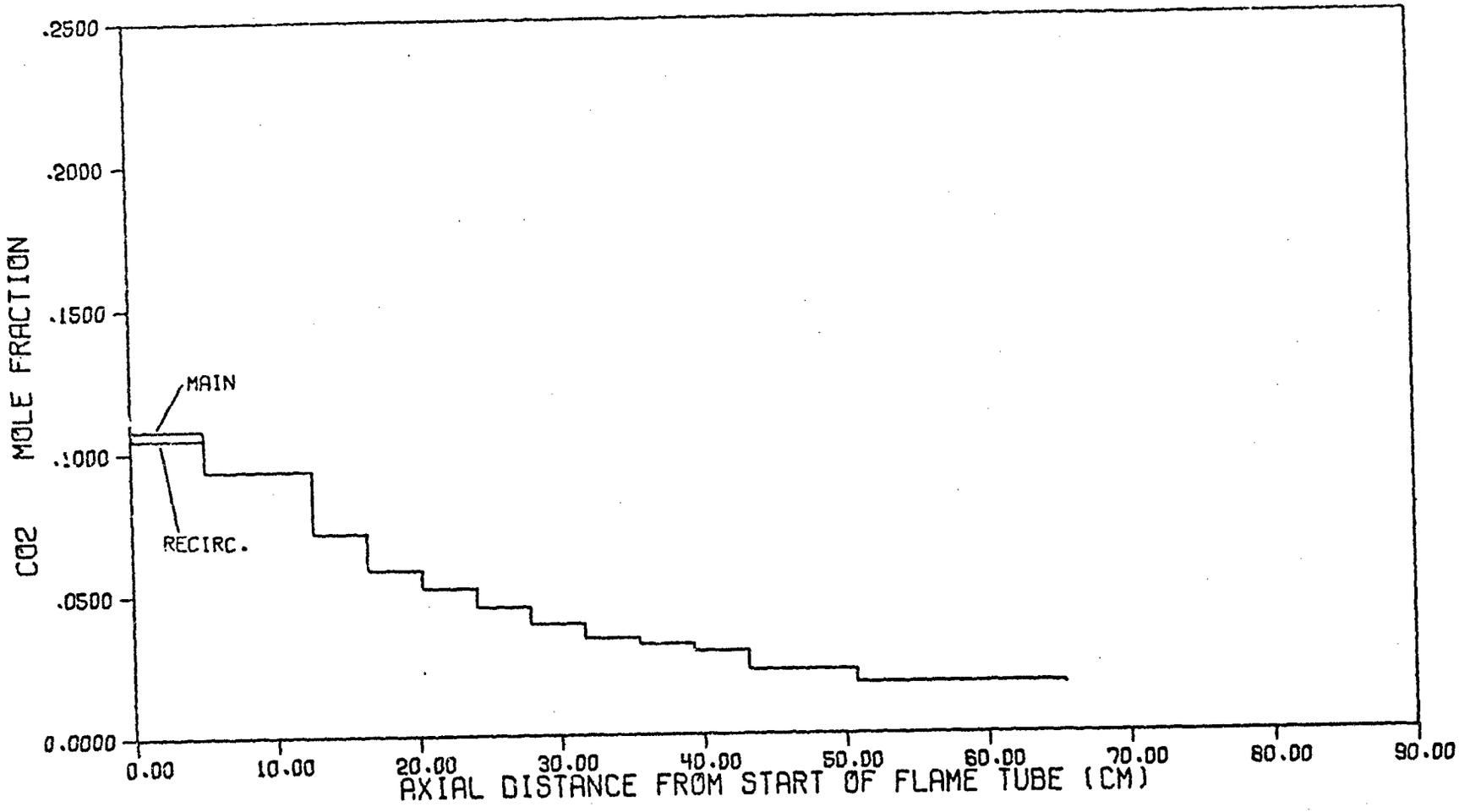

FIGURE 42. CO2 MOLE FRACTION DISTRIBUTION PREDICTED FOR NASA TEST CASE COMBUSTOR NO. 3 (RECIRC. RATIO=0.5\VOLUME RATIO=1.0).

amount of nitric oxide formed depends on the length of time spent at peak temperatures. Secondly, the exit nitric oxide concentration of 142 ppm is within the range of values observed in combustors (Cornelius and Wade, 1970).

We can make no experimental comparisons for the NASA Test Combustor No. 3 other than the generalizations mentioned above since this combustor is not a physical unit. Indeed for this reason no time-consuming parametric studies were performed.

CHAPTER VI

CONCLUSIONS AND FUTURE EFFORTS

A complete model for the analysis of all types of gas turbine combustors has been developed. It utilizes the fluid mechanical portion of the experimentally verified NASA combustor analysis program (Anon., 1968) to compute required distributions of airflow and static pressure. The combustion model itself consists of an assemblage of perfectly stirred reactors. Inside each perfectly stirred reactor a fully kinetic combustion mechanism for a general hydrocarbon is used to compute performance. The level of nitric oxide formation is also kinetically computed. Upon consideration of the physical flows inside the combustor, the volumes of these perfectly stirred reactors, the flows interconnecting them, and the fuel and air addition points were arranged to allow a reasonable approximation of the overall mixing behavior in terms of a minimum number of physically significant parameters. The predictions of the model yield approximate internal profiles of temperature and species concentrations which indicate performance and can be directly employed in a heat transfer analysis to predict flame tube wall temperatures (Owens and Mellor, 1971).

The kinetic analysis for general hydrocarbon combustion is based on the postulate that the combustion process of any hydrocarbon can be separated into three component processes:

1. a rapid partial oxidation of the parent hydrocarbon to carbon monoxide and water;
2. a single rate limiting step of carbon monoxide destruction (Reaction [24]);
3. a sequence of free radical production reactions not involving carbon;

where step 1 is assumed to have infinite rate compared to step 2. It was deduced that the accuracy of these simplifications should improve

as the complexity of the hydrocarbon increases.

The Zeldovich mechanism was taken to be responsible for the majority of nitric oxide formation, but the three-body association reaction of monatomic nitrogen and oxygen was included since it is known to be of increasing significance at high temperatures.

A study of conventional chemical reactor theory revealed techniques for modelling mixing by proper combinations of perfectly stirred reactors. It was found that an arbitrary residence time distribution can be approximated by combinations of plug flow reactors and perfectly stirred reactors with various interconnecting flows. Investigation of segregation showed that the residence time distribution alone is not sufficient to predict behavior due to the eddy dominated nature of the turbulent mixing processes. In particular, if the fluid segregates the initial distribution of reactants over the eddies, the rate of eddy intermixing, and the eddy residence time distribution must be determined. By considering various approximations of these functions a number of stirred reactors were interconnected to approximate the mixing processes.

The resulting overall combustor model was seen to possess several intrinsic merits, namely:

1. it is simple enough to facilitate solutions;
2. both mixing and kinetics are considered;
3. there is an exact correspondence between the flow zones in the model and in a combustor.

Therefore, it is inherently superior to those models which neglect mixing and/or kinetics, or those which rely heavily on exit tracer response functions and neglect internal structure.

It is presumptuous to make conclusions concerning the predictions of this model in view of the lack of experimental data. However, trend predictions inside the combustor are seen to be accurate, and the values of the variables at combustor exit fall in the range of values observed in experimental systems.

The major region of future refinements will be the primary zone model. A need exists for good work on the three recirculation modes and the exact influence of each on mixing and reaction. Relatively little is known concerning the internal structure of the initial vapori-

zation zone, in particular the droplet distribution and accompanying evaporation rates. The question concerning the existence of heterogeneous combustion is yet unresolved. The modes of entrainment of fuel vapor from the zone will define the initial mixture ratio segregation in the primary combustion zone, but this is poorly understood.

Future work using the current analytical model will include extensive parametric studies of the Allison J-33 combustor and the Boeing 502E combustor for several operating points. These studies should elucidate the effects of the various mixing parameters. These predictions will then be compared with experimental data on these combustors for the same operating points. The experimental facility and technique is described fully by Anderson and Mellor (1971). Comparison will be made on the basis of the internal profiles of temperature, carbon monoxide concentration and nitric oxide concentration. It is hoped that further refinements of the combustor modelling program will become apparent as a result of these comparisons.

LIST OF REFERENCES

Anderson, R. D. and Mellor, A. M. (1971), "An investigation of gas turbine combustors with high inlet air temperatures, Second Annual Report Part III: Experimental Developments," TM-71-3, Jet Propulsion Center, Purdue University, Lafayette, Indiana, TACOM Report No. 11322.

Anon. (1968), "Computer program for the analysis of annular combustors, Vol. I: Calculational procedures; Vol. II: Operating manual," Northern Res. Engr. Corp. Reports No. 1111-1 and 1111-2, (NASA CR 72374, 72375).

Baulch, D. L., Drysdale, D. A., and Lloyd, A. C. (1968a), "Critical evaluation of rate data for homogeneous, gas-phase reactions of interest in high temperature systems, No. 1," Dept. of Phys. Chem., The University, Leeds.

Baulch, D. L., Drysdale, D. D., and Lloyd, A. C. (1968b), "Critical evaluation of rate data for homogeneous, gas-phase reactions of interest in high temperature systems, No. 2," Dept. of Phys. Chem., The University, Leeds.

Baulch, D. L., Drysdale, D. D., and Lloyd, A. C. (1969a), "Critical evaluation of rate data for homogeneous, gas-phase reactions of interest in high temperature systems, No. 3," Dept. of Phys. Chem., The University, Leeds.

Baulch, D. L., Drysdale, D. D., and Lloyd, A. C. (1969b), "Critical evaluation of rate data for homogeneous, gas-phase reactions of interest in high temperature systems, No. 4," Dept. of Phys. Chem., The University, Leeds.

Beér, J. M. and Lee, K. B., 'The effect of the residence time distribustion on the performance and efficiency of combustors', Tenth Symposium (International) on Combustion, The Combustion Institute (1965) 1187-1202.

Bowman, C. T. (1968), "Application of kinetics calculations to the interpretation of shock tube data," WSCI Paper 68-50.

Bowman, C. T. (1970), "Investigation of nitric oxide formation kinetics in combustion processes: the hydrogen-oxygen nitrogen reaction," to be published Comb. Sci. Tech. 3.

Bowman, C. T. and Seery, D. J. (1968), "Ignition mechanisms of hydrocarbon fuels-methane and acetylene," WSCI Paper 68-41.

Camac, M. and Feinberg, R. M. (1967), "Formation of NO in shock-heated air," Eleventh Symposium (International) on Combustion, The Combustion Institute, 137-145.

Chigier, N. A. and Chervinsky, A. (1967), "Experimental investigation of swirling vortex motion in jets," Tr. ASME (J. Appl. Mech.) 34, 443-451.

Chinitz, W. (1965), "A theoretical analysis of nonequilibrium methane/air combustion," Pyrodynamics 3, 197-219.

Chinitz, W. and Baurer, T. (1966), "An analysis of nonequilibrium hydrocarbon/air combustion," Pyrodynamics 4, 119-154.

Cooper, P. W. and Marek, C. J. (1965), "Design of blue-flame oil burners utilizing vortex flow or attached jet entrainment," API Publication 1723-A.

Cornelius, W. and Wade, W. R. (1970), "The formation and control of nitric oxide in a regenerative gas turbine burner," SAE Paper No. 700708.

Crowe, C. T. and Pratt, D. T. (1970), "Gross characterization of mixing in combustion chambers based on a fluid dynamical model," Eastern States/Combustion Institute Fall Meeting Paper No. 6.

Danckwerts, P. V. (1953), "Continuous flow systems - distribution of residence times," Chem. Eng. Sci. 2, 1-13.

Danckwerts, P. V. (1958a), "Measurement of molecular homogeneity in a mixture," Chem. Eng. Sci. 7, 116-117.

Danckwerts, P. V. (1958b), "The effect of incomplete mixing on homogeneous reactions," Chem. Eng. Sci. 8, 83-102.

Edelman, R. B. (1970), "Some problems in combustion controlled by coupled mixing and kinetics," Paper presented at ESCI Meeting, Atlanta, Fall 1970.

Edelman, R. B. and Fortune, O. F. (1969), "A quasi-global chemical kinetic model for the finite rate combustion of hydrocarbon fuels with application to turbulent burning and mixing in hypersonic engines and nozzles," AIAA 7th Aerospace Sciences Meeting, Paper No. 69-86.

Field, M. A., Gill, D. W., Morgan, B. B. and Hawksley, P. G. W. (1967), Combustion of pulverized coal, British Coal Utilization Research Assoc.

Fletcher, R. S. and Heywood, J. B. (1971), "A model for nitric oxide emissions from aircraft gas turbine engines," AIAA 9th Aerospace Sciences Meeting, Paper No. 71-123.

Gilliland, E. R. and Mason, E. A. (1949), "Gas and solid mixing in fluidized beds," Ind. Eng. Chem. 41, 1191-1196.

Gilliland, E. R. and Mason, E. A. (1952), "Gas mixing in beds of fluidized solids," Ind. Eng. Chem. 44, 218-224.

Gradon, K. and Miller, S. C. (1967), "Combustion development on the Rolls-Royce Spey engine," Combustion in advanced turbine systems, Pergamon, London, 45-78.

Hammond, D. C., Jr. and Mellor, A. M. (1970a), "An investigation of gas turbine combustors with high inlet air temperatures, First Annual Report Part I - Analytical Developments," TM-70-2, Jet Propulsion Center, Purdue University, Lafayette, Indiana.

Hammond, D. C., Jr. and Mellor, A. M. (1970b), "A primary investigation of gas turbine combustor modelling," Comb. Sci. Tech. 2, 67-80.

Heywood, J. B., Fay, J. A., and Linden, L. H. (1970), "Jet aircraft polluant production and dispersion," AIAA Paper No. 70-115, AIAA 8th Aerospace Sciences Meeting.

Hiett, G. F. and Powell, G. E. (1962), "Three-dimensional probe for investigation of flow patterns," The Engineer 213, 165-170.

Hottel, H. C., Williams, G. C., Bonnell, A. H. (1958), "Application of stirred reactor theory to the prediction of combustor performance," comb. flame 2, 13-34.

Hottel, H. C., Williams, G. C., Nerheim, N. M., Schneider, G. R. (1965), "Kinetic studies in stirred reactors: combustion of carbon monoxide and propane," Tenth Symposium (International) on Combustion, The Combustion Institute, 111-121.

Hubble, P. E. (1967), "A numerical approach to the estimation of gas turbine combustion chamber performance," Combustion in advanced gas turbine systems, Pergamon, London, 229-256.

Jenkins, D. R., Spalding, D. B., and Yunlu, V. S. (1967), "Combustion of hydrogen and oxygen in a steady-flow adiabatic stirred reactor," Eleventh Symposium (International) on Combustion, The Combustion Institute, 779-790.

Jones, A. (1969), personal communication.

Jones, A. and Prothero, A. (1968), "The solution of the steady-state equations for an adiabatic stirred reactor," Comb. Flame 12, 457-464.

Kerr, N. M. and Fraser, D. (1965), "Swirl part 1: Effect on axisymmetric turbulent jets," J. Inst. Fuel 38, 519-526.

Lavoie, G. A., Heywood, J. B. and Keck, J. C. (1970), "Experimental and theoretical study of nitric oxide formation in internal combustion engines," Comb. Sci. Tech. 1, 313-326.

Lefebvre, A. H. (1966), "Theoretical aspects of gas turbine combustion performance," College of Aeronautics, Cranfield, Coa Note Aero, No. 163.

Lefebvre, A. H. (1967), "Factors controlling gas turbine combustion performance at high pressure," Combustion in advanced gas turbine systems, Pergamon, London, 211-226.

Levenspiel, O. (1962), Chemical reaction engineering, J. Wiley & Sons, New York.

Marteney, P. J. (1970), "Analytical study of the kinetics of formation of nitrogen oxide in hydrocarbon-air combustion," Comb. Sci. Tech. 1, 461-469.

Morgan, A. C. (1967), "The combustion of methane in a jet-mixed reactor," Sc.D. thesis in Chem. Eng., M.I.T.

Nerheim, N. M. (1960), Sc.D. thesis in Chem. Eng., M.I.T.

Newhall, H. K. (1969), "Kinetics of engine-generated nitrogen oxides and carbon monoxide," Twelfth Symposium (International) on Combustion, The Combustion Institute, 603-613.

Owens, C. W. and Mellor, A. M. (1971), "An investigation of gas turbine combustors with high inlet air temperatures, Second Annual Report Part II - Heat Transfer, " TM-71-2, Jet Propulsion Center, Purdue University, Lafayette, Indiana, TACOM Report No. 11328.

Penner, S. S. (1957), Chemistry problems in jet propulsion, Pergamon, New York.

Pratt, D. T. (1970), "The distribution of residence times in a confined round jet," Western States/Combustion Institute Paper No. WSCI-70-7.

Prothero, A. (1969), "Computing with thermochemical data," Comb. Flame 13, 399-408.

Schneider, G. R. (1960) Sc.D. thesis in Chem. Eng., M.I.T.

Spalding, D. B. and Jain, V. K. (1966), "The effects of finite recirculation in a stirred reactor," Comb. Flame 10, 37-43.

Stull, D. R. ed. (1965), "JANAF Thermochemical Tables," Dow Chemical Co., Midland, Mich., PB-168-370 et seq.

Tacina, R. R. and Grobman, J. (1969), "Analysis of total-pressure loss and airflow distribution for annular gas turbine combustors," NASA TN D-5385.

Thring, M. W. and Newby, M. P. (1953), "Combustion length of enclosed turbulent jet flames," Fourth Symposium (International) on Combustion, The Combustion Institute, 789-796.

Verduzio, L. and Campanaro, P. (1969), "The air recirculation ratio in can-type gas turbine combustors," Cranfield International Propulsion Symposium.

Way, B. (1955), "Combustion in the turbojet engine," Selected combustion problems II, AGARD, 296-327.

Zeldovich, Y. B., Sadovnikov, P. Ya., and Frank-Kamenetskii, D. A., (1947), "Oxidation of nitrogen in combustion," Academy of Sciences USSR, Inst. of Chem. Phys., Moscow, Leningrad.

APPENDIX A
DESCRIPTION OF THE KINETIC PERFECTLY STIRRED REACTOR PROGRAM FOR HYDROCARBON COMBUSTION

The function of this computer program is to predict the performance of a single stirred reactor by solving the coupled set of equations (2-5), (2-6), and (2-7). The current program is an extensive revision of the program developed by Jones and Prothero (1968) which solved the set of equations (2-5) and (2-6), i.e. solved for the concentrations for a specified reactor temperature. This formulation was unacceptable for use in the overall model; thus we included Eqn. (2-7) in the set allowing solutions for a specified inlet temperature. Curve fits for the thermochemical properties were abstracted from the work of Prothero (1969). The original kinetics data were altered in accordance with Table 9. A brief description of the main program and each subprogram follows (Jones, 1969).

THORTNA

THORTNA is the main control program which functions mainly as an input/output routine. Optionally, two levels of printed output and also punched card output will be produced.

INPTHD

INPTHD is a library data input routine. It reads a standard thermochemical data package from magnetic tape at the start of each program run. This data package contains values of the specific heat curve fit coefficients, the molecular weights, enthalpies and entropies of formation, and several arrays which define the various reactions.

SLCTNA

SLCTNA sets up the mechanism and rate constant matrices for the reactions chosen by selecting data from the library data package.

TSOLVE

TSOLVE performs the solution of the energy equation by matching inlet and exit specific enthalpies. It uses a golden section technique and calls GASMIX once per iteration.

GASMIX

Given an estimated reactor temperature from TSOLVE, GASMIX solves for the density and species concentrations existing in the reactor. A multi-dimensional extension of Newton's method is used. Both FUNCTN and DERIVS are called.

FUNCTN

FUNCTN evaluates the residuals of the species conservation equations which are written in the form $F(\sigma_i, \rho) = 0$.

DERIVS

DERIVS evaluates the Jacobian matrix of the partial derivatives of the species conservation equations.

SRENTHA - SRH298A

These function subprograms operate together to evaluate the molar enthalpies of a particular species as a function of temperature.

MATINV - MXPERM

These two subroutines are called by GASMIX to invert the Jacobian matrix of partial derivatives.

KDATA

KDATA is a block data subprogram which stores the values of the parameters which define the various rate constants.

To use this program for general hydrocarbon combustion the parent fuel must be converted to its equivalent in carbon monoxide and water,

and an appropriate heat transfer must be computed. This process is accomplished by the following global reaction:

$$\phi C_a H_b + (a + \frac{b}{4})\, O_2 \xrightarrow{k_f = \infty} \phi a CO + \phi(b/2)\, H_2O + [a(1-\phi/2) + (1-\phi)b/4]\, O_2 + Q$$

where the right hand side gives the true inlet mixture to the combustor, and Q is the heat transfer to the reactor when expressed as cal/gm of flow. Here ϕ is the equivalence ratio of the original hydrocarbon mixture.

This program is completely operational and detailed information will be supplied upon request. Typical computation times on a CDC 6500 machine range from 30 to 150 sec per case depending on the severity of the conditions imposed.

APPENDIX B
DESCRIPTION OF THE EQUILIBRIUM REACTOR PROGRAM

This program was designed to give an upper limit on the predictions of the kinetic program (Appendix A). As a result it utilizes the same library data package but processes the information in a slightly different manner. The program is an inhouse product and has not been previously presented. The numerical technique is rather unique: starting from some initial estimate of the composition, the current composition is used to evaluate all of the equilibrium constants and a temperature from the energy equation. A temperature is then calculated from each of the equilibrium constants. The deviation of each of these temperatures from the average is used to increment the composition, and the process repeats until some convergence criterion is met. Solutions can be performed for fixed reactor or inlet temperature. Again each subprogram will be briefly described.

EQRTR

EQRTR is the main program which serves only as an input/output routine. Optionally both printed and punched card output can be produced.

GSOLV

GSOLV is an organizational routine which controls the initialization and calling sequence of the operational routines.

EQDTIN

EQDTIN is the library data input routine for this program.

NEWNI

NEWNI computes the composition increments mentioned in discussing the numerical technique.

PRISOL

PRISOL is used by NEWNI in computing the composition increments. It solves the set of atomic species conservation equations.

TEMPKP

TEMPKP evaluates a temperature from each of the equilibrium constant values.

TENERG

TENERG evaluates a temperature by solving the energy equation.

Typical computation times for this program on the CDC 6500 machine range from 20 to 60 sec depending heavily on the accuracy of the optionally supplied initial estimate. We will supply, on request, a more complete description of this program.

APPENDIX C
DESCRIPTION OF THE GAS TURBINE COMBUSTOR ANALYSIS PROGRAM

This program performs the analysis of a complete gas turbine combustor based on the overall model. The basic computational device is the kinetic perfectly stirred reactor program described in Appendix A. Certain inputs to the program are required and they will be summarized here:

1. the combustor geometry;
2. the predicted airflow and pressure distributions from the NASA program;
3. an estimated fuel distribution;
4. the total fuel flow and temperature;
5. the total airflow and temperature;
6. estimates of the primary zone recirculation ratio and volume ratio;
7. the species and reactions to be considered.

The same thermochemical data package is utilized. To compact the program as much as possible it was written in overlayed form (cf. Fig. 43). To conserve computer time an internal abort/restart sequence was written into the program. The abort sequence functions if the program detects an error (insufficient time, incorrect input, non-convergence, etc.) and at that point all internal information is dumped to magnetic tape. Using the restart sequence the program can be started at any point either for error correction or parametric studies. For instance, when running two cases which differ only in secondary air addition, the program could be started at the point where the distribution first differs, thereby using a portion of the previous calculations. This feature will be useful when changing the secondary combustion zones while the primary zone description remains fixed. A description of each routine's function follows.

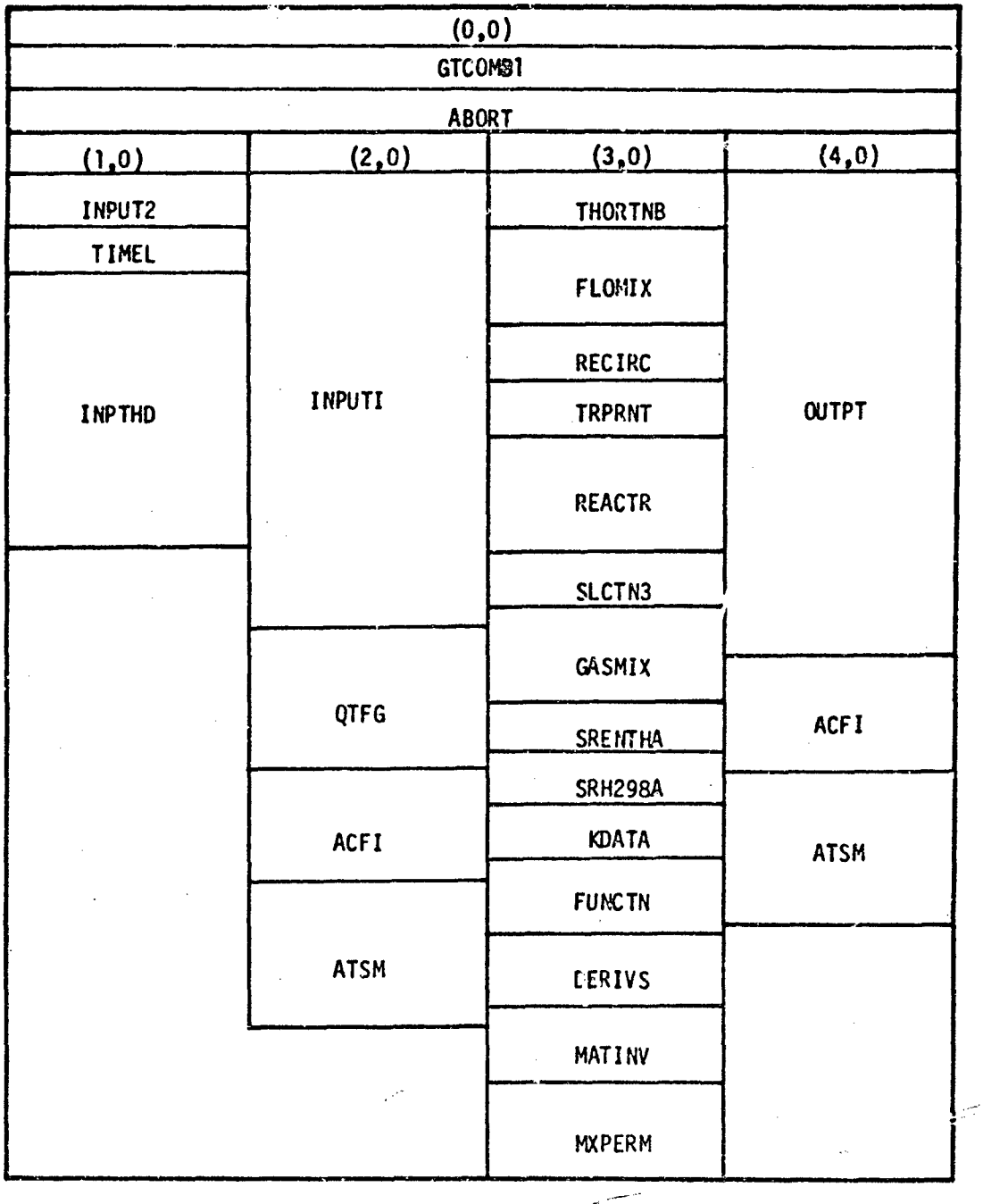

Fig. 43 Overlay structure of the gas turbine combustor analysis program.

GTGOMB1

This is the resident main control program; it directs the calling sequence of the other overlays and computes the total time consumed by each. It also contains all the input/output buffers.

ABORT

As the name implies this is the abort sequence routine. If an error is detected, this routine is called, and it dumps all internal information to magnetic tape. An appropriate error message is issued to the output device. ABORT is also called at the completion of computations to save the internal information for future runs.

INPUT2

INPUT2 is the main program of the library data input overlay. It performs two calls, one on INPTHD and one on TIMEL. The function of INPTHD was described in Appendix A.

TIMEL

TIMEL is an assembly language coded routine which evaluates the total time available to the program for execution. This time is used in the abort sequence.

INPUT1

INPUT1 is the main program of the case data input overlay. It reads the previously mentioned input data, and sets up the combustor model by assigning volumes, flows, and pressures to all of the reactors.

QTFG

QTFG is used by INPUT1 to integrate the combustor dimensions in order to compute the volume.

ATSM - ACFI

These two subroutines are used by INPUT1 and OUTPT to interpolate values for the various reactor parameters from the tabulated distribution functions.

THORTNB

THORTNB is the main program of the computational overlay. It controls the processing in that overlay.

FLOMIX

FLOMIX is used to initialize the input conditions for each reactor. It performs the partial oxidation calculation discussed in Appendix A.

RECIRC

RECIRC solves for the performance of the primary zone model.

REACTR

REACTR performs the actual solution for each reactor. It is a slight revision of TSOLVE described in Appendix A.

TRPRNT

TRPRNT serves as an intermediate output routine for debugging purposes.

The remainder of the computational routines were described in Appendix A.

OUTPT

OUTPT prints out the solution predicted by the computational overlay. In addition it can plot the input distributions and output profiles as functions of axial position and/or mean residence time.

The exact configuration of this program is in a state of flux. For the test case presented in Chapter V the total computation time was about 1100 sec on the CDC 6500 machine.